Supporting Information for

Fast and Accurate Quantum Crystallography: from Small to Large, from Light to Heavy

Lorraine A. Malaspina,[a] Erna K. Wieduwilt,[a,b] Justin Bergmann,[a,%] Florian Kleemiss,[a,c] Benjamin Meyer,[b,&] Manuel F. Ruiz-López,[b] Rumpa Pal,[a,§] Emanuel Hupf,[a,$] Jens Beckmann,[a] Ross O. Piltz,[d] Alison J. Edwards,[d] Simon Grabowsky,[a,c*] Alessandro Genoni[b*]

[a] *Institut für Anorganische Chemie und Kristallographie, Fachbereich 2 – Biologie/Chemie, Universität Bremen, Leobener Straße 3 und 7, 28359 Bremen, Germany*

[b] *Université de Lorraine, CNRS, Laboratoire de Physique et Chimie Théoriques (LPCT), 1 Boulevard Arago, 57078 Metz, France*

[c] *Departement für Chemie und Biochemie, Universität Bern, Freiestrasse 3, 3012 Bern, Switzerland*

[d] *Australian Nuclear Science and Technology Organisation, Australian Centre for Neutron Scattering, New Illawarra Rd, Lucas Heights NSW 2234, Australia*

Present Addresses:

[%] *Lund University, Department of Theoretical Chemistry, Chemical Center, P.O. Box 124, S-22100 Lund, Sweden*

[&] *Laboratory for Computational Molecular Design (LCMD), Institute of Chemical Sciences and Engineering (ISIC), École Polytechnique Fédérale de Lausanne (EPFL), CH-1015 Lausanne, Switzerland*

[§] *Division of Physics, Faculty of Pure and Applied Sciences, University of Tsukuba, 1-1-1 Tennodai, Tsukuba, Ibaraki, 305-8571, Japan*

[$] *Department of Chemistry, University of Alberta, 11227 Saskatchewan Drive, Edmonton, Alberta, Canada T6G 2G2*

Correspondence to Alessandro Genoni (Alessandro.Genoni@univ-lorraine.fr) and Simon Grabowsky (simon.grabowsky@dcb.unibe.ch)

Table of Contents

Theoretical bases of the HAR-ELMO technique

Hirshfeld Atom Refinement. In all its variants (traditional and new HAR-ELMO strategy) the Hirshfeld Atom Refinement is a self-consistent refinement procedure consisting in the following steps: i) the starting point is always a molecular geometry from a previous independent atom model refinement that represents at least the asymmetric unit of the crystallographic structure; ii) using the current geometry, a wavefunction is computed: in traditional HAR, a tailor-made quantum mechanical calculation (at Hartree-Fock or Density Functional Theory level) is directly performed, while, in the new HAR-ELMO strategy, the wavefunction is obtained by transferring ELMOs from the constructed libraries; iii) from the obtained wavefunction, a molecular electron density is calculated and afterwards partitioned into atomic contributions through the Hirshfeld stockholder partitioning technique; iv) the resulting Hirshfeld atoms (atomic density functions) are then used for the computation of the global calculated structure factors that allow the evaluation of the statistical agreement with the experimental structure factors (χ^2); v) the statistical agreement is minimized with respect to the atomic coordinates and ADPs using standard least-squares refinement to obtain a new molecular geometry and new ADPs; vi) if convergence is achieved (maximum shift of any refined parameter over its standard uncertainty (s.u) lower than 0.01, namely Δparam/s.u.<0.01) , the new atomic positions and ADPs represent the refined crystallographic structure, otherwise the new molecular geometry is the starting point for a new iteration from point (ii) to point (v).

Theory of Extremely Localized Molecular Orbitals. Extremely localized molecular orbitals (ELMOs)[S1] are molecular orbitals strictly localized on small molecular subunits (e.g., atoms, bonds and functional groups) that are obtained by imposing *a priori* a localization scheme that subdivides the molecule under investigation into fragments that may overlap. This fragmentation allows the definition of a local basis set $\beta_i = \{|\chi_{i\mu}\rangle\}_{\mu=1}^{M_i}$ for each subunit. Each of the subunits is constituted only by those basis functions that are centered on the atoms that belong to the fragment. These

basis sets are afterwards exploited to expand the ELMOs of each subunit and, for instance, the generic α-th ELMO for the *i*-th fragment can be written in this way:

$$| \varphi_{i\alpha} \rangle = \sum_{\mu=1}^{\mathrm{M}_i} C_{i\mu,i\alpha} \; | \chi_{i\mu} \rangle \qquad \text{(S1)}$$

Following Stoll,[S1] a single Slater determinant constructed with extremely localized molecular orbitals defined by equation (S1) describes the system under examination:

$$|\Psi_{ELMO}\rangle = \frac{1}{\sqrt{(2N)!\, det[\mathbf{S}]}} \; \hat{A} \left[\prod_{i=1}^{f} \prod_{\alpha=1}^{n_i} \varphi_{i\alpha} \, \bar{\varphi}_{i\alpha} \right] \qquad \text{(S2)}$$

where $\hat{A}$ is the usual antisymmetrizer, n_i is the number of occupied ELMOs for the *i*-th fragment, $\varphi_{i\alpha}$ is a spinorbital with spatial part $\varphi_{i\alpha}$ and spin part α and $\bar{\varphi}_{i\alpha}$ is a spinorbital with spatial part $\varphi_{i\alpha}$ and spin part β. Furthermore, $det[\mathbf{S}]$ is the determinant of the overlap-matrix of the occupied ELMOs, which is actually due to the non-orthogonality of the ELMOs.

ELMOs result from the variational minimization of the ELMO energy (S2) with respect to expansion coefficients $\{C_{i\mu,i\alpha}\}$ in (S1) and it is possible to show that this is mathematically equivalent to self-consistently solving the following modified Hartree-Fock equations (namely, the Stoll equations) for each fragment:[S1]

$$\hat{F}_i |\varphi_{i\alpha}\rangle = \; \varepsilon_{i\alpha} \, |\varphi_{i\alpha}\rangle \qquad \text{(S3)}$$

with $\hat{F}_i$ as the modified Fock operator for the *i*-th subunit, namely:

$$\hat{F}_i = \left(1 - \hat{\rho} \; + \hat{\rho}_i^{\dagger}\right) \hat{F} (1 - \hat{\rho} \; + \hat{\rho}_i) \qquad \text{(S4)}$$

where $\hat{F}$ is the usual Fock operator, $\hat{\rho}$ is the global density operator (which depends on all the occupied ELMOs of the system) and $\hat{\rho}_i$ is the density operator for the *i*-th fragment (which, on the contrary, depends only on the occupied ELMOs of the subunit) .

As an example, in Figure S1 we show the different kinds of ELMOs that can be obtained for the water molecule by defining a localization pattern strictly corresponding to the Lewis structure of the system (Figure S1-A): i) an ELMO describing the oxygen core electrons (Figure S1-B); ii) two ELMOs associated with the two oxygen lone pairs (Figure S1-C and Figure S1-D); iii) two ELMOs corresponding to the two O-H bonds of the molecules (Figure S1-E and Figure S1-F).

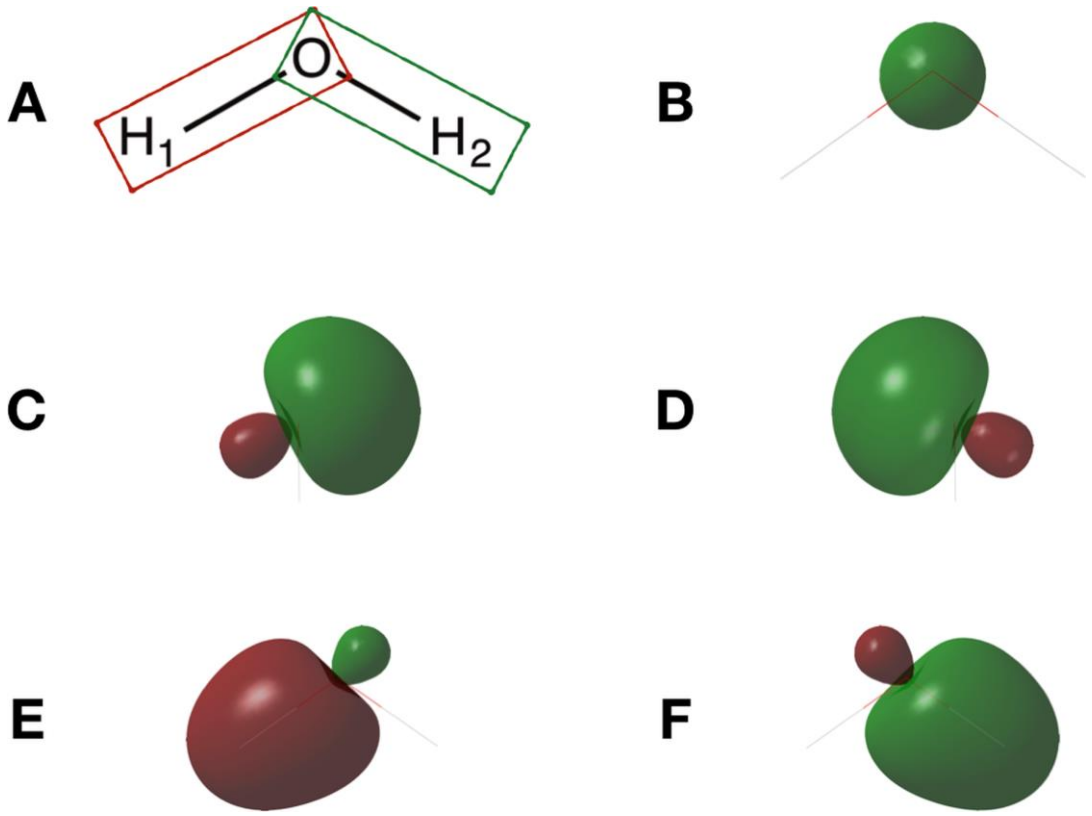

Figure S1: (A) Lewis structure of the water molecule and corresponding localization scheme: the two overlapping fragments O-H1 and O-H2 are explicitly depicted, while, for the sake of clarity, atomic fragment O associated with the core and lone pair electrons of the oxygen atom is not shown; (B) ELMO describing the core electrons of the oxygen atom; (C) and (D) ELMOs describing the lone pairs of the oxygen atom; (E) ELMO describing the O-H1 bond of the molecule; (F) ELMO describing the O-H2 bond of the molecule. All the ELMOs were computed using the cc-pVDZ basis-set and were plotted considering a 0.15 a.u. isosurface.

ELMOs transferability and rotation. As a consequence of their extreme localization, ELMOs are orbitals easily transferable from one molecule to another, and particularly from a model system (which is usually the small molecule on which the orbital is originally computed) to the target system under investigation. Following Philipp and Friesner,[S2] this can be done by defining a suitable rotation matrix **P** that transforms the ELMO coefficients (see equation (S1)) obtained in the geometry of the model system to the ELMO coefficients in the geometry of the target molecule. As already indicated in detail in previous publications about ELMO transferability and libraries,[S3-S5] the rotation matrix is obtained through the definition *i)* of a reference frame (**a**, **c**, **d**) in the model molecule and *ii)* of a reference frame (**a**', **c**', **d**') in the target system (see Figure S2). These reference frames originate from the choice of

two atomic triads (one for the model molecule and one for the target system) that ensure the uniqueness of the rotation.

If we indicate the two triads for the model and target molecules as (A_1, A_2, A_3) and (A_1', A_2', A_3'), respectively, the vectors defining the two reference frames are the following ones: **a** (**a**') is the position vector of A_2 (A_2') relative to A_1 (A_1') (see Figure S2), while **c** (**c**') and **d** (**d**') result from the following vector products:

$$\begin{cases} \mathbf{c} = \mathbf{a} \times \mathbf{b} & (\mathbf{c}' = \mathbf{a}' \times \mathbf{b}') \\ \mathbf{d} = \mathbf{c} \times \mathbf{a} & (\mathbf{d}' = \mathbf{c}' \times \mathbf{a}') \end{cases} \qquad (S5)$$

with **b** (**b'**) as the position vector of A_3 (A_3') with respect to A_1 (A_1') (see Figure S2).

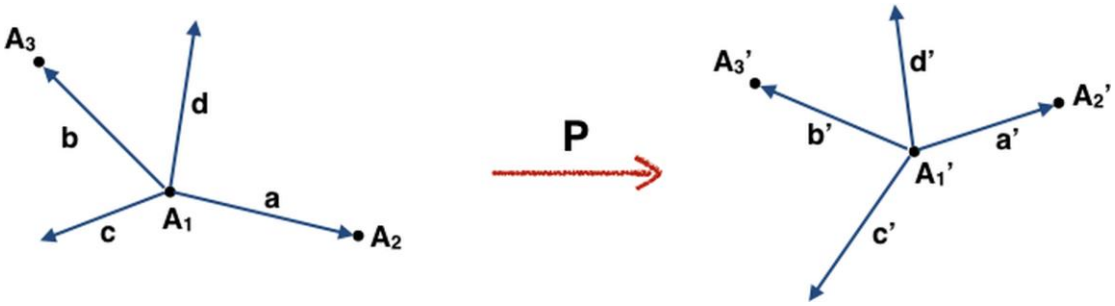

Figure S2: Schematic representation of reference frames and atomic triads that are necessary to define matrix **P** associated with the rotation of the ELMOs from the geometry of the model system (left) to the geometry of the target molecule (right).

For ELMOs localized only on one atom (i.e., ELMOs corresponding to core or lone-pair electrons) the atomic triads are constituted of the atom on which the ELMO is localized and, in general, by two other bonded atoms. For ELMOs describing two-center bonds, the triads are given by the two atoms that form the bond and by an atom representing the local dissymmetry of the bond under consideration.[S6] For three-center ELMOs (e.g., ELMOs used to describe electronic delocalization such as in peptide bonds or aromatic rings[S5]), the triads of atoms are automatically chosen. For ELMOs localized on more than three atoms, the definition of triads (and, consequently, of reference frames) that simultaneously take into account the orientation of all the atoms in the subunit is obviously impossible and this is the reason why all the ELMOs available in the current databanks are localized at the most on three atoms (see next subsection).

Rotation matrix **P** that leads from reference frame (**a**, **c**, **d**) to reference frame (**a**', **c**', **d**') is the "key-matrix" that allows the construction of all the matrices for the rotation

of all kinds of basis functions and associated ELMO coefficients. In fact, it can be easily shown[S3] that, excluding *s*-type atomic orbitals, which are invariant owing to their spherical symmetry, the *p*-type basis functions (and the related coefficients) can be exactly transformed by matrix **P**, while basis functions (and corresponding coefficients) with angular momentum greater than 1 can be rotated using transformation matrices expressed in function of **P**.

Structure of the ELMO libraries. As already mentioned in the main text, the current ELMO libraries[S5] enable the description of all the possible fragments of a water molecule and of the twenty natural amino acids in all their possible protonation states and forms (namely, N-terminal, C-terminal and non-terminal forms). They have been constructed by computing ELMOs on proper model molecules that take into account the chemical environment of the considered fragments. At the moment, the ELMO databases are available for five standard basis sets of quantum chemistry (i.e., 6-31G, 6-311G, 6-31G(d,p), 6-311G(d,p) and cc-pVDZ) and contain molecular orbitals localized on one-atom and two-atom fragments, which are associated with core/lone pair and bonding electrons, respectively, and molecular orbitals localized on three-atom fragments, which properly describe the delocalized nature of the electronic structure in some particular regions of proteins and polypeptides (e.g., in carboxylic groups, peptide bonds or aromatic rings).

All the ELMOs in the current version of the databanks were computed on optimized geometries (at B3LYP/6-311++G(d,p) level) of model molecules properly designed to take into account the usual chemical environment of the fragments of interest in polypeptides and proteins. In particular, for each fragment, except for the one corresponding to the peptide bond, the model molecules were constructed using the *Nearest Functional Group Approximation* (NFGA), which consists in considering the subunit of interest and its nearest neighbor functional groups capped with hydrogen atoms.[S3] For peptide bonds the simpler *Nearest Bond Approximation* (NBA) was taken into account, according to which the model molecule consists of the fragment under investigation and its nearest neighbor bonds always capped with hydrogen atoms.[S3]

In the ELMO libraries, for each fragment of the different amino acids, not only the coefficients of the corresponding occupied and virtual ELMOs are stored, but also the coordinates associated with the atomic triads in the model molecule, which are crucial

to define the rotation of the molecular orbitals from the geometry of the model system to the geometry of the target molecule (see previous subsection).

The transfer of the ELMOs from the databanks to target structures is carried out through the in-house program ELMOdb. The software basically parses PDB files of polypeptides or proteins and, for each of their residues, it carries out the transfer procedure for one fragment at a time.

As already mentioned in the main text, the ELMOdb program has been designed also to read tailor-made ELMOs associated with special fragments of molecules that are not covered by the current version of the databanks. These ELMOs must be determined on proper model systems and afterwards stored (together with the atomic coordinates of the associated model molecule triads) in a specific folder to which the ELMOdb program has access. As an example and also for the sake of completeness, the model molecules used to compute the ELMOs exploited in the HAR-ELMO refinements of the coordination compounds investigated in this paper are indicated in the section “Refinement of coordination compounds” of this Supporting Information.

A complete overview on the construction and organization of the ELMO databanks and on the main features of the ELMOdb program can be found in the original paper about the ELMO libraries.[S5]

Validation of HAR-ELMO

Measurement details

The results presented here involve the comparison of the results obtained through the HAR and HAR-ELMO approaches for the following X-ray datasets:

- Glycyl-*L*-alanine, at 12 K, λ= 0.5259(2) Å, data set taken from ref. S7 (ref. 26 in the main text)
- Glycyl-*L*-alanine, at 50 K, λ= 0.5259(2) Å, data set taken from ref. S7
- Glycyl-*L*-alanine, at 100 K, λ= 0.5259(2) Å, data set taken from ref. S7
- Glycyl-*L*-alanine, at 150 K, λ= 0.5259(2) Å, data set taken from ref. S7
- Glycyl-*L*-alanine, at 295 K, λ= 0.5259(2) Å, data set taken from ref. S7
- *L*-alanine, at 23 K, λ= 0.71073 Å, data set taken from ref. ref. S8 (ref. 35 in the main text)
- *L*-alanine, at 100 K, λ= 0.71073 Å, new measurement (see Table S1 and main text)
- *L*-alanine, at 150 K, λ= 0.71073 Å, new measurement (see Table S1 and main text)

Neutron-diffraction data sets are available for all structures except for *L*-alanine and Glycyl-*L*-alanine at 100 K:

- Glycyl-*L*-alanine, at 12 K, λ= 0.8313(2) Å, data set taken from ref. S9 (ref. 36 in the main text)
- Glycyl-*L*-alanine, at 50 K, λ= 0.8313(2) Å, data set taken from ref. S9
- Glycyl-*L*-alanine, at 150 K, λ= 0.8313(2) Å, data set taken from ref. S9
- Glycyl-*L*-alanine, at 295 K, λ= 0.8313(2) Å, data set taken from ref. S9
- *L*-alanine, at 23 K, λ= 0.750 to 1.500 Å (Laue), new measurement (see Table S1 and main text)
- *L*-alanine, at 150 K, λ= 0.750 to 1.500 Å (Laue), new measurement (see Table S1 and main text)

Table S1: Measurement details for the new X-ray and neutron single-crystal diffraction experiments of *L*-alanine.

Compound	***L*-alanine**			
Chemical formula	$C_3\ H_7\ N_1\ O_2$			
M_r **(u)**	89.0947			
Crystal system	Orthorhombic			
Space group	$P\ 2_12_12_1$			
***a, b, c* (Å)**	5.9279(10)* 12.2597(17) 5.7939(9)	5.9596(2)* 12.2828(3) 5.7899(1)	5.9587(2) 12.2796(4) 5.7876(2)	5.9596(2) 12.2828(3) 5.7899(1)
V **(Å^3)**	421.07(7)	423.82(2)	423.48(2)	423.82(2)
Z	4	4	4	4
Radiation type	Neutron	Neutron	X-ray (MoKα)	X-ray (MoKα)
Wavelength (Å)	0.750 to 1.500	0.750 to 1.500	0.71073	0.71073
Temperature (K)	23	150	100(2)	150(2)
Crystal size (mm)	1.9x1.6x1.0	3.5x1.9x1.0	0.46x0.26x 0.17	0.29x0.21x 0.19
Absorption cor.	none	none	multi-scan	multi-scan
μ **(mm^{-1})**	0.0	0.0	0.117	0.117
***T*min**	-	-	0.943	0.631
***T*max**	-	-	0.996	0.754
Extinction cor:[S10]	8.8(5)	5.0(6)	none	none
Resolution (Å)	0.500	0.500	0.45	0.55
hkl ranges	*h*= -11, 9 *k*= -18, 23 *l*=-11, 11	*h*=-11, 11 *k*=-24, 24 *l*=-10, 10	*h*=-13, 11 *k*=-27, 27 *l*=-12, 12	*h*=-10, 10 *k*=-21, 22 *l*=-10, 10
Theta min			3.318	3.317
Theta max	71.48	71.11	52.157	40.238
Theta full	71.39	71.01	25.242	25.242
Complet. (max)	0.874	0.875	0.992	0.999
Complet. (full)	0.874	0.875	0.987	0.998
Refl. Measured	35505	94436	31869	21264
Unique refl.	1541	1554	4783	2667
Unique obs. refl.	1486	1310	4611	2602
Obs. criteria	I>2σ(I)	I>2σ(I)	F>0 F/u(F)>3.0 |F_calc|>10^{-3}	F>0 F/u(F)>3.0 |F_calc|>10^{-3}
Rint	0.0470	0.1015	0.0223	0.0402
Rsym	0.0519	0.0937	0.0148	0.0212

*For the refinements of the Laue neutron-diffraction experiments, the cell parameters of the respective X-ray diffraction data sets at the same temperatures were used.

Refinement details

Table S2: Refinements against X-ray data for Gly-*L*-Ala at 12 K, CCDC deposition nos.: 1917823-1917825.

	HAR	**HAR-ELMO**	**IAM**
R*[*F*>3*σ*(*F*)], *wR*(*F*), *S	0.016, 0.061, 1.27	0.017, 0.061, 1.35	0.025, 0.061, 2.44
No. of reflections	2394	2394	2394
No. of parameters	181	181	131
H-atom treatment	All H-atom parameters refined (anisotropically)	All H-atom parameters refined (anisotropically)	H atoms refined isotropically
$\Delta\rho_{max}$, $\Delta\rho_{min}$ (eÅ^{-3})	0.14, −0.17	0.14, −0.18	0.20, −0.21

Table S3: Refinements against X-ray data for Gly-*L*-Ala at 50 K, CCDC deposition nos.: 1917826-1917828.

	HAR	**HAR-ELMO**	**IAM**
R*[*F*>3*σ*(*F*)], *wR*(*F*), *S	0.018, 0.065, 1.22	0.019, 0.065, 1.31	0.026, 0.065, 2.14
No. of reflections	2295	2295	2295
No. of parameters	181	181	131
H-atom treatment	All H-atom parameters refined (anisotropically)	All H-atom parameters refined (anisotropically)	H atoms refined isotropically
$\Delta\rho_{max}$, $\Delta\rho_{min}$ (eÅ^{-3})	0.12, −0.13	0.12, −0.13	0.17, −0.18

Table S4: Refinements against X-ray data for Gly-*L*-Ala at 100 K, CCDC deposition nos.: 1917829-1917831.

	HAR	**HAR-ELMO**	**IAM**
R*[*F*>3*σ*(*F*)], *wR*(*F*), *S	0.017, 0.082, 1.56	0.018, 0.082, 1.66	0.026, 0.082, 3.10
No. of reflections	2456	2456	2456
No. of parameters	181	181	131
H-atom treatment	All H-atom parameters refined (anisotropically)	All H-atom parameters refined (anisotropically)	H atoms refined isotropically
$\Delta\rho_{max}$, $\Delta\rho_{min}$ (eÅ^{-3})	0.14, −0.20	0.13, −0.17	0.17, −0.20

Table S5: Refinements against X-ray data for Gly-*L*-Ala at 150 K, CCDC deposition nos.: 1917832-1917834.

	HAR	**HAR-ELMO**	**IAM**
R*[*F*>3*σ(F)*], *wR(F), S	0.016, 0.064, 1.53	0.017, 0.064, 1.65	0.025, 0.064, 3.09
No. of reflections	2440	2440	2440
No. of parameters	181	181	131
H-atom treatment	All H-atom parameters refined (anisotropically)	All H-atom parameters refined (anisotropically)	H atoms refined isotropically
$\Delta\rho_{max}$, $\Delta\rho_{min}$ (eÅ^{-3})	0.12, −0.13	0.13, −0.14	0.14, −0.19

Table S6: Refinements against X-ray data for Gly-*L*-Ala at 295 K, CCDC deposition nos.: 1917835-1917837.

	HAR	**HAR-ELMO**	**IAM**
R*[*F*>3*σ(F)*], *wR(F), S	0.019, 0.075, 1.42	0.021, 0.075, 1.55	0.030, 0.075, 2.74
No. of reflections	2357	2357	2357
No. of parameters	181	181	131
H-atom treatment	All H-atom parameters refined (anisotropically)	All H-atom parameters refined (anisotropically)	H atoms refined isotropically
$\Delta\rho_{max}$, $\Delta\rho_{min}$ (eÅ^{-3})	0.13, −0.15	0.12, −0.14	0.14, −0.17

Table S7: Refinements against X-ray data for *L*-Ala at 23 K, CCDC deposition nos.: 1917816-1917818.

	HAR	**HAR-ELMO**	**IAM**
R*[*F*>3*σ(F)*], *wR(F), S	0.020, 0.069, 1.18	0.020, 0.069, 1.29	0.028, 0.069, 2.28
No. of reflections	2405	2405	2405
No. of parameters	118	118	83
H-atom treatment	All H-atom parameters refined (anisotropically)	All H-atom parameters refined (anisotropically)	H atoms refined isotropically
$\Delta\rho_{max}$, $\Delta\rho_{min}$ (eÅ^{-3})	0.11, −0.10	0.11, −0.11	0.28, −0.27

Table S8: Refinements against X-ray data for *L*-Ala at 100 K, CCDC deposition nos.: 1917810-1917812.

	HAR	**HAR-ELMO**	**IAM**
R*[*F*>3*σ(F)*], *wR(F), S	0.020, 0.065, 2.10	0.020, 0.065, 2.30	0.027, 0.065, 4.13
No. of reflections	4611	4611	4611
No. of parameters	118	118	83
H-atom treatment	All H-atom parameters refined (anisotropically)	All H-atom parameters refined (anisotropically)	H atoms refined isotropically
$\Delta\rho_{max}$, $\Delta\rho_{min}$ (eÅ^{-3})	0.15, −0.22	0.16, −0.27	0.27, −0.25

Table S9: Refinements against X-ray data for *L*-Ala at 150 K, CCDC deposition nos.: 1917820-1917822.

	HAR	**HAR-ELMO**	**IAM**
R*[*F*>3*σ(F)*], *wR(F), S	0.020, 0.074, 1.78	0.021, 0.074, 1.88	0.028, 0.074, 2.62
No. of reflections	2602	2602	2602
No. of parameters	118	118	83
H-atom treatment	All H-atom parameters refined (anisotropically)	All H-atom parameters refined (anisotropically)	H atoms refined isotropically
$\Delta\rho_{max}$, $\Delta\rho_{min}$ (eÅ^{-3})	0.17, −0.15	0.16, −0.16	0.30, −0.20

Table S10: Refinement against neutron data for *L*-Ala at 23 K and 150 K, CCDC deposition nos.: 1917813, 1917685.

Temperature (K)	23	150
R*[*F*>3*σ(F)*], *wR(F), S	0.033, 0.027, 1.00	0.038, 0.033, 1.00
No. of reflections	1483	1305
No. of parameters	119	119
H-atom treatment	All H-atom parameters refined (anisotropically)	All H-atom parameters refined (anisotropically)
$\Delta\rho_{max}$, $\Delta\rho_{min}$ (eÅ^{-3})	1.43, −1.68	1.03, −1.17

Methodology for validation of HAR-ELMO

HAR refinements were performed at RHF/6-311G(d,p) level. Corresponding HAR-ELMO refinements were performed by transferring ELMOs from the ELMO libraries also using the 6-311G(d,p) basis-set.

No self-consistent field of cluster charges was used in any of the refinements since it is not available in the ELMOdb program, although it is known that the use of cluster charges leads to better hydrogen bond distances for groups involved in strong intermolecular interactions such as hydrogen bonds.[S11] The ELMO libraries contain pre-computed ELMOs, which, at the moment, cannot be updated according to the crystal environment represented by the surrounding cluster charges.

In HAR and HAR-ELMO, all hydrogen atoms were refined using anisotropic displacement parameters. Therefore the IAM results will be excluded from all the ADP statistics.

The statistics presented here are based on the following quantities:

1) - the mean ratio of the bond lengths $\langle r_A/r_B \rangle$

- the mean ratio of the diagonal ADPs $\langle U^{ii}_A/U^{ii}_B \rangle$

2) - the mean absolute differences (MADs) of the bond lengths (r_A and r_B) $\langle |\Delta r_{A\text{-}B}| \rangle$

- the mean absolute differences of the diagonal ADPs $\langle |\Delta U^{ii}_{A\text{-}B}| \rangle$

- the mean absolute differences of all ADPs $\langle |\Delta U^{ij}_{A\text{-}B}| \rangle$.

Note that the off-diagonal terms are generally small in magnitude and their differences tend to conceal deviations of the diagonal terms.

3) The root-mean-squared differences (wRMSDs) of bond distances and ADPs weighted by the combined standard uncertainties (csus):

The wRMSDs of the bond lengths measure the average deviation of the bond distances obtained through method A from the bond distances obtained through method B (given in equation (S6)).

The wRMSDs of the ADPs measure the average deviation of all ADPs obtained through method A from the ADPs resulting from method B (given in equation (S7)).

$$wRMSD = \left\langle \frac{(r_A - r_B)^2}{s.u.(r_A)^2 + s.u.(r_B)^2} \right\rangle^{\frac{1}{2}} (S6)$$

$$wRMSD = \left\langle \frac{\left(U_A^{ij} - U_B^{ij}\right)^2}{s.u.\left(U_A^{ij}\right)^2 + s.u.\left(U_B^{ij}\right)^2} \right\rangle^{\frac{1}{2}} (S7)$$

The expected values for the previous statistical quantities are the following:
- Type (1) should be close to 1 for good statistical agreement;
- Type (2) should be close to 0 for good statistical agreement;
- Type (3) should be 0 for exact agreement, close to 1 for good statistical agreement.

However, in the calculations of the wRMSD, standard uncertainties (s.u.) are used (see equations (S6) and (S7)). Therefore, considering that standard uncertainties are normally underestimated, values ranging from 1.5 to 2.0 are not uncommon for wRMSDs.

Comparison of hydrogen bond distances

Table S11: Statistical results for X-H bond distances, averaged among all bonds.

Compound	Method (A / B)	$\langle r_A/r_B \rangle$	$\langle \lvert \Delta r_{A\text{-}B} \rvert \rangle$ (in Å)	wRMSD
Gly-*L*-Ala 12 K	HAR / Neutron	0.996	0.006	1.295
	HAR-ELMO / Neutron	0.995	0.010	1.393
	IAM / Neutron	0.871	0.139	11.588
	HAR / HAR-ELMO	1.001	0.011	1.406
Gly-*L*-Ala 50 K	HAR / Neutron	1.003	0.010	1.236
	HAR-ELMO / Neutron	1.002	0.011	1.414
	IAM / Neutron	0.883	0.125	12.807
	HAR / HAR-ELMO	1.001	0.009	0.885
Gly-*L*-Ala 100 K	HAR / Neutron	-	-	-
	HAR-ELMO / Neutron	-	-	-
	IAM / Neutron	-	-	-
	HAR / HAR-ELMO	1.000	0.011	1.425
Gly-*L*-Ala 150 K	HAR / Neutron	1.000	0.008	1.378
	HAR-ELMO / Neutron	1.000	0.013	1.997
	IAM / Neutron	0.880	0.128	10.767
	HAR / HAR-ELMO	1.000	0.012	1.432
Gly-*L*-Ala 295 K	HAR / Neutron	0.994	0.011	1.061
	HAR-ELMO / Neutron	0.993	0.020	1.784
	IAM / Neutron	0.887	0.120	9.113
	HAR / HAR-ELMO	1.001	0.013	1.448
***L*-Ala 23 K**	HAR / Neutron	0.991	0.010	1.875
	HAR-ELMO / Neutron	0.974	0.028	3.995
	IAM / Neutron	0.916	0.090	9.070
	HAR / HAR-ELMO	1.018	0.019	2.171
***L*-Ala 100 K**	HAR / Neutron	-	-	-
	HAR-ELMO / Neutron	-	-	-
	IAM / Neutron	-	-	-
	HAR / HAR-ELMO	1.012	0.012	2.326
***L*-Ala 150 K**	HAR / Neutron	0.995	0.009	1.186
	HAR-ELMO / Neutron	0.981	0.020	2.276
	IAM / Neutron	0.902	0.105	9.733
	HAR / HAR-ELMO	1.014	0.014	1.242

Table S12: Average bond distances and statistical results for X-H bond distances according to the bond type, distances in Å, units of differences are Å. The numbers in brackets are the sample standard deviations from the averaging procedure.

Compound	Method (A / B)	Bond type	$\langle r(X\text{—}H)\rangle$ (method A)	$\langle r_A/r_B\rangle$	$\langle \lvert\Delta r_{A\text{-}B}\rvert\rangle$	wRMSD
Gly-*L*-Ala 12 K	Neutron reference	N-H	1.039(11)	N/A	N/A	N/A
		C-H	1.096(10)	N/A	N/A	N/A
	HAR/ Neutron	N-H	1.031(23)	0.992	0.010	1.855
		C-H	1.095(14)	0.998	0.004	0.708
	HAR-ELMO/ Neutron	N-H	1.025(10)	0.987	0.014	1.790
		C-H	1.097(19)	1.000	0.007	1.049
	IAM/ Neutron	N-H	0.889(29)	0.855	0.151	12.226
		C-H	0.966(32)	0.881	0.131	11.142
	HAR / HAR-ELMO	N-H	as above	1.006	0.017	1.896
		C-H	as above	0.998	0.007	0.948
Gly-*L*-Ala 50 K	Neutron reference	N-H	1.037(13)	N/A	N/A	N/A
		C-H	1.093(9)	N/A	N/A	N/A
	HAR/ Neutron	N-H	1.038(22)	1.001	0.008	0.894
		C-H	1.098(16)	1.005	0.012	1.419
	HAR-ELMO/ Neutron	N-H	1.033(7)	0.996	0.009	0.987
		C-H	1.100(17)	1.006	0.013	1.638
	IAM/ Neutron	N-H	0.901(11)	0.869	0.136	10.166
		C-H	0.976(30)	0.893	0.117	14.299
	HAR / HAR-ELMO	N-H	as above	1.005	0.016	1.262
		C-H	as above	0.999	0.005	0.493
Gly-*L*-Ala 100 K	Neutron reference	N-H	-	N/A	N/A	N/A
		C-H	-	N/A	N/A	N/A
	HAR/ Neutron	N-H	1.028(20)	-	-	-
		C-H	1.095(14)	-	-	-
	HAR-ELMO/ Neutron	N-H	1.023(17)	-	-	-
		C-H	1.099(12)	-	-	-
	IAM/ Neutron	N-H	0.902(19)	-	-	-
		C-H	0.965(32)	-	-	-
	HAR / HAR-ELMO	N-H	as above	1.005	0.016	1.833
		C-H	as above	0.996	0.008	1.071

Table S12: continued.

Compound	Method (A / B)	Bond type	⟨r(X—H)⟩ (method A)	⟨rA/rB⟩	⟨|ΔrA-B|⟩	wRMSD
Gly-*L*-Ala 150 K	Neutron reference	N-H	1.040(12)	N/A	N/A	N/A
		C-H	1.091(10)	N/A	N/A	N/A
	HAR/ Neutron	N-H	1.030(16)	0.991	0.011	1.706
		C-H	1.097(13)	1.006	0.007	1.107
	HAR-ELMO/ Neutron	N-H	1.026(12)	0.987	0.018	2.307
		C-H	1.100(15)	1.009	0.010	1.760
	IAM/ Neutron	N-H	0.891(26)	0.857	0.149	12.134
		C-H	0.977(41)	0.896	0.114	9.751
	HAR / HAR-ELMO	N-H	as above	1.004	0.017	1.904
		C-H	as above	0.997	0.008	1.002
Gly-*L*-Ala 295 K	Neutron reference	N-H	1.040(11)	N/A	N/A	N/A
		C-H	1.085(10)	N/A	N/A	N/A
	HAR/ Neutron	N-H	1.026(11)	0.987	0.014	1.331
		C-H	1.084(22)	0.998	0.009	0.835
	HAR-ELMO/ Neutron	N-H	1.024(17)	0.985	0.026	2.271
		C-H	1.084(28)	0.999	0.015	1.366
	IAM/ Neutron	N-H	0.883(36)	0.849	0.157	11.291
		C-H	0.990(47)	0.913	0.095	7.308
	HAR / HAR-ELMO	N-H	as above	1.002	0.019	2.010
		C-H	as above	1.000	0.009	0.894

Table S12: continued.

Compound	Method (A / B)	Bond type	⟨r(X—H)⟩ (method A)	⟨rA/rB⟩	⟨|ΔrA-B|⟩	wRMSD
***L*-Ala 23 K**	Neutron reference	N-H	1.044(10)	N/A	N/A	N/A
		C-H	1.095(4)	N/A	N/A	N/A
	HAR/ Neutron	N-H	1.028(13)	0.984	0.016	2.437
		C-H	1.091(8)	0.996	0.006	1.304
	HAR-ELMO/ Neutron	N-H	1.000(27)	0.958	0.044	5.296
		C-H	1.079(12)	0.985	0.017	2.624
	IAM/ Neutron	N-H	0.965(68)	0.924	0.079	8.923
		C-H	0.998(20)	0.911	0.098	9.178
	HAR / HAR-ELMO	N-H	as above	1.028	0.027	2.775
		C-H	as above	1.011	0.012	1.572
***L*-Ala 100 K**	Neutron reference	N-H	-	-	-	-
		C-H	-	-	-	-
	HAR/ Neutron	N-H	1.036(15)	-	-	-
		C-H	1.088(11)	-	-	-
	HAR-ELMO/ Neutron	N-H	1.023(11)	-	-	-
		C-H	1.076(3)	-	-	-
	IAM/ Neutron	N-H	0.927(22)	-	-	-
		C-H	0.981(27)	-	-	-
	HAR / HAR-ELMO	N-H	as above	1.012	0.013	2.103
		C-H	as above	1.011	0.012	2.481
***L*-Ala 150 K**	Neutron reference	N-H	1.042(10)	N/A	N/A	N/A
		C-H	1.091(5)	N/A	N/A	N/A
	HAR/ Neutron	N-H	1.035(13)	0.993	0.013	1.490
		C-H	1.087(5)	0.996	0.006	0.892
	HAR-ELMO/ Neutron	N-H	1.020(19)	0.979	0.022	2.486
		C-H	1.073(8)	0.983	0.018	2.104
	IAM/ Neutron	N-H	0.938(41)	0.899	0.105	9.548
		C-H	0.985(31)	0.903	0.106	9.870
	HAR / HAR-ELMO	N-H	as above	1.014	0.014	1.145
		C-H	as above	1.013	0.014	1.309

Table S13: Intermolecular hydrogen bonds of Gly-*L*-Ala. For atomic labels, see the CIFs deposited with the Cambridge Database and with this journal as Supporting Information

.D-H..A	Model	12 K	50 K	100 K	150 K	295 K
		D-H Distance in Å				
N1-H11 …O1	Neutron	1.022(4)	1.018(4)	-	1.025(4)	1.023(6)
	HAR	0.997(7)	1.007(9)	1.002(6)	1.008(6)	1.009(7)
	HAR-ELMO	1.020(7)	1.027(9)	1.025(6)	1.034(6)	1.045(7)
	IAM	0.854(12)	0.889(13)	0.880(11)	0.859(11)	0.834(11)
N2-H12 ...O2	Neutron	1.044(5)	1.045(5)	-	1.040(5)	1.042(7)
	HAR	1.047(7)	1.058(9)	1.039(7)	1.045(7)	1.034(8)
	HAR-ELMO	1.029(7)	1.042(9)	1.021(8)	1.031(7)	1.023(9)
	IAM	0.893(11)	0.903(14)	0.909(11)	0.909(11)	0.901(12)
N2-H22 …O1	Neutron	1.045(5)	1.041(5)	-	1.053(5)	1.043(7)
	HAR	1.039(8)	1.046(9)	1.024(9)	1.028(8)	1.030(9)
	HAR-ELMO	1.015(9)	1.029(9)	1.003(10)	1.009(9)	1.007(11)
	IAM	0.923(13)	0.914(12)	0.923(14)	0.913(13)	0.916(14)
N2-H32 …O2	Neutron	1.044(5)	1.042(4)	-	1.041(5)	1.049(7)
	HAR	1.039(7)	1.039(9)	1.045(8)	1.039(7)	1.029(9)
	HAR-ELMO	1.037(8)	1.031(9)	1.042(9)	1.031(8)	1.021(10)
	IAM	0.884(10)	0.895(12)	0.894(11)	0.883(10)	0.881(11)

Table S13: continued.

.D-H..A	Model	12 K	50 K	100 K	150 K	295 K
				H…A Distance in Å		
N1-H11 …O1	Neutron	1.869(5)	1.865(4)	-	1.868(5)	1.892(7)
	HAR	1.894(7)	1.887(8)	1.892(6)	1.891(6)	1.907(7)
	HAR-ELMO	1.871(7)	1.866(9)	1.868(6)	1.865(6)	1.873(7)
	IAM	2.037(12)	2.010(13)	2.013(11)	2.037(11)	2.076(11)
N2-H12 ...O2	Neutron	1.712(5)	1.713(5)	-	1.721(5)	1.737(8)
	HAR	1.717(7)	1.706(9)	1.727(7)	1.724(7)	1.750(8)
	HAR-ELMO	1.734(7)	1.719(9)	1.744(7)	1.738(7)	1.761(9)
	IAM	1.855(11)	1.845(14)	1.844(11)	1.847(11)	1.871(12)
N2-H22 …O1	Neutron	1.686(5)	1.694(5)	-	1.682(5)	1.685(8)
	HAR	1.696(9)	1.692(9)	1.715(9)	1.709(9)	1.714(10)
	HAR-ELMO	1.719(9)	1.707(9)	1.733(10)	1.727(9)	1.736(12)
	IAM	1.810(13)	1.825(12)	1.814(15)	1.824(13)	1.826(14)
N2-H32 …O2	Neutron	1.728(5)	1.735(5)	-	1.740(5)	1.744(8)
	HAR	1.738(7)	1.739(10)	1.739(8)	1.742(7)	1.766(9)
	HAR-ELMO	1.739(9)	1.747(11)	1.741(9)	1.748(9)	1.769(10)
	IAM	1.885(11)	1.882(13)	1.881(11)	1.891(11)	1.906(11)
				D…A Distance in Å		
N1-H11 …O1	Neutron	2.876(2)	2.870(2)	-	2.879(2)	2.904(4)
	HAR	2.8745(4)	2.8752(8)	2.8773(8)	2.8813(9)	2.8969(9)
	HAR-ELMO	2.8745(5)	2.8746(8)	2.8776(9)	2.8815(9)	2.8972(9)
	IAM	2.8761(8)	2.8759(11)	2.8778(10)	2.8827(11)	2.8989(12)
N2-H12 ...O2	Neutron	2.747(3)	2.751(3)	-	2.754(3)	2.772(4)
	HAR	2.7489(5)	2.7488(8)	2.7519(8)	2.7551(8)	2.7696(9)
	HAR-ELMO	2.7495(5)	2.7493(9)	2.7526(8)	2.7558(9)	2.7705(10)
	IAM	2.7465(8)	2.7457(12)	2.7498(10)	2.7529(11)	2.7671(12)
N2-H22 …O1	Neutron	2.716(2)	2.721(2)	-	2.718(3)	2.713(4)
	HAR	2.7161(5)	2.7175(7)	2.7168(8)	2.7182(8)	2.7219(9)
	HAR-ELMO	2.7163(5)	2.7179(7)	2.7168(9)	2.7184(9)	2.7233(10)
	IAM	2.7169(9)	2.7180(9)	2.7178(11)	2.7201(11)	2.7248(13)
N2-H32 …O2	Neutron	2.723(2)	2.726(2)	-	2.728(3)	2.739(4)
	HAR	2.7253(5)	2.7250(8)	2.7244(8)	2.7277(8)	2.7360(9)
	HAR-ELMO	2.7256(5)	2.7255(8)	2.7247(8)	2.7280(9)	2.7368(9)
	IAM	2.7239(8)	2.7242(10)	2.7230(10)	2.7265(11)	2.7358(12)

Table S13: continued.

.D-H..A	Model	12 K	50 K	100 K	150 K	295 K
		D-H…A Angle in °				
N1-H11 …O1	Neutron	167.8(4)	168.3(3)	-	168.3(4)	169.3(5)
	HAR	167.2(6)	166.2(8)	167.1(5)	166.7(5)	166.3(6)
	HAR-ELMO	167.4(6)	166.4(9)	167.5(5)	166.8(6)	166.0(7)
	IAM	167.4(12)	164.3(13)	167.4(11)	168.0(12)	168.8(12)
N2-H12 ...O2	Neutron	170.8(4)	171.5(4)	-	171.4(4)	171.3(7)
	HAR	167.8(8)	167.9(8)	168.0(7)	168.1(6)	167.8(7)
	HAR-ELMO	168.5(8)	169.1(8)	168.7(7)	168.5(7)	168.3(8)
	IAM	175.6(10)	175.1(11)	174.4(11)	174.3(10)	172.7(11)
N2-H22 …O1	Neutron	167.6(4)	167.7(4)	-	167.1(4)	167.4(6)
	HAR	166.2(7)	165.6(9)	165.0(7)	166.0(7)	165.1(8)
	HAR-ELMO	166.7(7)	166.5(9)	165.8(8)	166.5(7)	166.0(9)
	IAM	166.7(11)	164.9(12)	165.7(12)	166.8(12)	166.4(12)
N2-H32 …O2	Neutron	157.6(4)	157.1(4)	-	157.1(5)	156.8(7)
	HAR	157.1(7)	156.8(10)	155.5(7)	156.7(6)	155.5(8)
	HAR-ELMO	157.4(8)	156.9(11)	155.7(8)	157.3(8)	156.7(9)
	IAM	157.8(10)	156.2(14)	156.2(10)	157.2(10)	156.4(11)

Table S14: Intermolecular hydrogen bonds for *L*-alanine. For atomic labels and symmetry codes, see the CIFs deposited with the Cambridge Database and with this journal as Supporting Information.

D-H..A	**Model**	**12 K**	**100 K**	**150 K**
			D-H Distance in Å	
N1-H1…O1	Neutron	1.0352(17)	-	1.035(2)
	HAR	1.024(7)	1.052(4)	1.042(10)
	HAR-ELMO	0.973(9)	1.035(5)	1.023(11)
	IAM	0.935(11)	0.917(7)	0.914(13)
N1-H2...O2	Neutron	1.0441(19)	-	1.040(2)
	HAR	1.018(7)	1.031(4)	1.021(8)
	HAR-ELMO	1.000(8)	1.017(5)	1.001(9)
	IAM	0.917(10)	0.914(6)	0.914(10)
N1-H3…O1	Neutron	1.0534(13)	-	1.0524(19)
	HAR	1.042(7)	1.024(4)	1.042(9)
	HAR-ELMO	1.027(8)	1.017(5)	1.037(9)
	IAM	1.040(12)	-	0.984(11)
N1-H3…O2	Neutron	1.0534(13)	-	1.0524(19)
	HAR	1.042(7)	1.024(4)	1.042(9)
	HAR-ELMO	1.027(8)	1.017(5)	1.037(9)
	IAM	1.040(12)	0.952(6)	0.984(11)

Table S14: continued.

D-H..A	Model	12 K	100 K	150 K
			H…A Distance in Å	
N1-H1…O1	Neutron	1.8355(18)	-	1.841(2)
	HAR	1.855(7)	1.836(4)	1.845(10)
	HAR-ELMO	1.900(9)	1.847(5)	1.858(11)
	IAM	1.918(11)	1.941(7)	1.945(13)
N1-H2...O2	Neutron	1.802(2)	-	1.809(3)
	HAR	1.831(6)	1.820(4)	1.833(9)
	HAR-ELMO	1.847(7)	1.832(5)	1.850(10)
	IAM	1.937(10)	1.937(6)	1.940(10)
N1-H3…O1	Neutron	2.5496(15)	-	2.541(2)
	HAR	2.573(7)	2.578(4)	2.580(9)
	HAR-ELMO	2.577(8)	2.575(5)	2.579(9)
	IAM	2.558(12)	-	2.596(12)
N1-H3…O2	Neutron	1.7495(15)	-	1.756(2)
	HAR	1.757(7)	1.779(4)	1.759(9)
	HAR-ELMO	1.773(8)	1.787(4)	1.766(9)
	IAM	1.764(12)	1.854(6)	1.822(11)
			D…A Distance in Å	
N1-H1…O1	Neutron	2.8354(9)	-	2.8402(11)
	HAR	2.8348(6)	2.8391(2)	2.8394(4)
	HAR-ELMO	2.8353(6)	2.8398(2)	2.8397(5)
	IAM	2.8321(8)	2.8372(4)	2.8373(6)
N1-H2...O2	Neutron	2.8153(9)	-	2.8199(12)
	HAR	2.8149(6)	2.8194(2)	2.8205(4)
	HAR-ELMO	2.8151(6)	2.8199(3)	2.8208(5)
	IAM	2.8145(8)	2.8185(4)	2.8188(6)
N1-H3…O1	Neutron	3.3371(9)	-	3.3326(11)
	HAR	3.3364(7)	3.3299(2)	3.3314(4)
	HAR-ELMO	3.3368(7)	3.3301(3)	3.3315(4)
	IAM	3.3358(9)	-	3.3326(6)
N1-H3…O2	Neutron	2.7922(9)	-	2.7971(10)
	HAR	2.7918(6)	2.7955(2)	2.7964(4)
	HAR-ELMO	2.7919(6)	2.7955(2)	2.7965(4)
	IAM	2.7910(8)	2.7956(4)	2.7965(6)

Table S14: continued.

D-H..A	Model	12 K	100 K	150 K
		D-H…A Angle in °		
N1-H1…O1	Neutron	161.25(15)	-	161.3(2)
	HAR	159.1(7)	158.2(4)	158.3(9)
	HAR-ELMO	160.3(8)	159.5(4)	159.7(10)
	IAM	165.1(11)	165.4(6)	164.6(11)
N1-H2...O2	Neutron	162.59(16)	-	162.8(2)
	HAR	161.4(6)	162.2(3)	161.8(7)
	HAR-ELMO	162.1(7)	162.9(4)	162.6(8)
	IAM	159.6(9)	161.4(6)	160.7(9)
N1-H3…O1	Neutron	131.02(13)	-	131.47(17)
	HAR	129.7(5)	130.0(3)	128.6(6)
	HAR-ELMO	130.5(5)	130.8(3)	129.2(6)
	IAM	131.1(8)	-	131.7(8)
N1-H3…O2	Neutron	169.62(15)	-	169.26(19)
	HAR	171.5(6)	171.7(3)	172.8(7)
	HAR-ELMO	170.9(7)	170.9(4)	172.4(8)
	IAM	168.6(10)	169.5(6)	170.2(10)

Table S15: Symmetry operations for intermolecular hydrogen bonds of Gly-*L*-Ala and *L*-Ala.

Compound	D-H..A	Symmetry operation
Gly-*L*-Ala	N1-H11…O1	1/2-x,2-y,-1/2+z
	N2-H12...O2	3/2-x,2-y,-1/2+z
	N2-H22…O1	1/2+x,3/2-y,1-z
	N2-H32…O2	1-x,1/2+y,3/2-z
L-Ala	N1-H1…O1	3/2-x,-y,-1/2+z
	N1-H2...O2	1/2+x,1/2-y,1-z
	N1-H3…O1	x,y,-1+z
	N1-H3…O2	x,y,-1+z

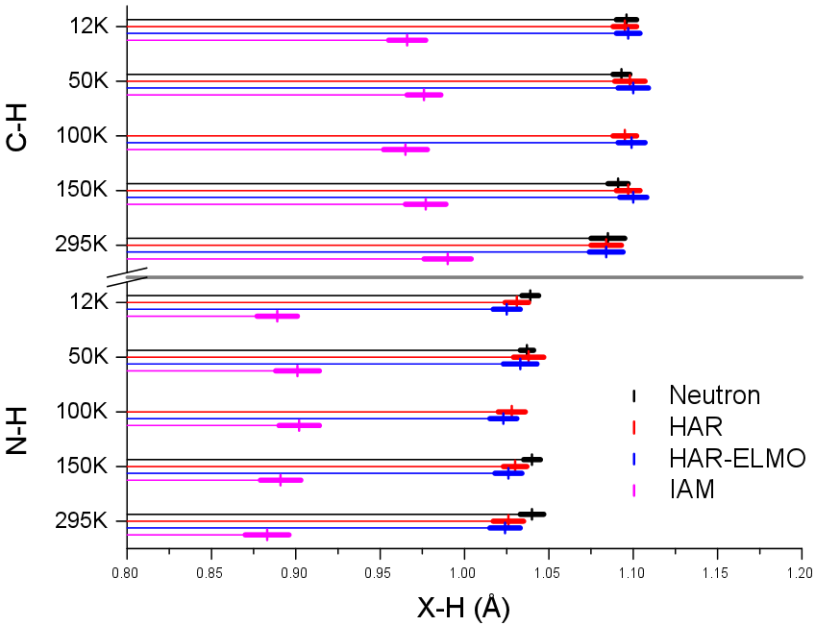

Figure S3: Graphical representation of Table S12 for X-H bond lengths in Gly-*L*-Ala.

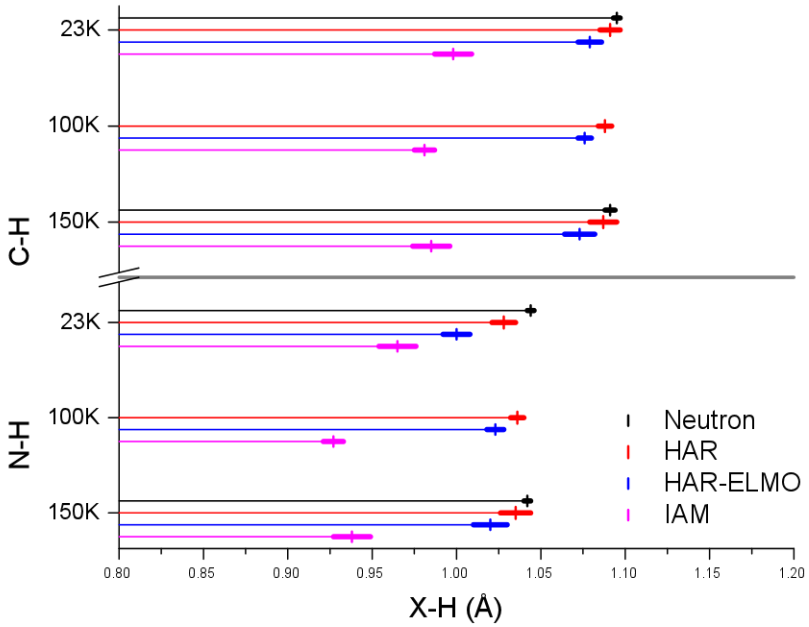

Figure S4: Graphical representation of Table S12 for X-H bond lengths in *L*-Ala.

Comparison of hydrogen ADPs

Table S16: Statistical results for hydrogen atom ADPs for Gly-*L*-Ala, units of differences are Å^2.

Method (A/B)	**12 K**	**50 K**	**100 K**	**150 K**	**295 K**
			wRMSD		
HAR/neutron	1.363	1.342	-	2.262	1.629
HAR-ELMO/neutron	1.466	1.263	-	2.144	1.658
HAR-ELMO/HAR	0.779	0.699	0.812	0.870	0.713
			$\mathbf{< \lvert U^{ij}_A - U^{ij}_B \rvert >}$		
HAR/neutron	0.0053	0.0048	-	0.0078	0.0096
HAR-ELMO/neutron	0.0058	0.0055	-	0.0079	0.0109
HAR-ELMO/HAR	0.0034	0.0033	0.0034	0.0036	0.0047
			$\mathbf{< \lvert U^{ii}_A - U^{ii}_B \rvert >}$		
HAR/neutron	0.0067	0.0053	-	0.0051	0.0106
HAR-ELMO/neutron	0.0071	0.0064	-	0.0063	0.0121
HAR-ELMO/HAR	0.0040	0.0043	0.0045	0.0049	0.0059
			$\mathbf{< U^{ii}_A / U^{ii}_B >}$		
HAR/neutron	1.060	1.021	-	1.056	1.116
HAR-ELMO/neutron	1.147	1.104	-	1.102	1.147
HAR-ELMO/HAR	1.108	1.119	1.063	1.053	1.030

Table S17: Statistical results for hydrogen atom ADPs for *L*-Ala, units of differences are Å^2.

Method (A/B)	**23 K**	**100 K**	**150 K**
		wRMSD	
HAR/neutron	1.958	-	1.283
HAR-ELMO/neutron	2.311	-	1.586
HAR-ELMO/HAR	0.991	1.571	0.656
		$< \lvert U^{ij}_A - U^{ij}_B \rvert >$	
HAR/neutron	0.0063	-	0.0047
HAR-ELMO/neutron	0.0082	-	0.0063
HAR-ELMO/HAR	0.0043	0.0035	0.0030
		$< \lvert U^{ii}_A - U^{ii}_B \rvert >$	
HAR/neutron	0.0069	-	0.0056
HAR-ELMO/neutron	0.0100	-	0.0077
HAR-ELMO/HAR	0.0049	0.0037	0.0032
		$< U^{ii}_A / U^{ii}_B >$	
HAR/neutron	1.328	-	1.042
HAR-ELMO/neutron	1.441	-	1.110
HAR-ELMO/HAR	1.044	1.070	1.063

Comparison of non-hydrogen ADPs

MADs (mean absolute differences) of non-hydrogen ADPs between independent X-ray and neutron measurements are often used as a quality control for the data and the refinements methods. For very high-quality data, MADs for non-hydrogen ADPs are expected to be in the range 0.0002 to 0.0005 Å^2.[S11-S13] For the Gly-*L*-Ala data used here it is known that the results for the non-H ADPs are inferior (MADs in the range 0.0010 to 0.0014 Å^2).[S7] It is believed that this is due to missing oblique-incidence correction.

Table S18: Statistical results for non-hydrogen atom ADPs of Gly-*L*-Ala, units of differences are Å^2.

Method (A/B)	**12 K**	**50 K**	**100 K**	**150 K**	**295 K**
			wRMSD		
IAM/neutron	2.273	2.212	-	2.068	1.468
HAR/neutron	2.578	2.669	-	2.251	1.468
HAR-ELMO/neutron	2.715	2.755	-	2.357	1.526
HAR-ELMO/HAR	1.559	1.374	1.570	1.583	1.536
			$\langle \lvert U^{ij}_A - U^{ij}_B \rvert \rangle$		
IAM/neutron	0.00108	0.00107	-	0.00122	0.00147
HAR/neutron	0.00110	0.00122	-	0.00118	0.00133
HAR-ELMO/neutron	0.00119	0.00129	-	0.00125	0.00136
HAR-ELMO/HAR	0.00020	0.00022	0.00019	0.00021	0.00029
			$\langle \lvert U^{ii}_A - U^{ii}_B \rvert \rangle$		
IAM/neutron	0.00140	0.00144	-	0.00149	0.00177
HAR/neutron	0.00167	0.00178	-	0.00168	0.00149
HAR-ELMO/neutron	0.00177	0.00189	-	0.00176	0.00161
HAR-ELMO/HAR	0.00019	0.00021	0.00018	0.00019	0.00028
			$\langle U^{ii}_A / U^{ii}_B \rangle$		
IAM/neutron	0.863	0.889	-	0.937	1.011
HAR/neutron	0.749	0.784	-	0.891	0.966
HAR-ELMO/neutron	0.735	0.773	-	0.885	0.958
HAR-ELMO/HAR	0.977	0.984	0.990	0.993	0.992

Table S19: Statistical results for non-hydrogen atom ADPs for *L*-Ala units of differences are Å^2.

Method (A/B)	**23 K**	**100 K**	**150 K**
		wRMSD	
IAM/neutron	3.667	-	51.759
HAR/neutron	2.832	-	8.419
HAR-ELMO/neutron	2.936	-	8.385
HAR-ELMO/HAR	1.018	2.278	1.012
		$\mathbf{< \lvert U^{ij}_A - U^{ij}_B \rvert >}$	
IAM/neutron	0.00032	-	0.00156
HAR/neutron	0.00034	-	0.00162
HAR-ELMO/neutron	0.00036	-	0.00163
HAR-ELMO/HAR	0.00008	0.00012	0.00010
		$\mathbf{< \lvert U^{ii}_A - U^{ii}_B \rvert >}$	
IAM/neutron	0.00043	-	0.00272
HAR/neutron	0.00058	-	0.00295
HAR-ELMO/neutron	0.00060	-	0.00297
HAR-ELMO/HAR	0.00009	0.00013	0.00011
		$\mathbf{< U^{ii}_A / U^{ii}_B >}$	
IAM/neutron	0.967	-	0.821
HAR/neutron	0.913	-	0.805
HAR-ELMO/neutron	0.909	-	0.804
HAR-ELMO/HAR	0.995	0.999	0.998

	Neutron	HAR	HAR-ELMO
Gly-*L*-Ala 12 K[1]	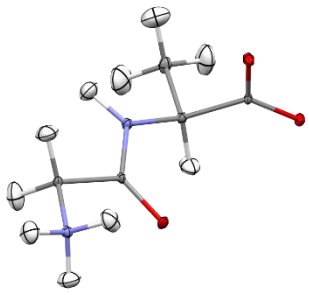	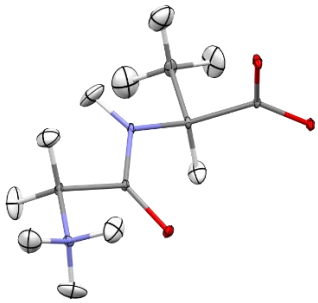	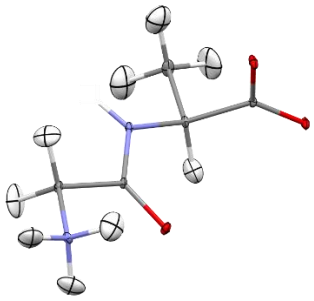
Gly-*L*-Ala 50 K	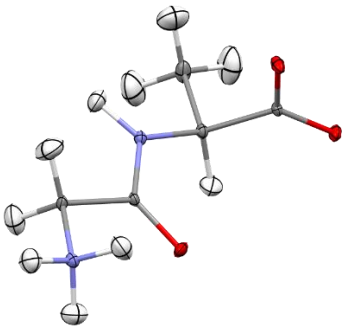	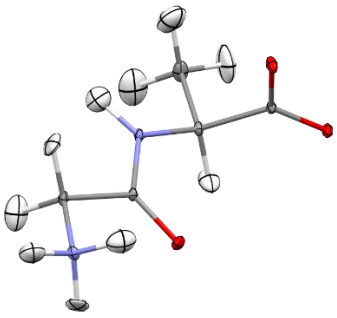	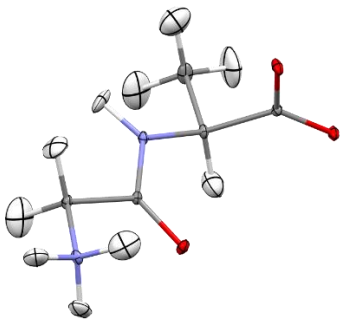
Gly-*L*-Ala 100 K	-	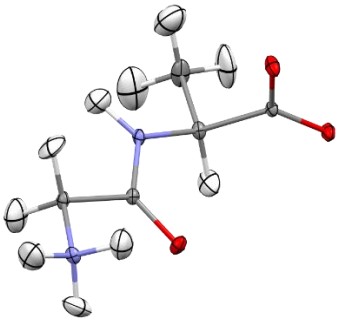	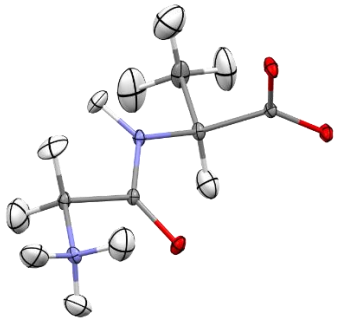
Gly-*L*-Ala 150 K	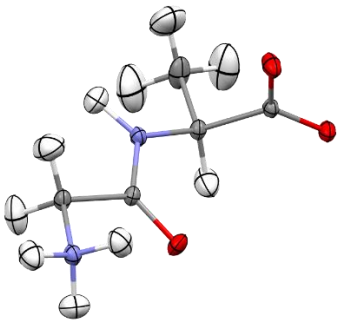	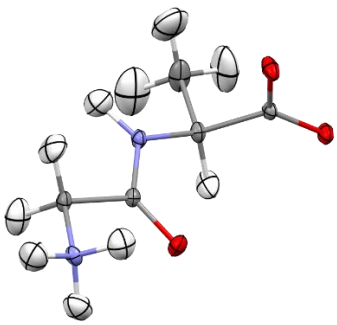	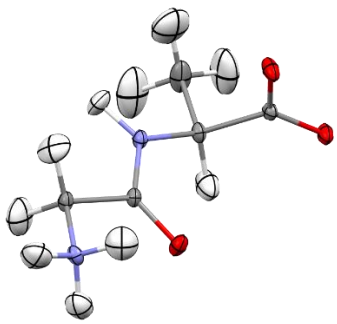
Gly-*L*-Ala 295 K	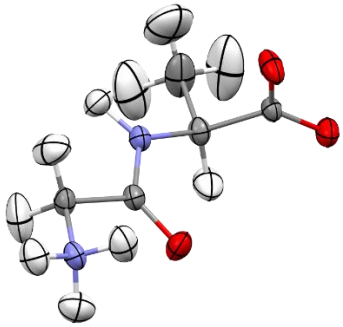	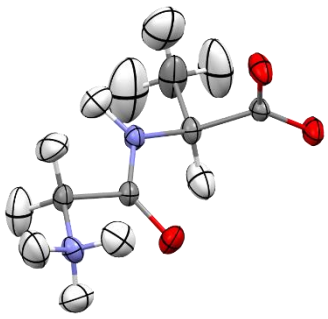	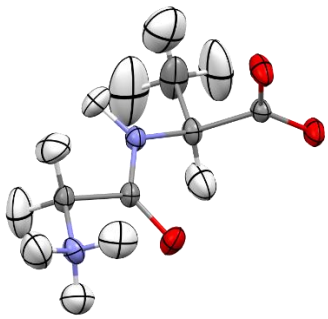

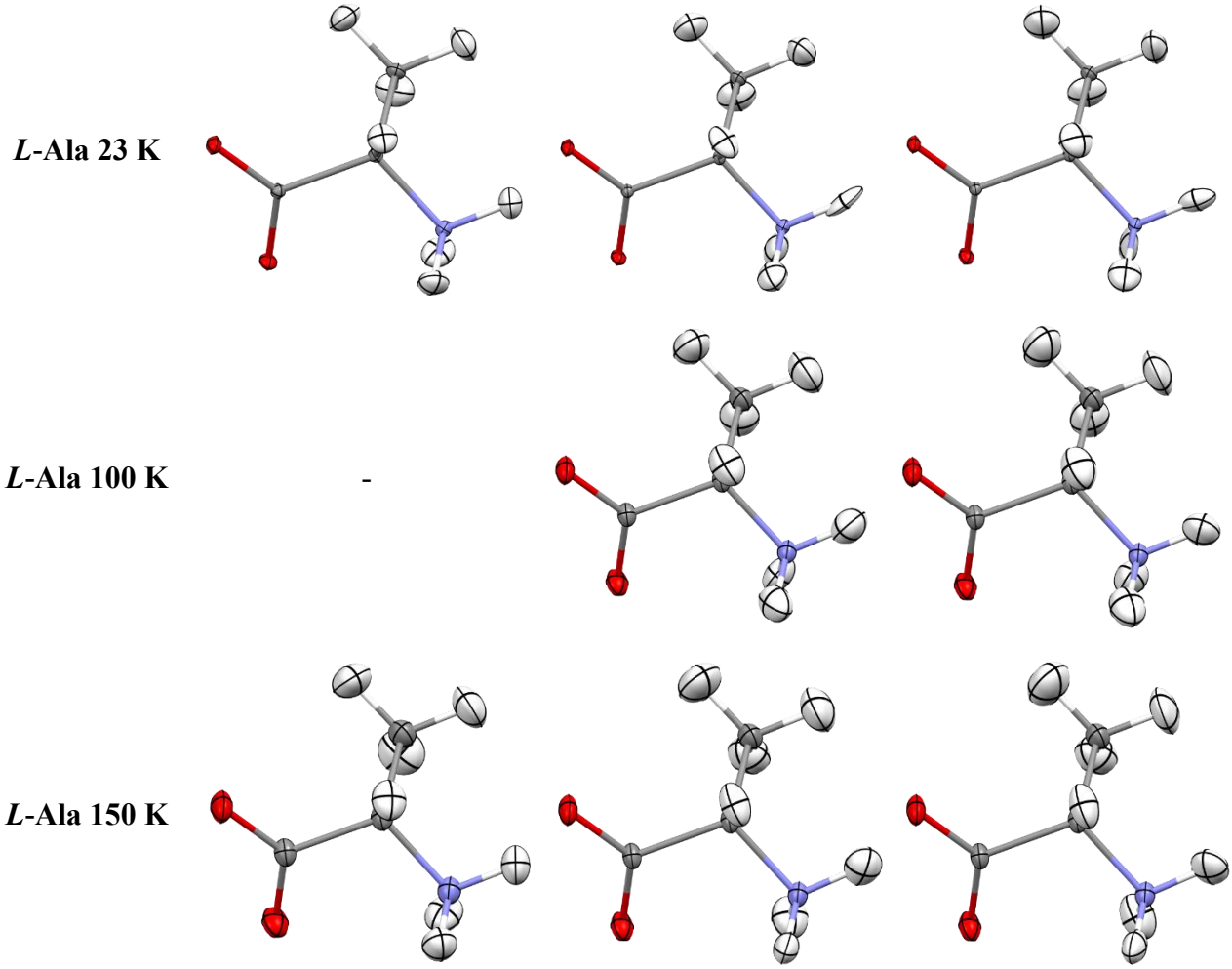

Figure S5: Molecular representations of the refined structures with 50% probability ADPs for Gly-*L*-Ala and *L*-Ala at all temperatures.

[1]For Gly-*L*-Ala 12 K, H(11) is non-positive definite (NPD), but this is only due to the small ADPs. Except for U_{33}, the values are still matching the Uijs resulting from HAR, which are not NPD, within one standard deviation. The H(11) Uijs (U_{11} U_{22} U_{33} U_{23} U_{13} U_{12}, respectively) resulting from the HAR and HAR-ELMO refinements are:

HAR: 0.019(4) 0.021(5) 0.024(3) 0.006(4) -0.014(3) 0.008(4) Å^2

HAR-ELMO: 0.011(4) 0.020(5) 0.013(3) 0.000(4) -0.017(3) 0.004(4) Å^2

Comparison of Fractal Dimension plots

Gly-*L*-Ala – Fractal Dimension plots according to Meindl & Henn[S14]

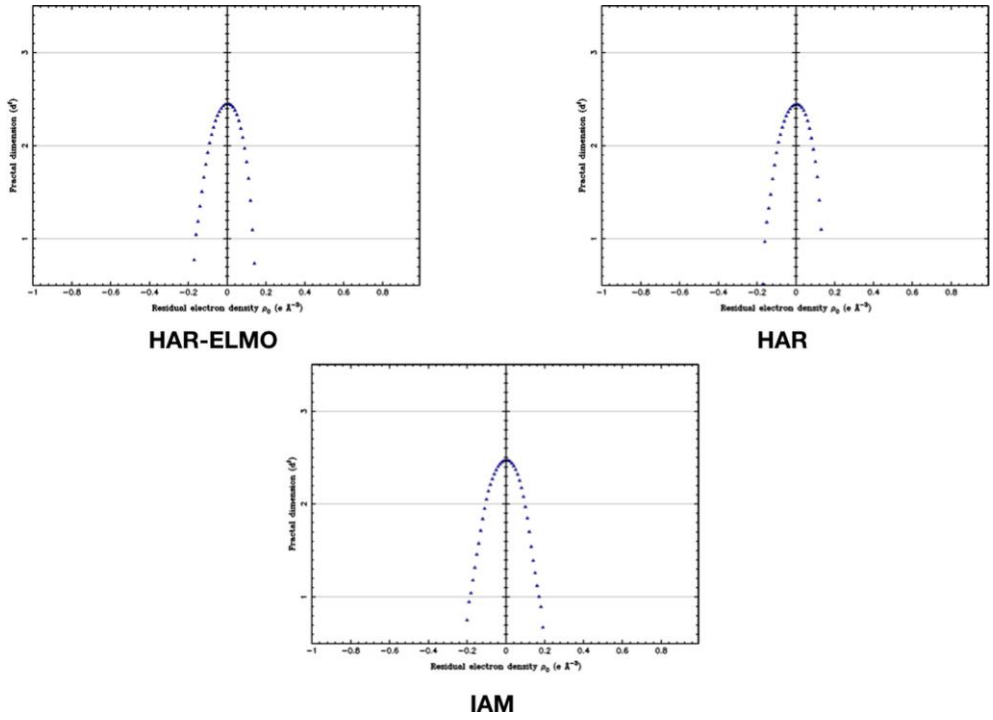

Figure S6: Fractal dimension plots for the HAR-ELMO, HAR and IAM refinements of Gly-*L*-Ala at 12 K.

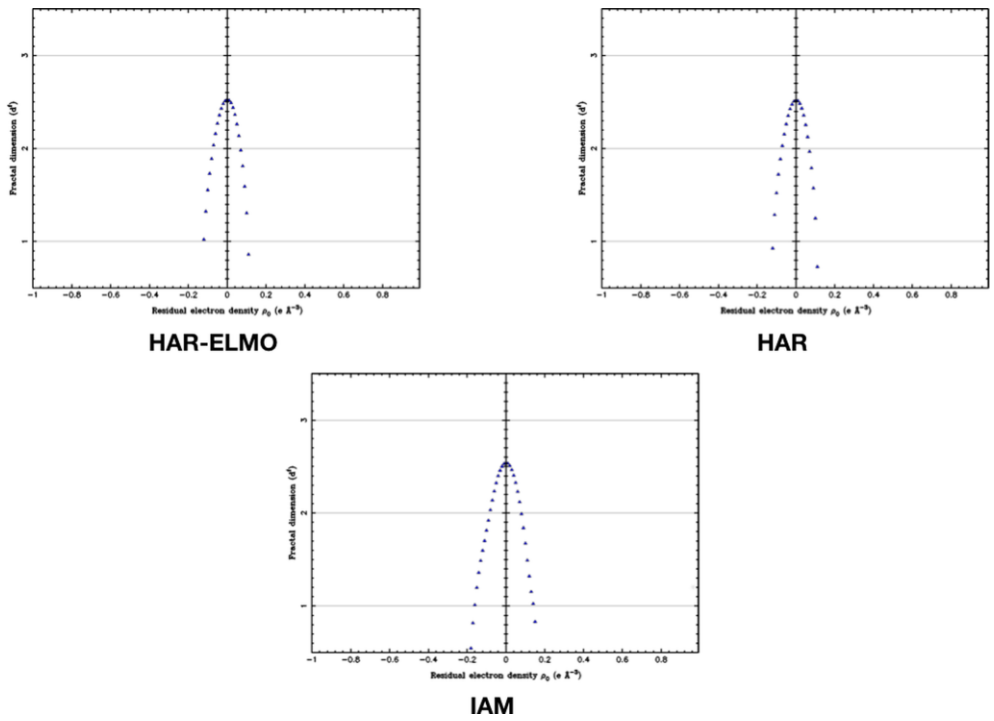

Figure S7: Fractal dimension plots for the HAR-ELMO, HAR and IAM refinements of Gly-*L*-Ala at 50 K.

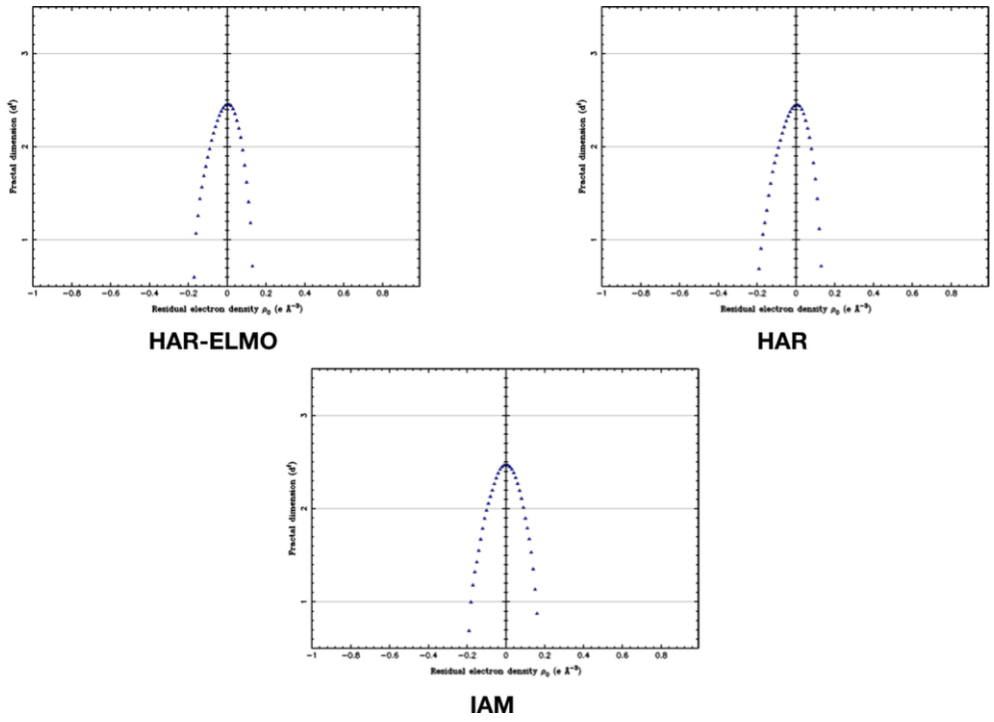

Figure S8: Fractal dimension plots for the HAR-ELMO, HAR and IAM refinements of Gly-*L*-Ala at 100 K.

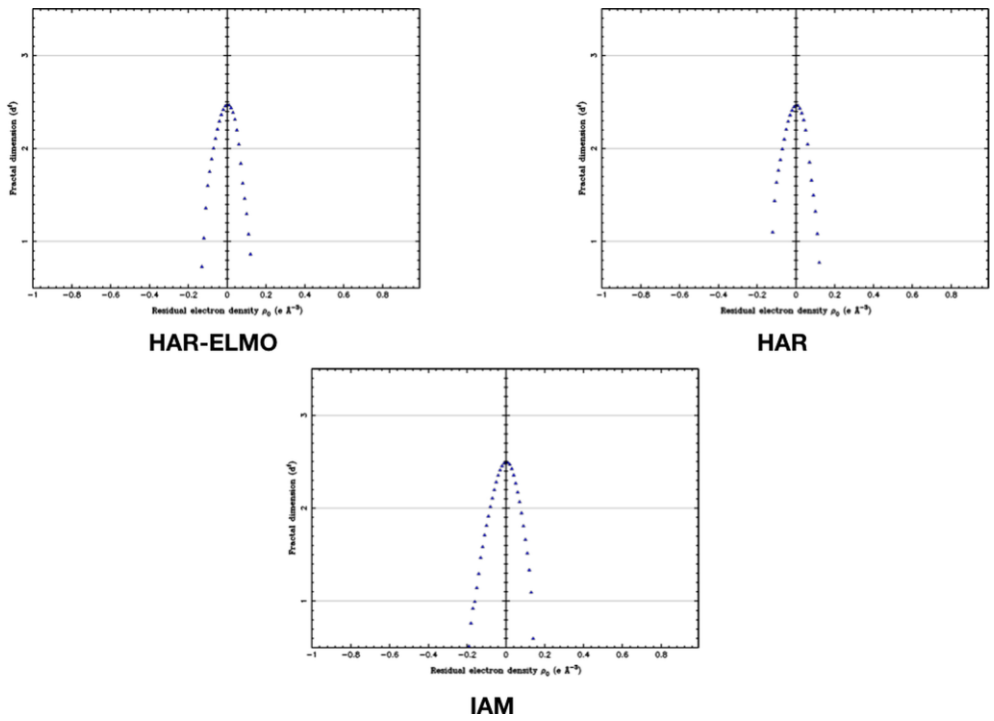

Figure S9: Fractal dimension plots for the HAR-ELMO, HAR and IAM refinements of Gly-*L*-Ala at 150 K.

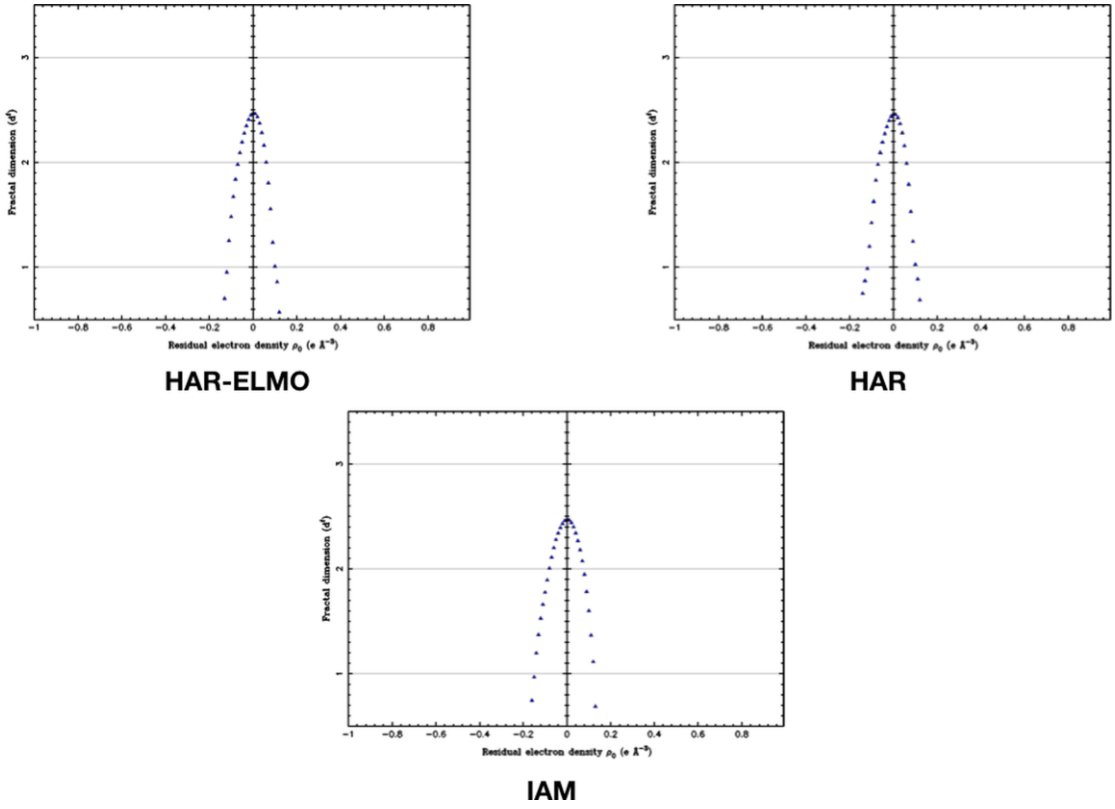

Figure S10: Fractal dimension plots for the HAR-ELMO, HAR and IAM refinements of Gly-*L*-Ala at 295 K.

L-Alanine – Fractal Dimension plots according to Meindl & Henn[S14]

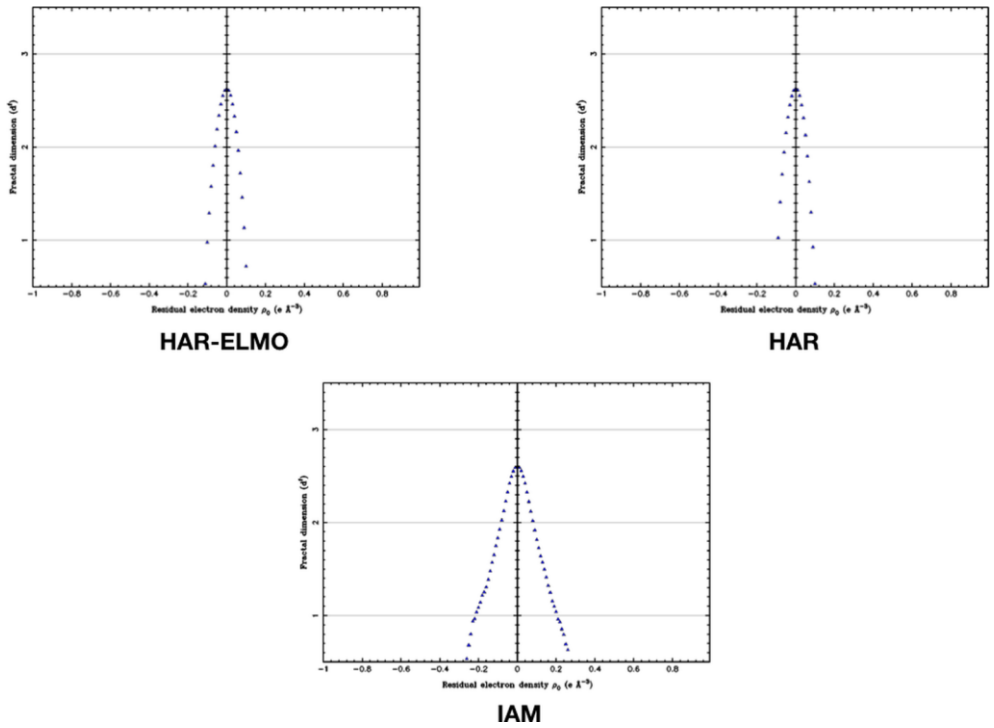

Figure S11: Fractal dimension plots for the HAR-ELMO, HAR and IAM refinements of *L*-Ala at 23 K.

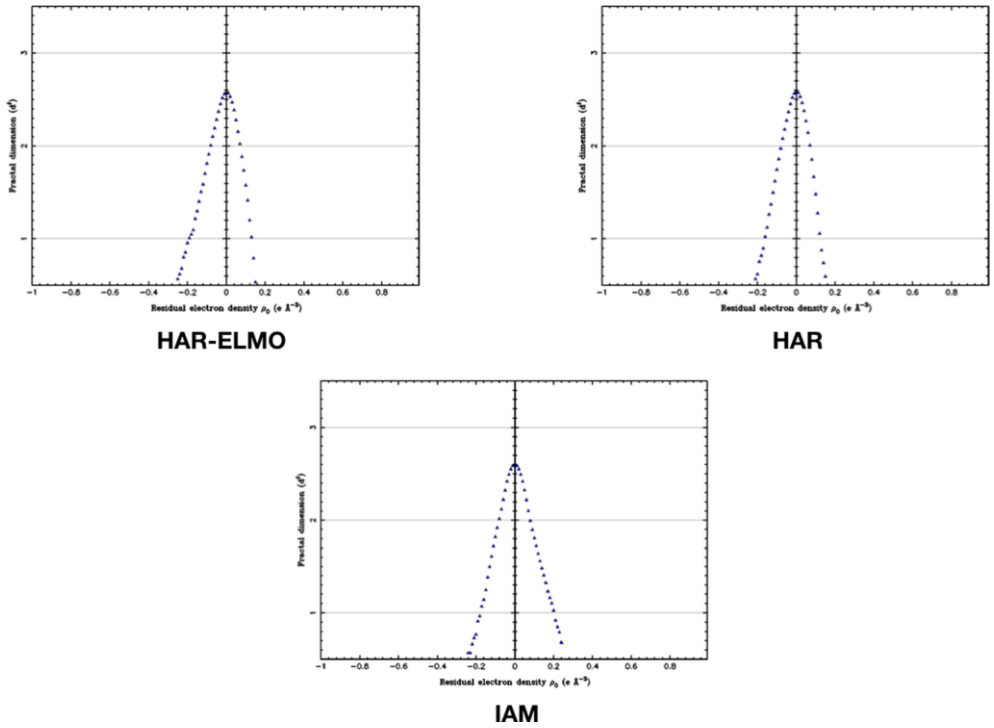

Figure S12: Fractal dimension plots for the HAR-ELMO, HAR and IAM refinements of *L*-Ala at 100 K.

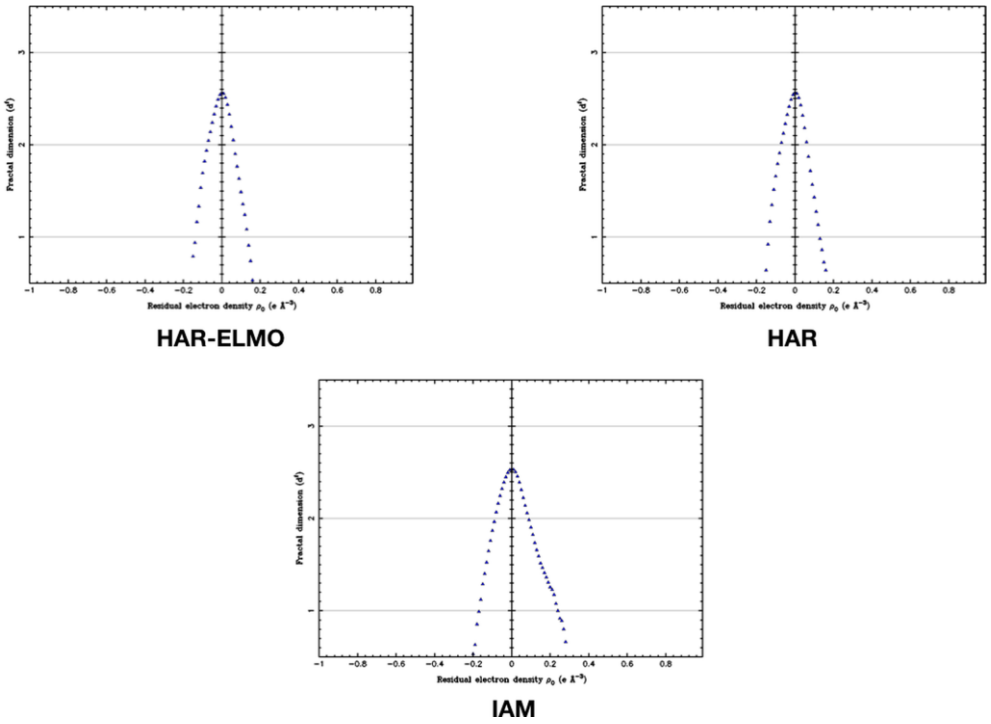

Figure S13: Fractal dimension plots for the HAR-ELMO, HAR and IAM refinements of *L*-Ala at 150 K.

Comparison of Normal Probability plots

Gly-*L*-Ala – Normal Probability plots

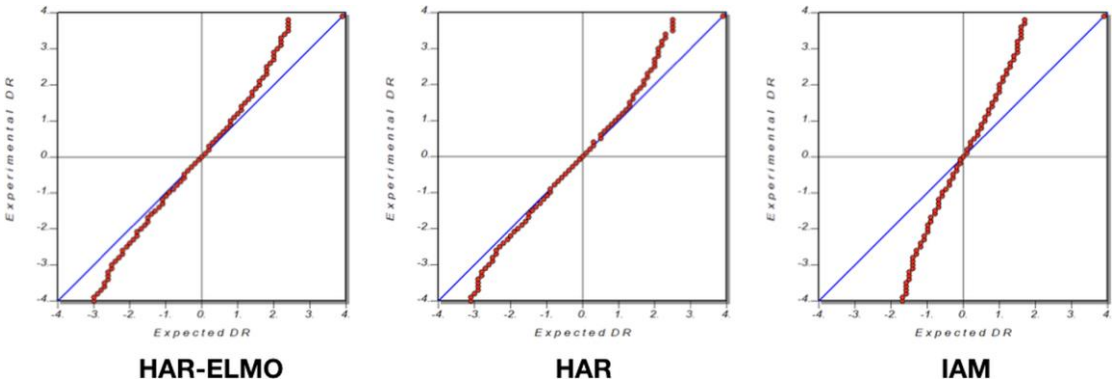

Figure S14: Normal probability plots for the HAR-ELMO, HAR and IAM refinements of Gly-*L*-Ala at 12 K.

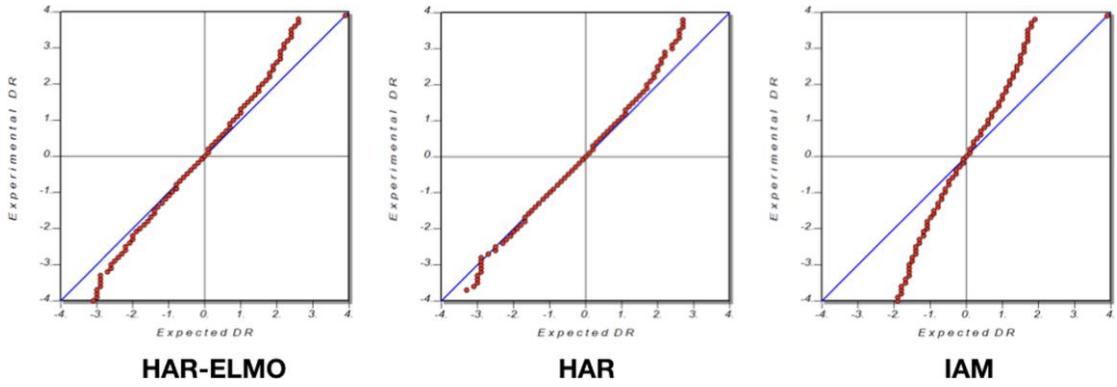

Figure S15: Normal probability plots for the HAR-ELMO, HAR and IAM refinements of Gly-*L*-Ala at 50 K.

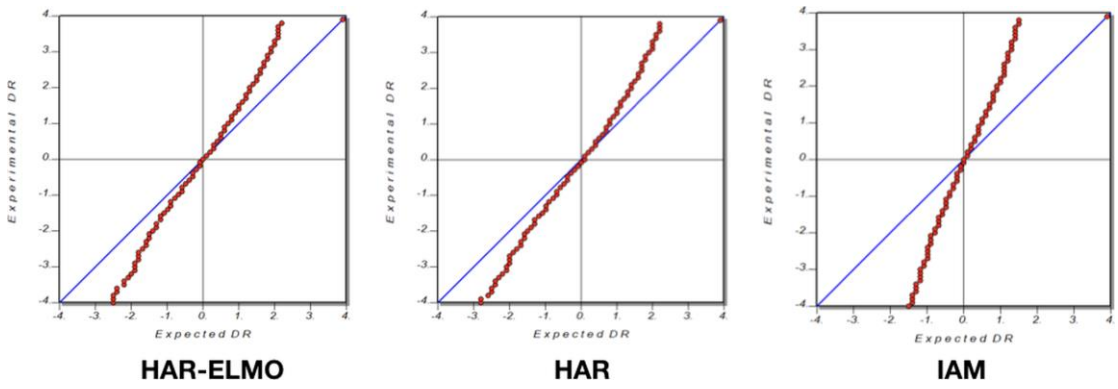

Figure S16: Normal probability plots for the HAR-ELMO, HAR and IAM refinements of Gly-*L*-Ala at 100 K.

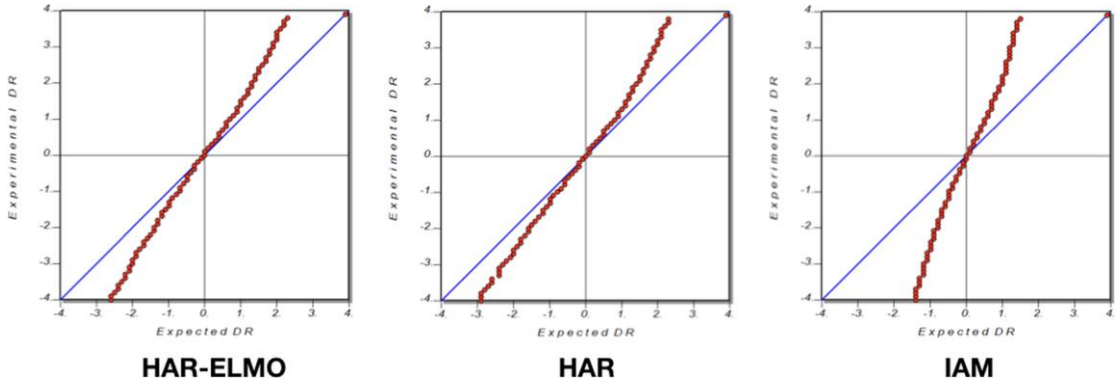

Figure S17: Normal probability plots for the HAR-ELMO, HAR and IAM refinements of Gly-*L*-Ala at 150 K.

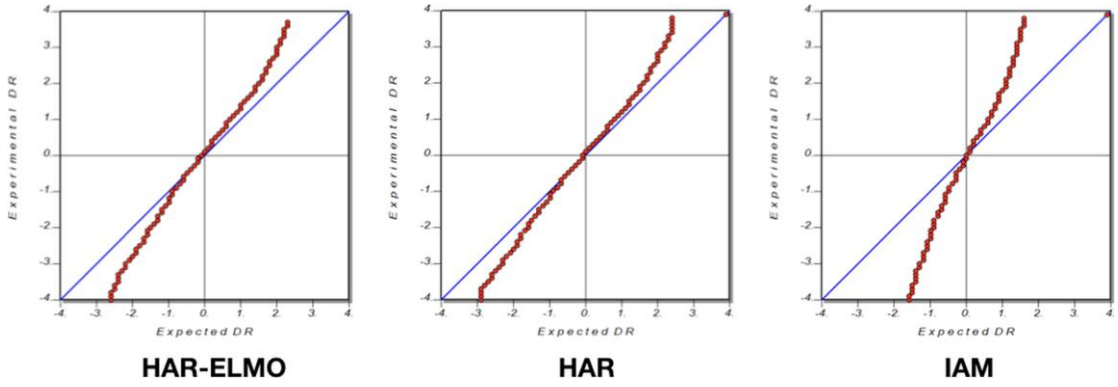

Figure S18: Normal probability plots for the HAR-ELMO, HAR and IAM refinements of Gly-*L*-Ala at 295 K.

L-Alanine – Normal Probability plots

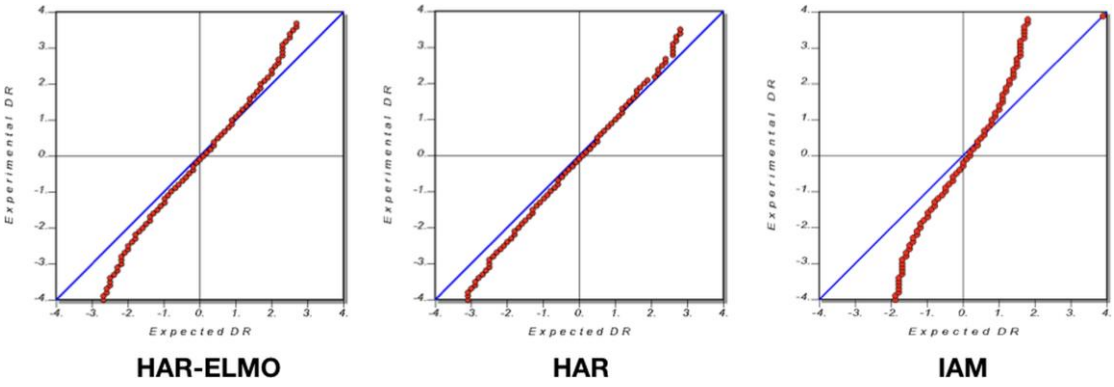

Figure S19: Normal probability plots for the HAR-ELMO, HAR and IAM refinements of *L*-Ala at 23 K.

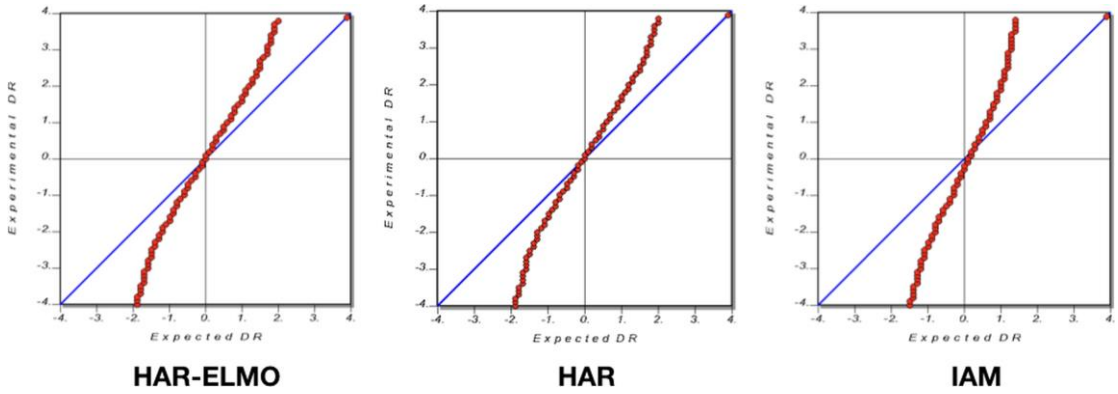

Figure S20: Normal probability plots for the HAR-ELMO, HAR and IAM refinements of *L*-Ala at 100 K.

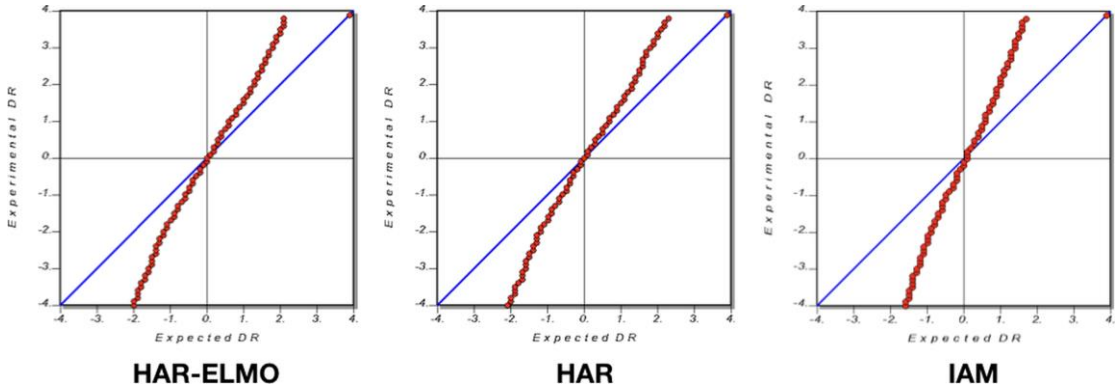

Figure S21: Normal probability plots for the HAR-ELMO, HAR and IAM refinements of *L*-Ala at 150 K.

Comparison of Averaged-K-curve plots

Gly-*L*-Ala – Averaged K-curve plots

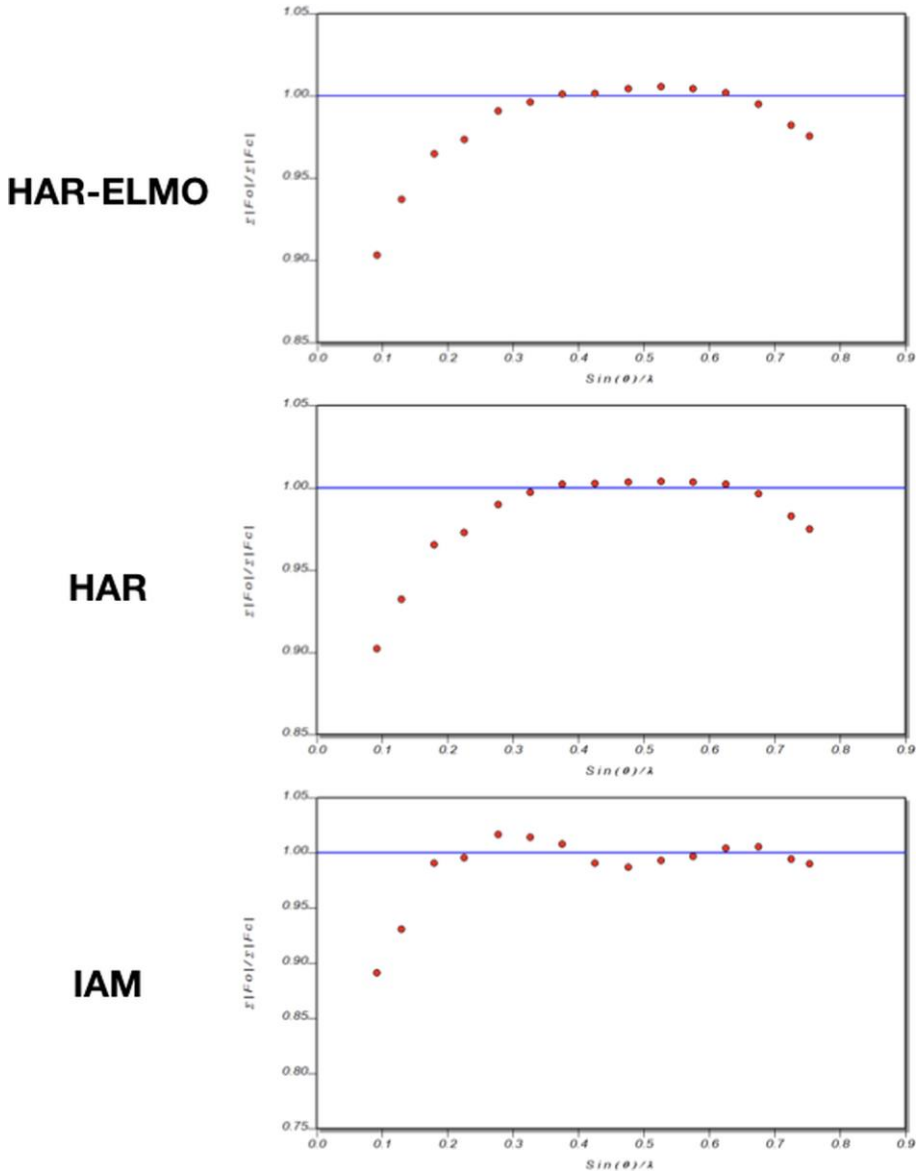

Figure S22: Averaged K-curve plots for the HAR-ELMO, HAR and IAM refinements of Gly-*L*-Ala at 12 K.

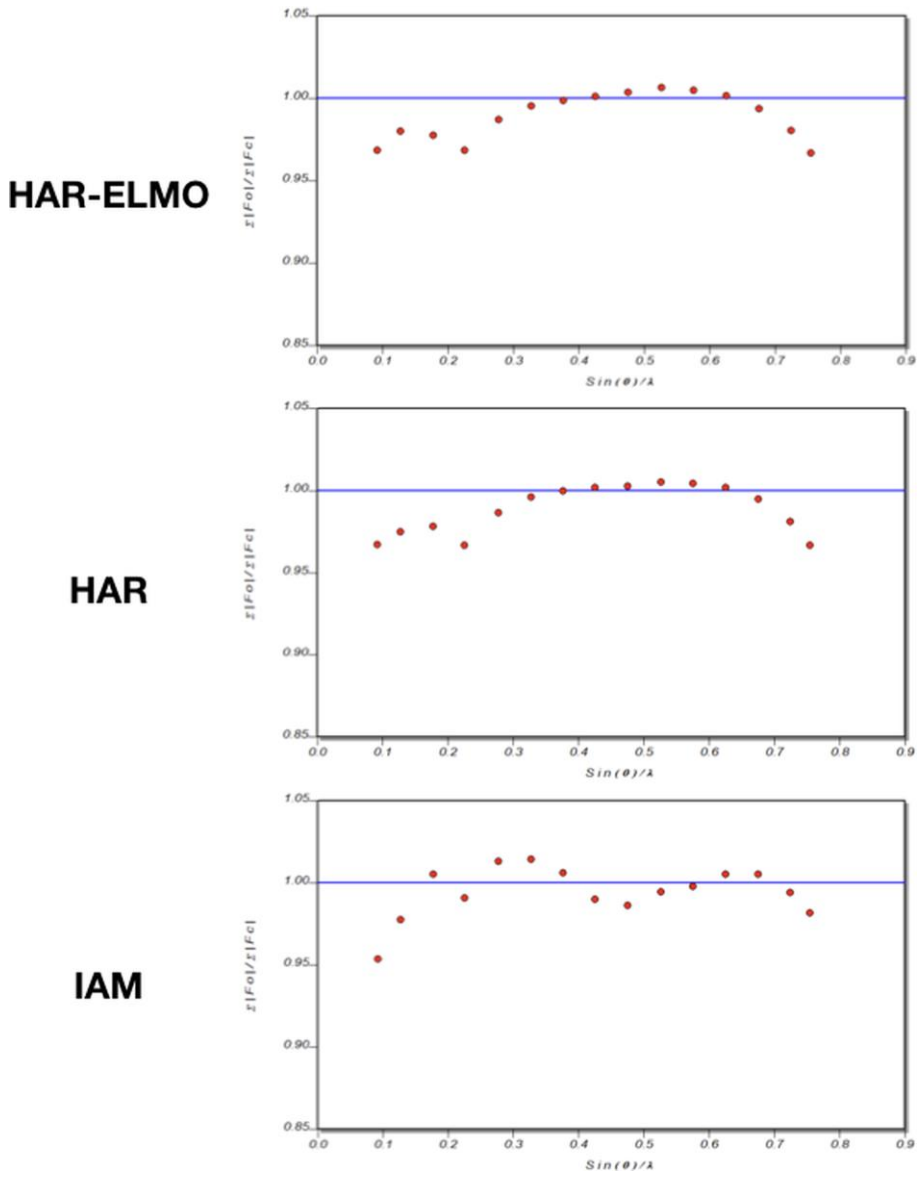

Figure S23: Averaged K-curve plots for the HAR-ELMO, HAR and IAM refinements of Gly-*L*-Ala at 50 K.

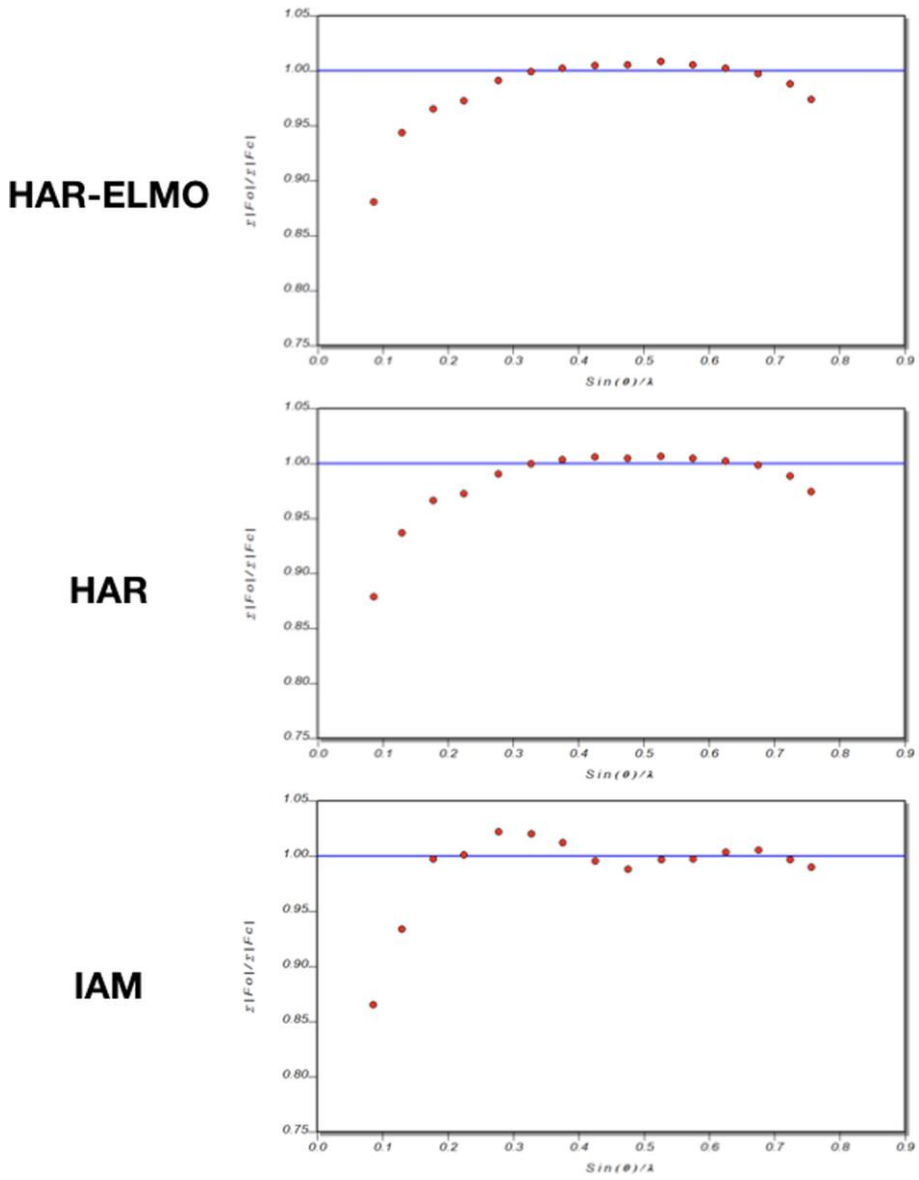

Figure S24: Averaged K-curve plots for the HAR-ELMO, HAR and IAM refinements of Gly-*L*-Ala at 100 K.

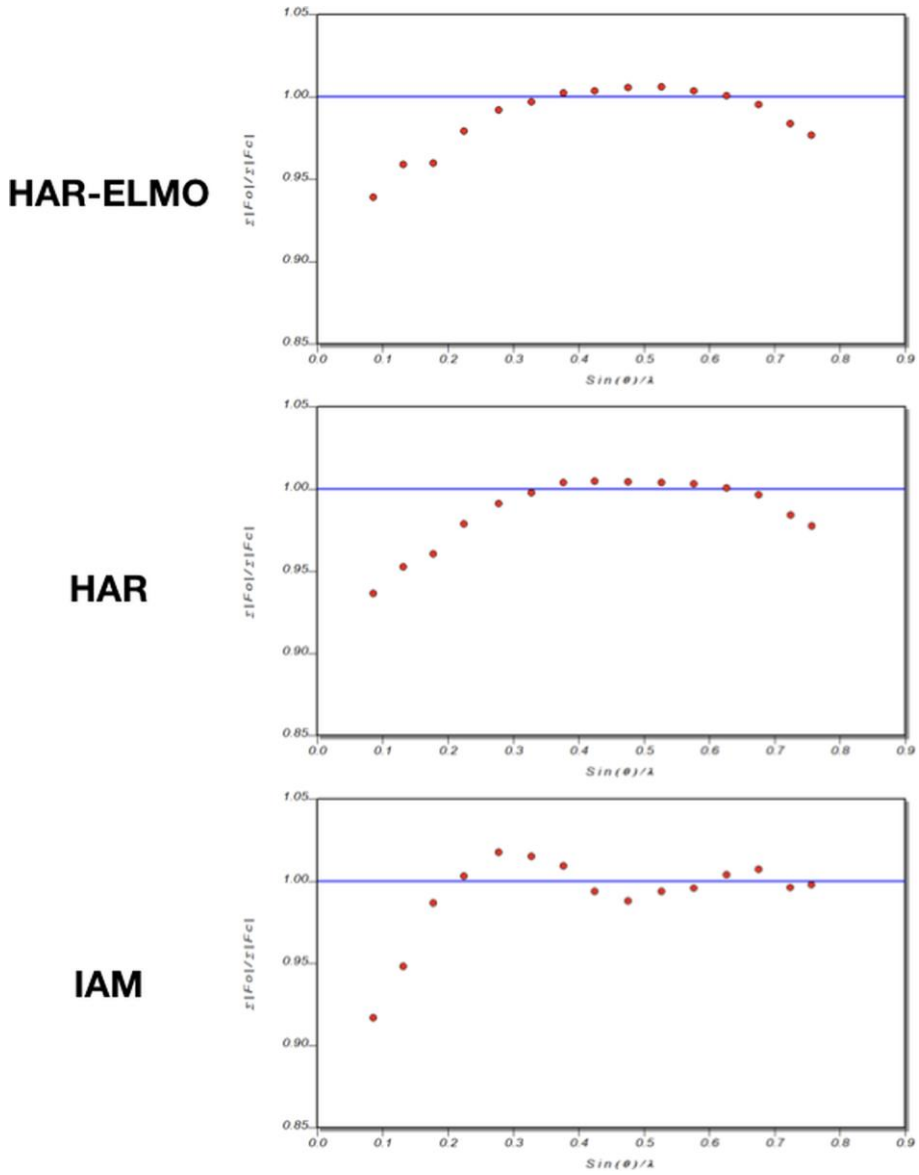

Figure S25: Averaged K-curve plots for the HAR-ELMO, HAR and IAM refinements of Gly-*L*-Ala at 150 K.

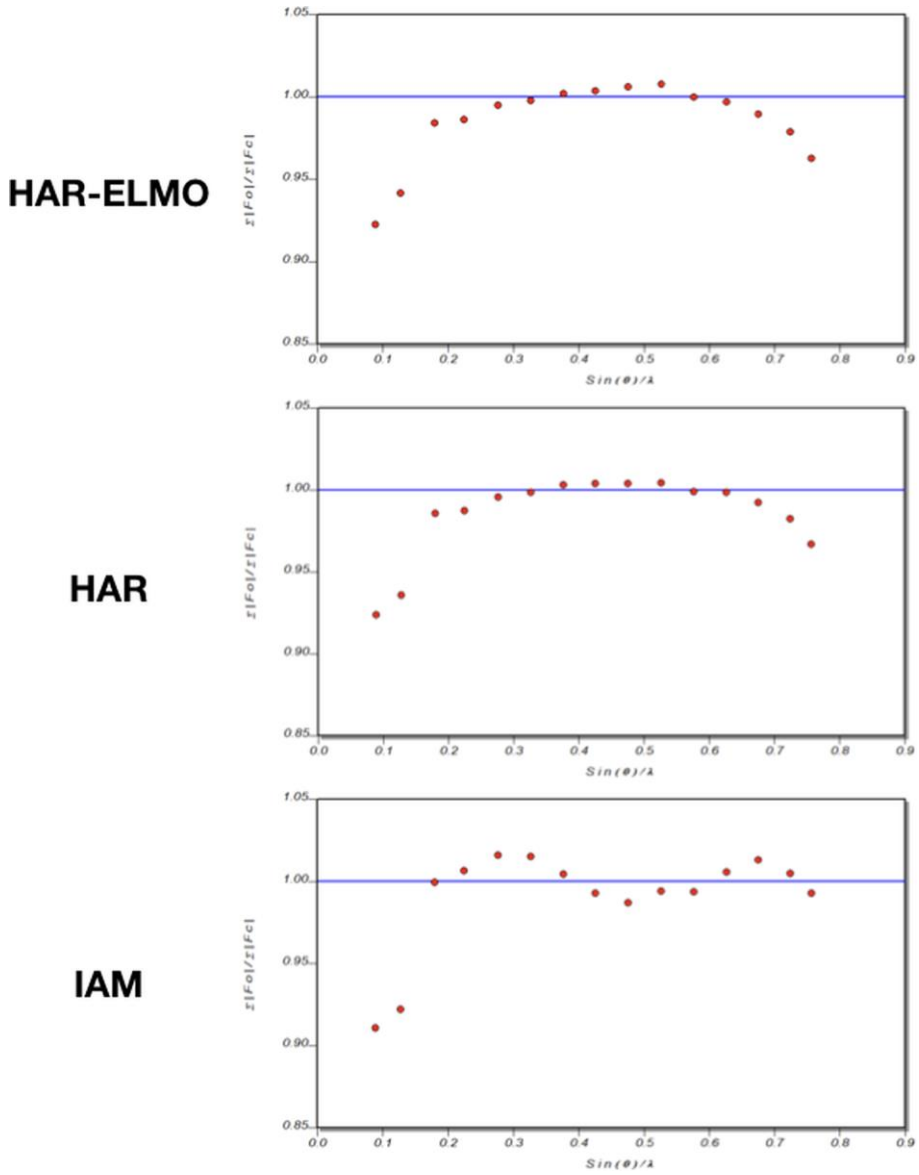

Figure S26: Averaged K-curve plots for the HAR-ELMO, HAR and IAM refinements of Gly-*L*-Ala at 295 K.

L-Alanine – Averaged K-curve plots

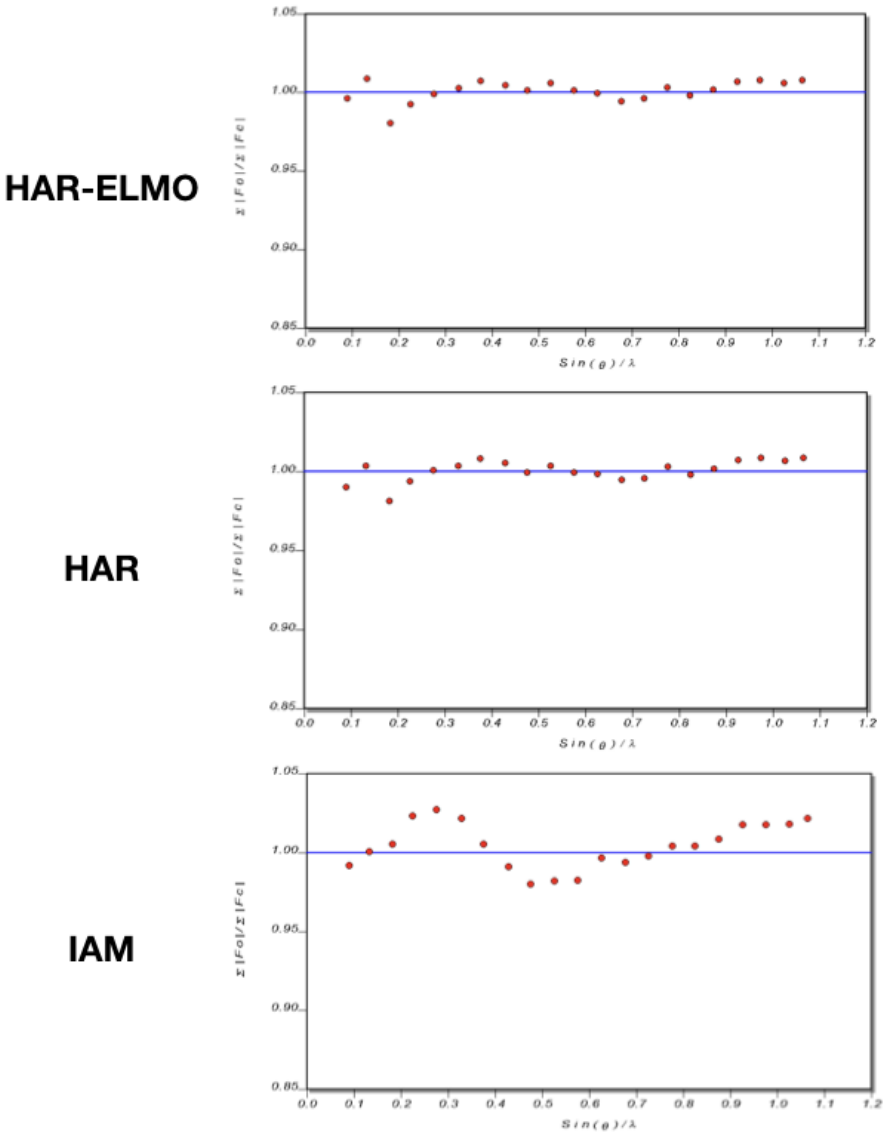

Figure S27: Averaged K-curve plots for the HAR-ELMO, HAR and IAM refinements of *L*-Ala at 23 K.

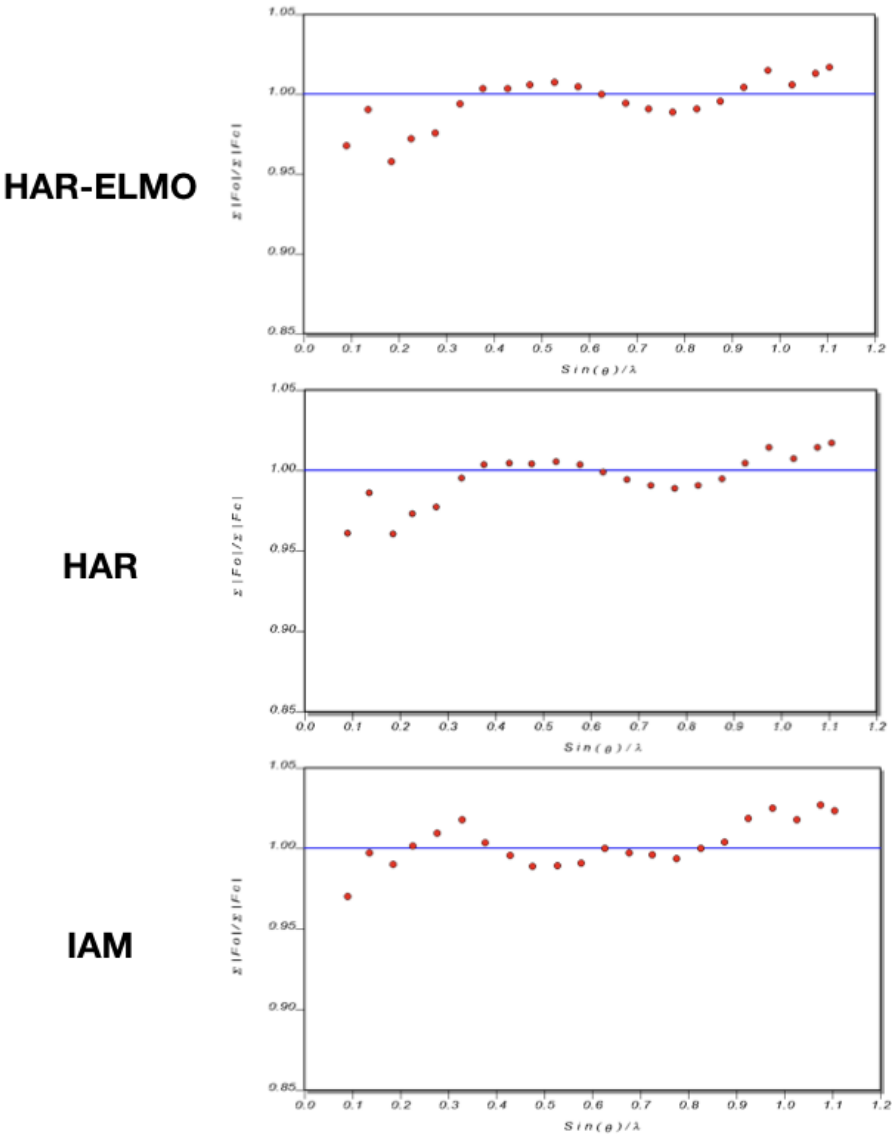

Figure S28: Averaged K-curve plots for the HAR-ELMO, HAR and IAM refinements of *L*-Ala at 100 K.

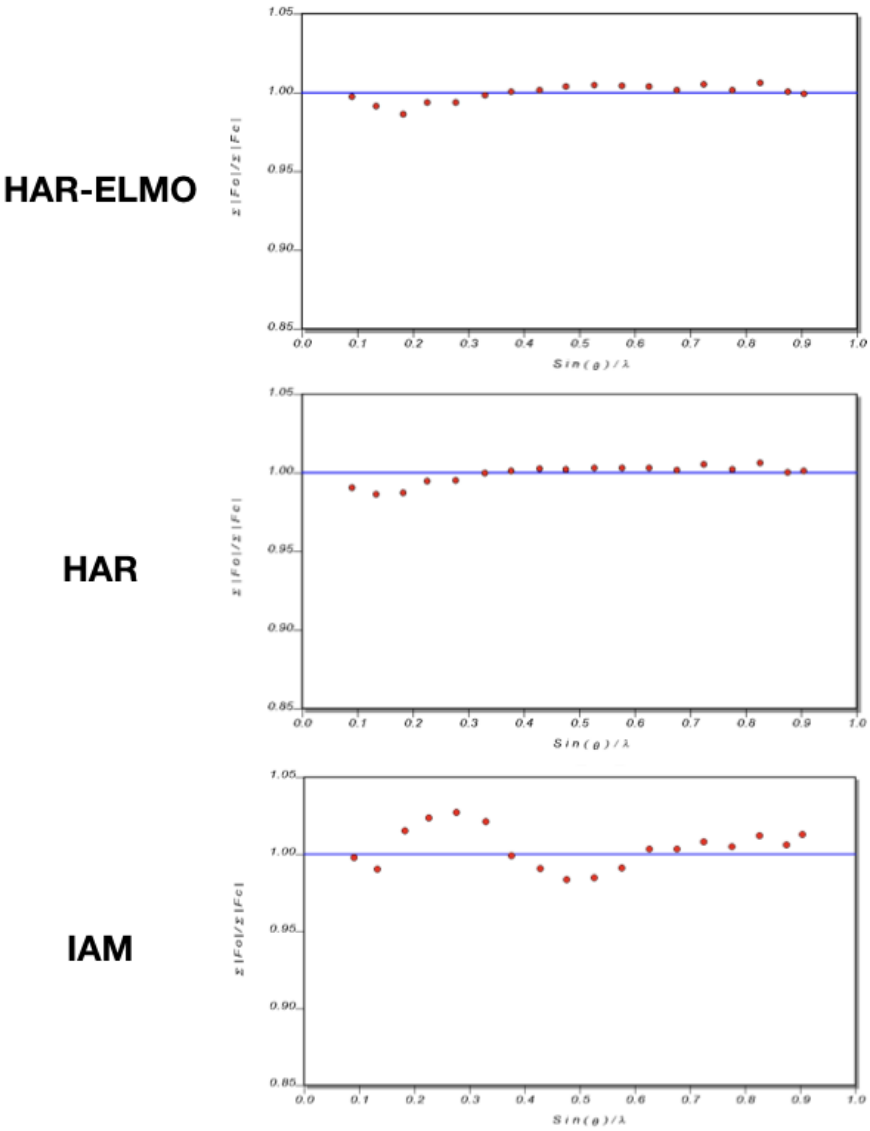

Figure S29: Averaged K-curve plots for the HAR-ELMO, HAR and IAM refinements of *L*-Ala at 150 K.

Comparison of Complete-K-curve plots

Gly-*L*-Ala – Complete K-curve plots

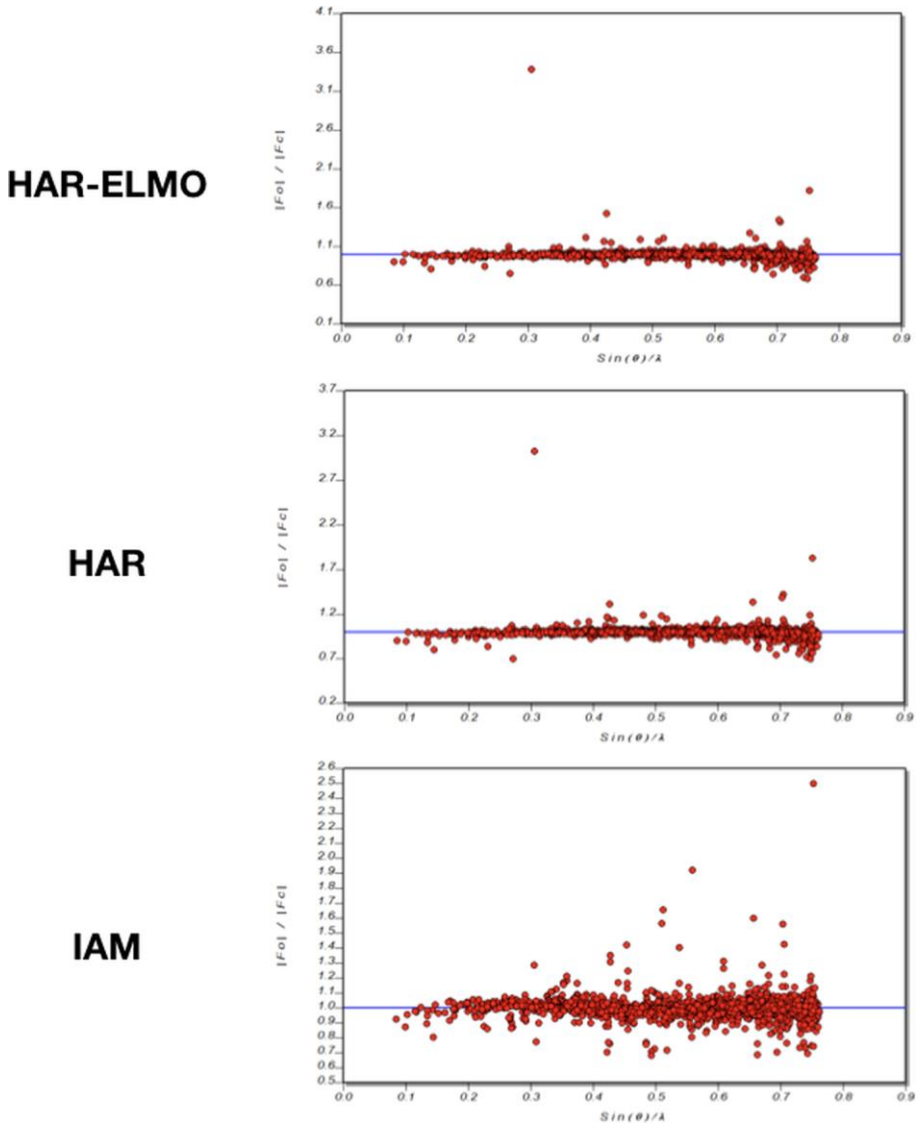

Figure S30: Complete K-curve plots for the HAR-ELMO, HAR and IAM refinements of Gly-*L*-Ala at 12 K.

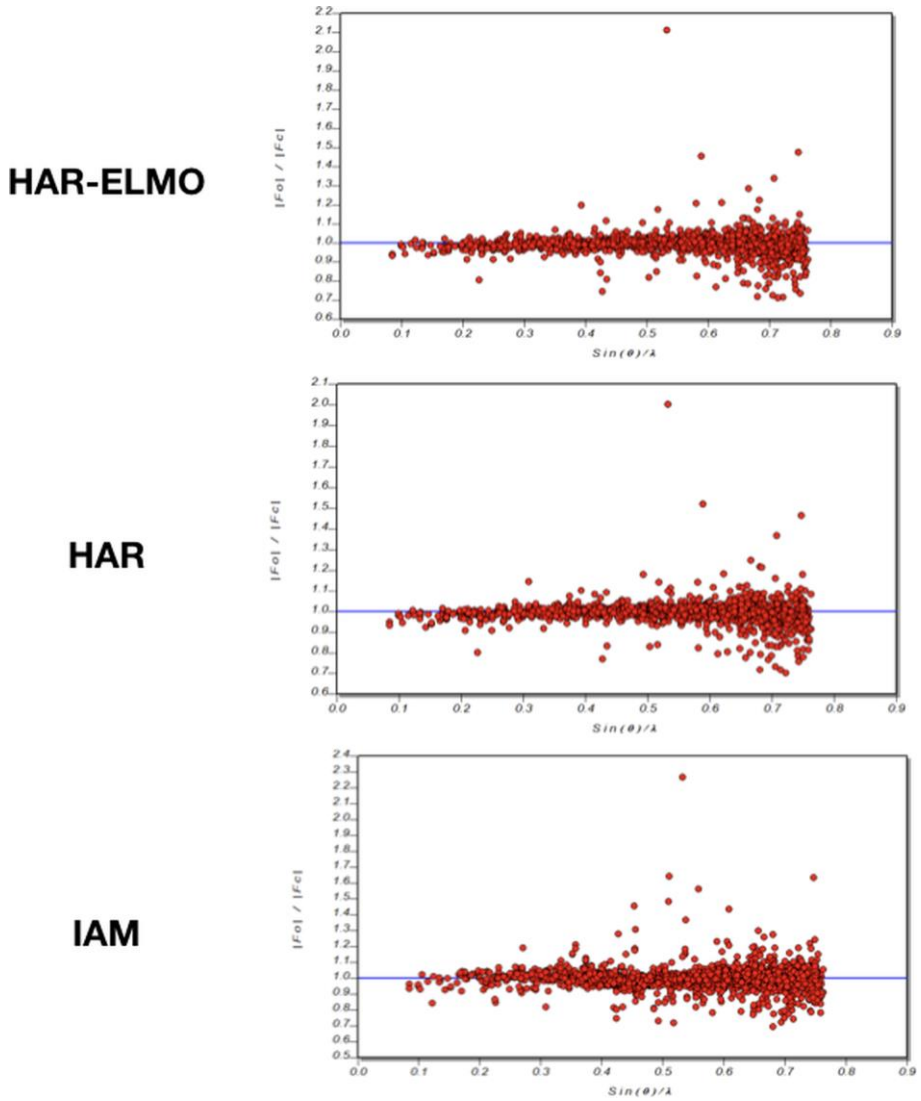

Figure S31: Complete K-curve plots for the HAR-ELMO, HAR and IAM refinements of Gly-*L*-Ala at 50 K.

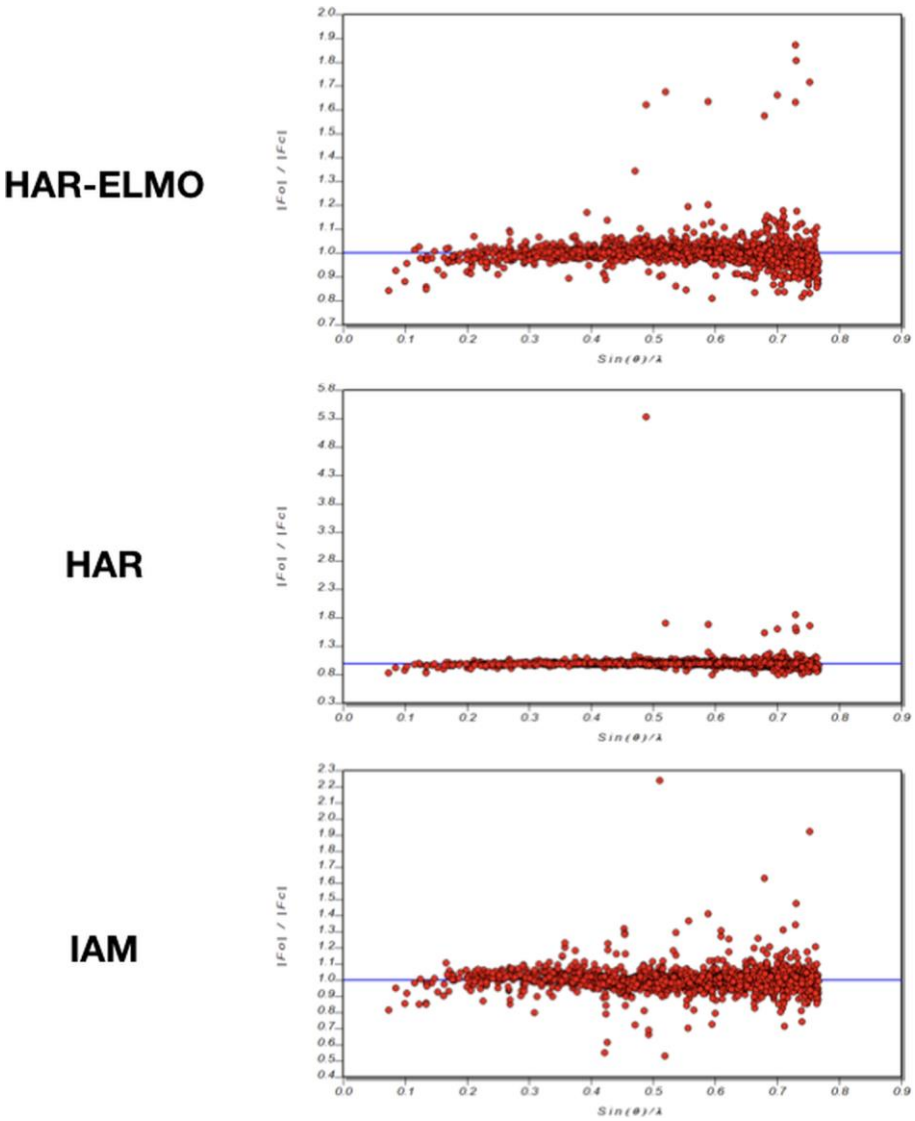

Figure S32: Complete K-curve plots for the HAR-ELMO, HAR and IAM refinements of Gly-*L*-Ala at 100 K.

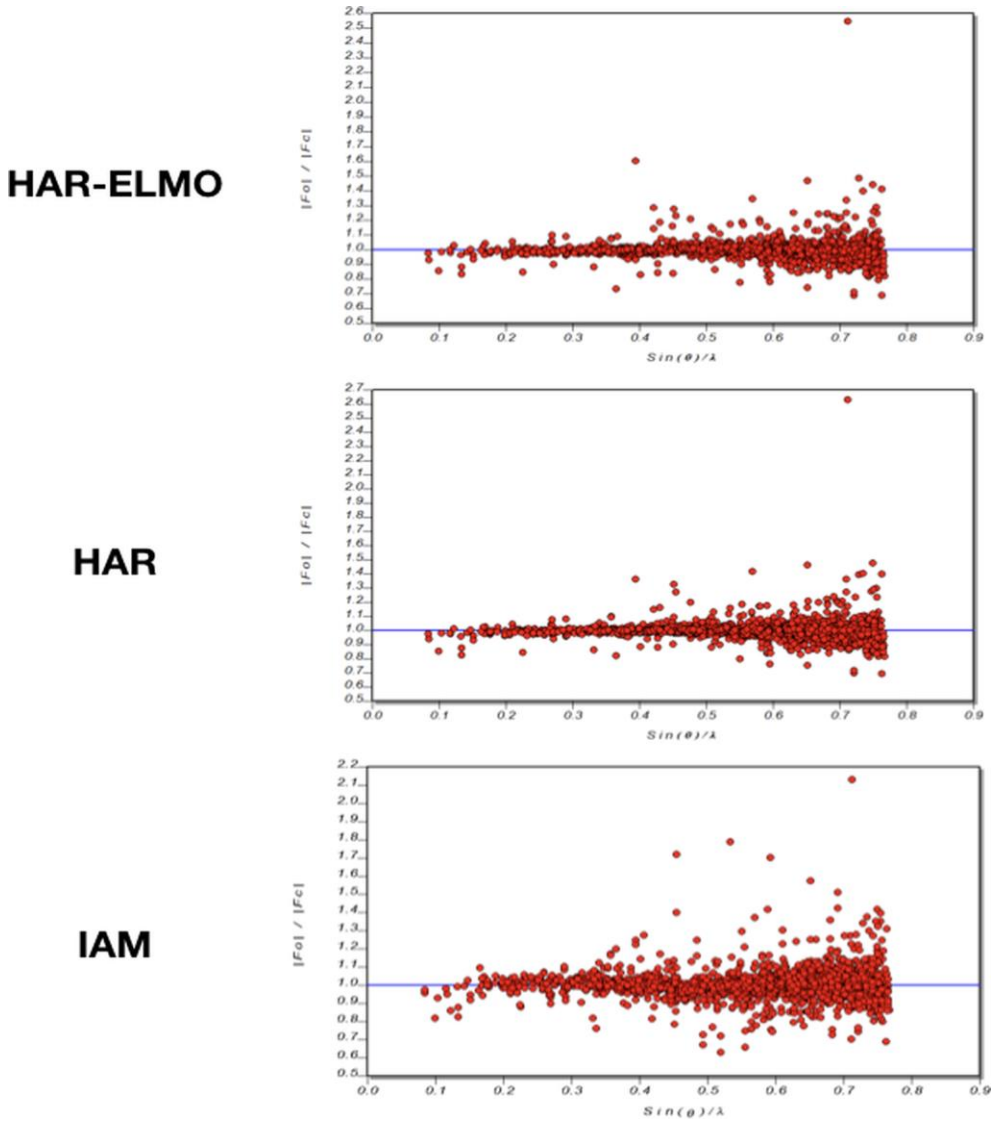

Figure S33: Complete K-curve plots for the HAR-ELMO, HAR and IAM refinements of Gly-*L*-Ala at 150 K.

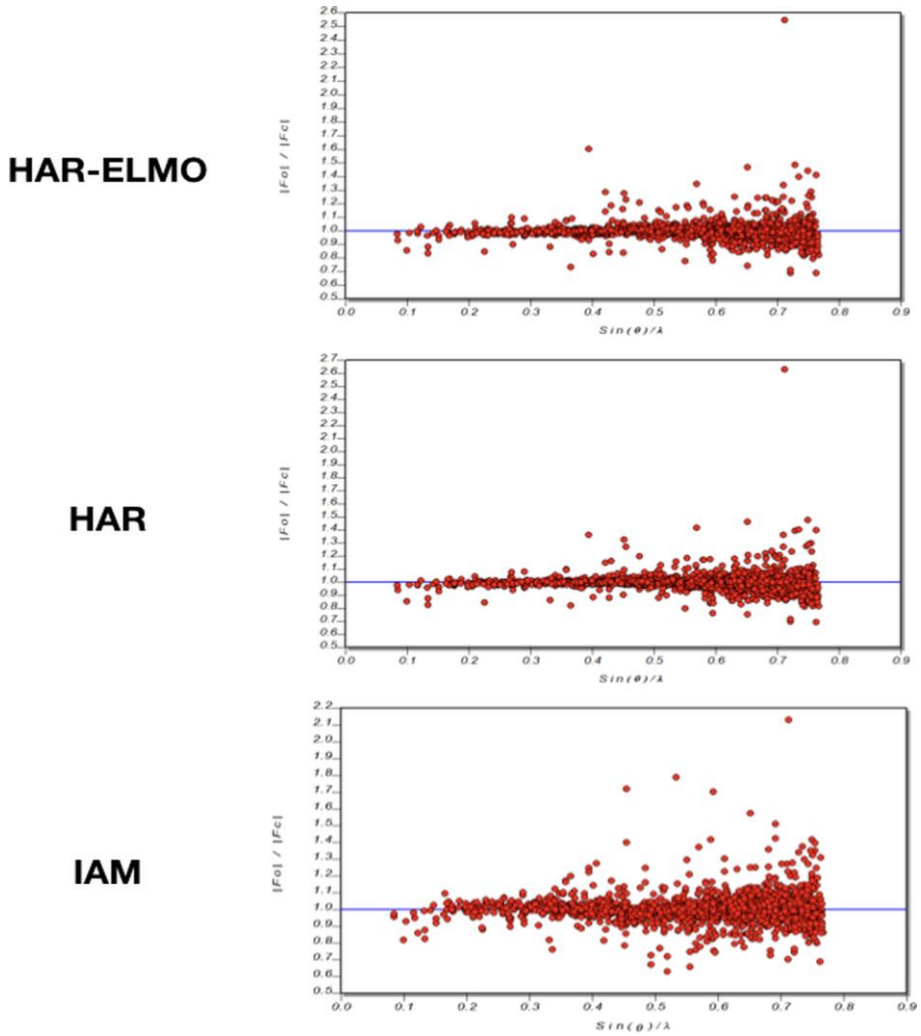

Figure S34: Complete K-curve plots for the HAR-ELMO, HAR and IAM refinements of Gly-*L*-Ala at 295 K.

L-Alanine – Complete K-curve plots

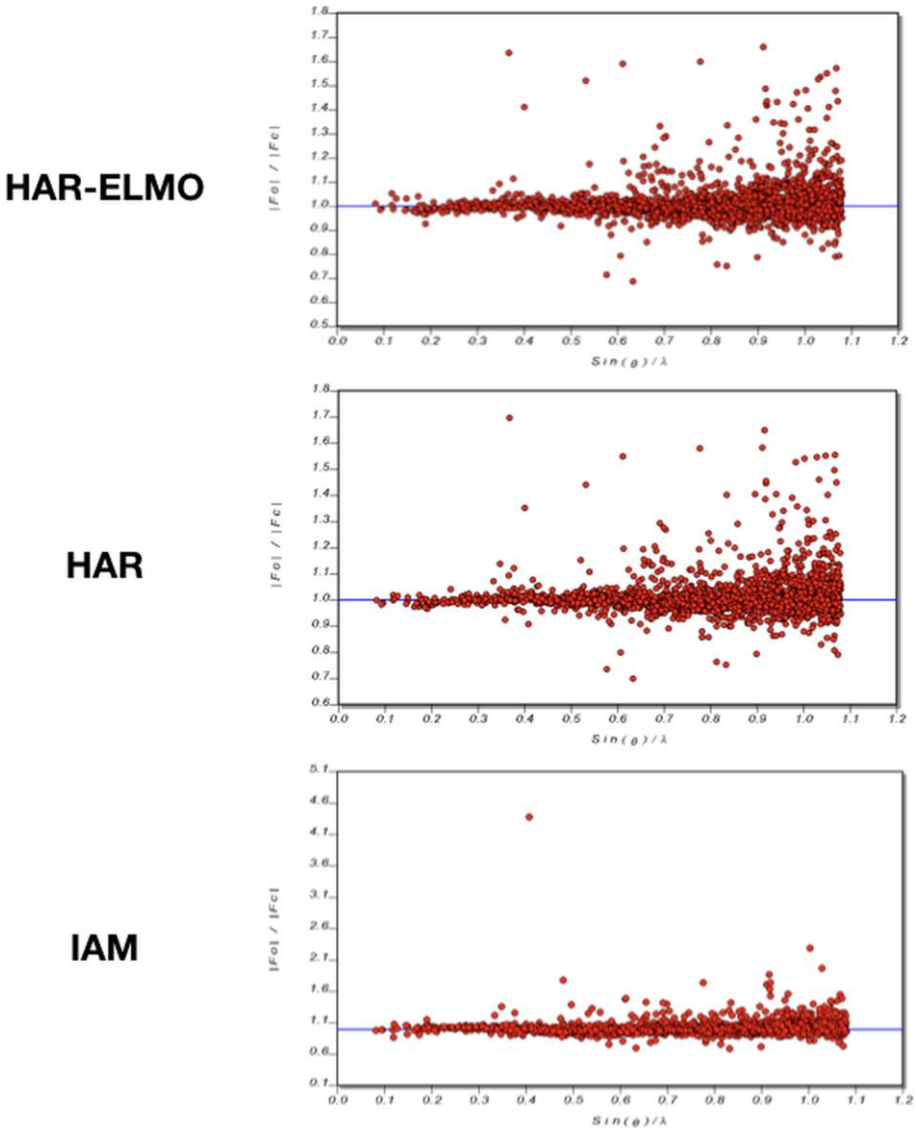

Figure S35: Complete K-curve plots for the HAR-ELMO, HAR and IAM refinements of *L*-Ala at 23 K.

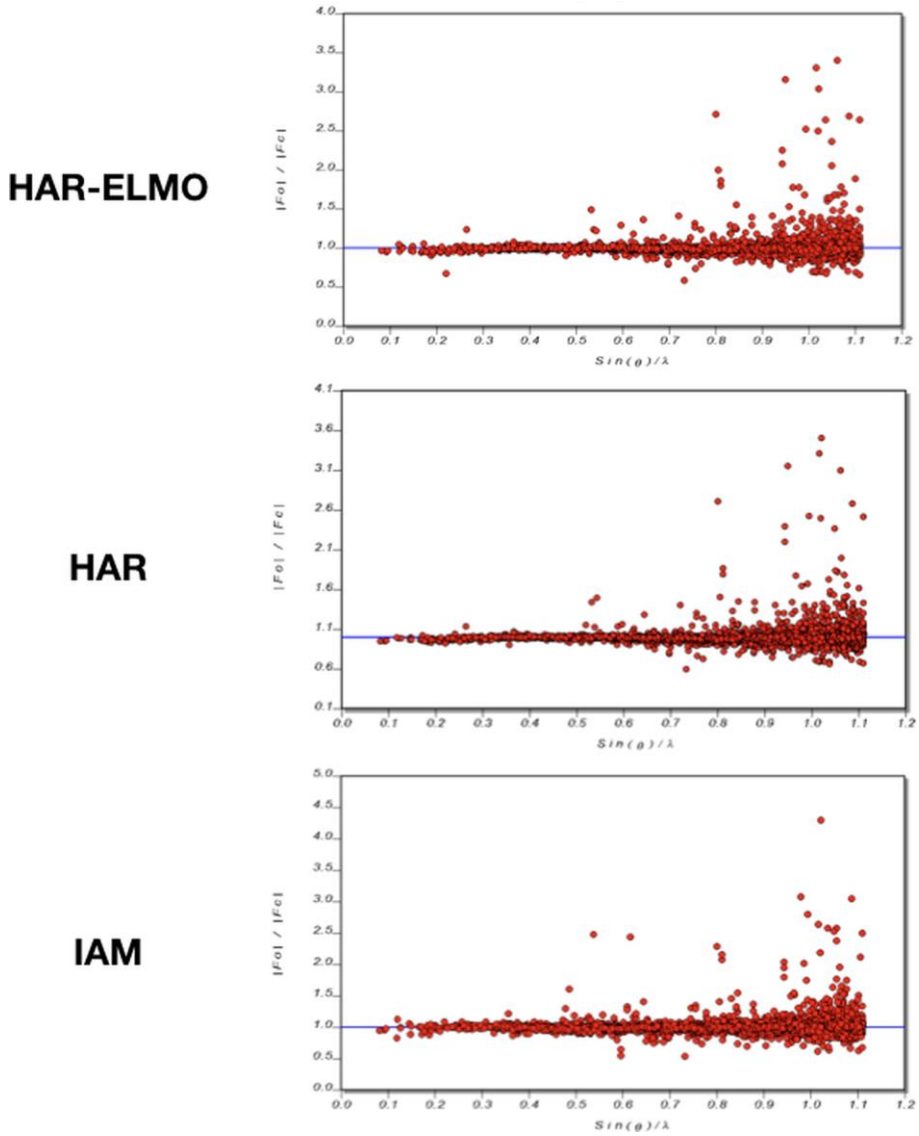

Figure S36: Complete K-curve plots for the HAR-ELMO, HAR and IAM refinements of *L*-Ala at 100 K.

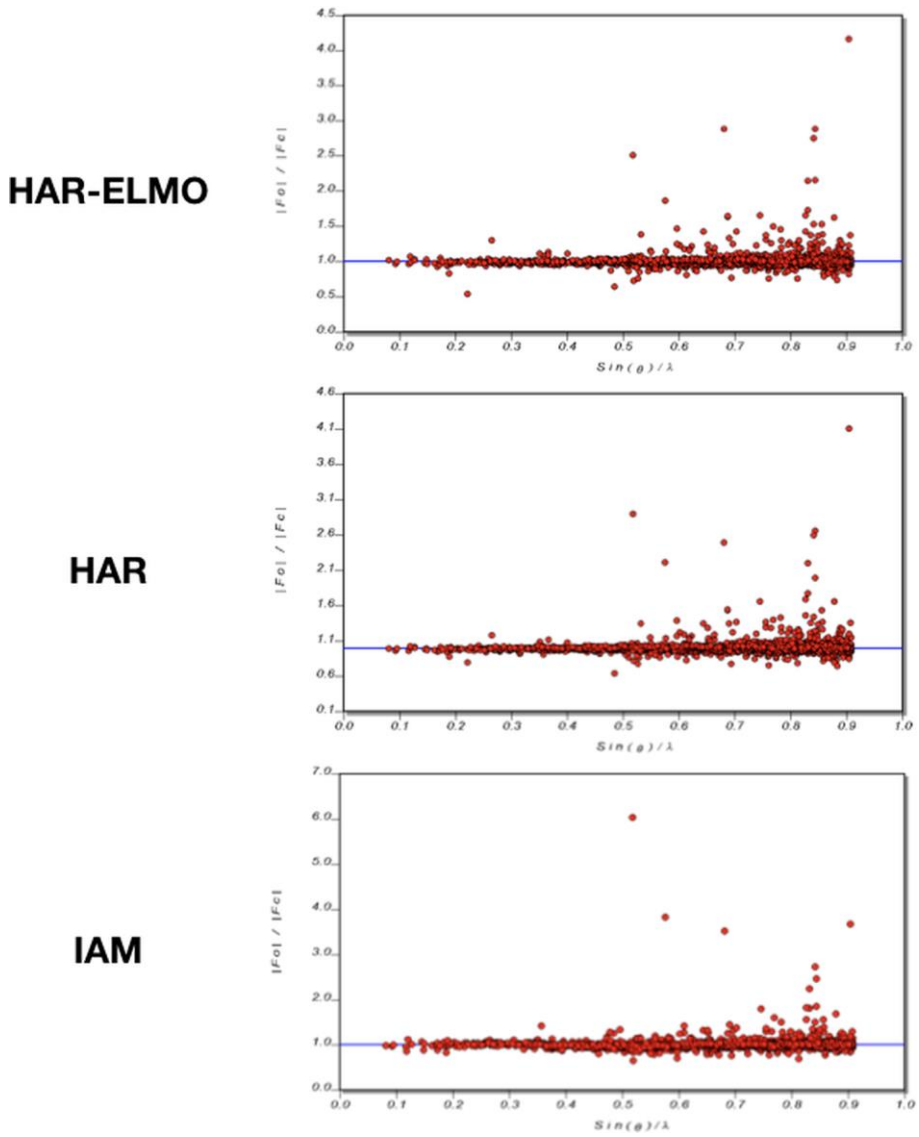

Figure S37: Complete K-curve plots for the HAR-ELMO, HAR and IAM refinements of *L*-Ala at 150 K.

Comparison of residual and deformation densities

Gly-*L*-Ala – Residual Densities (carboxylate group plane)

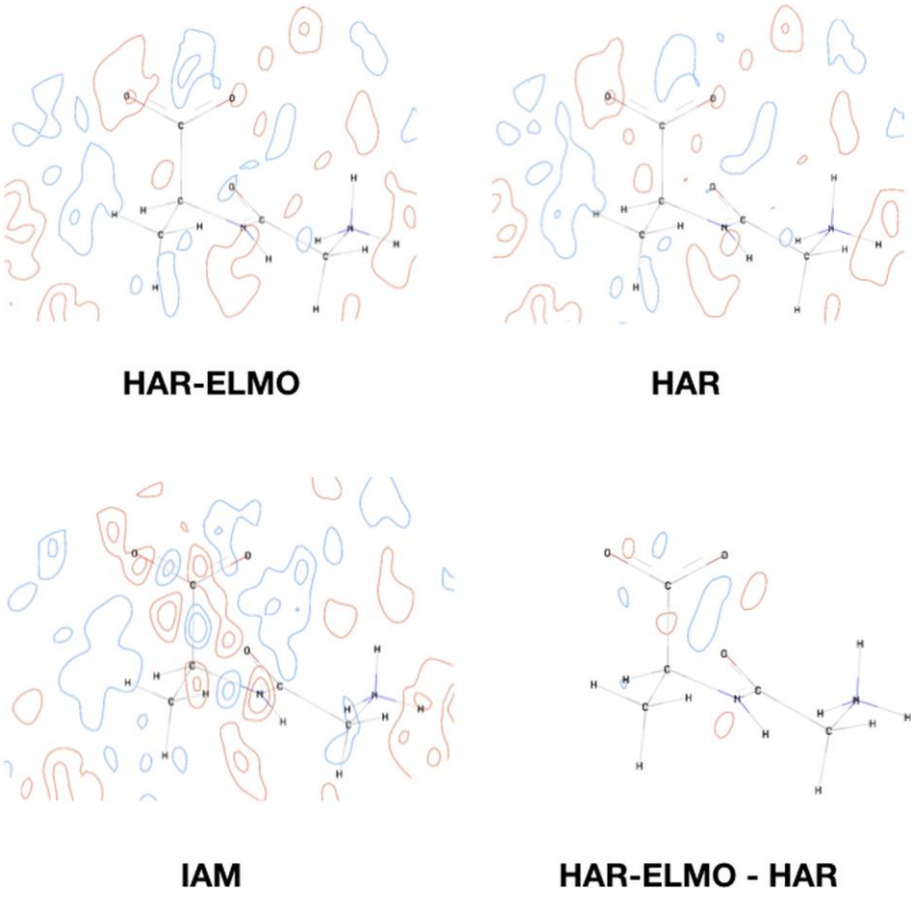

Figure S38: Residual density maps for Gly-*L*-Ala in the plane of the carboxylic group for the HAR-ELMO, HAR and IAM refinements at 12 K. The difference between the HAR-ELMO and HAR residual density maps is also shown. Contour levels: 0.05 and 0.10 eÅ^{-3} for the HAR-ELMO, HAR and IAM maps and 0.02 eÅ^{-3} for the HAR-ELMO – HAR difference map. Colours in the residual density maps: blue (positive) and red (negative).

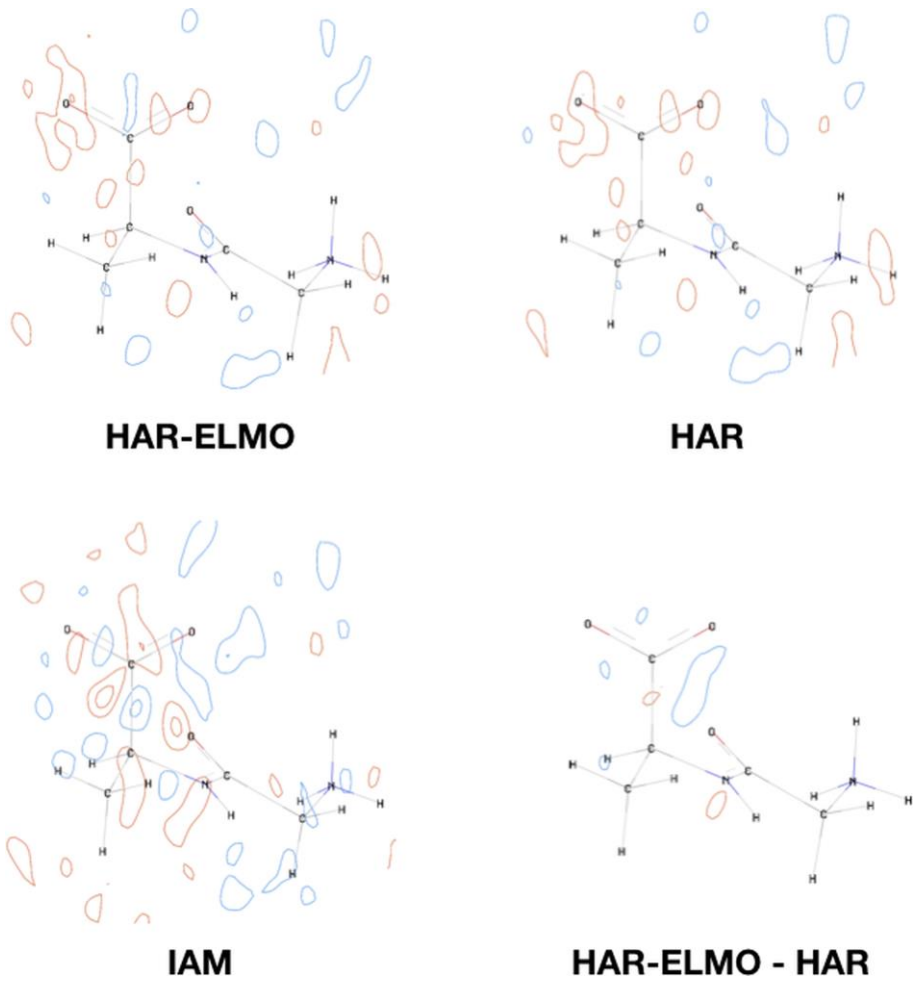

Figure S39: Residual density maps for Gly-*L*-Ala in the plane of the carboxylic group for the HAR-ELMO, HAR and IAM refinements at 50 K. The difference between the HAR-ELMO and HAR residual density maps is also shown. Contour levels: 0.05 and 0.10 eÅ^{-3} for the HAR-ELMO, HAR and IAM maps and 0.025 eÅ^{-3} for the HAR-ELMO – HAR difference map. Colours in the residual density maps: blue (positive) and red (negative).

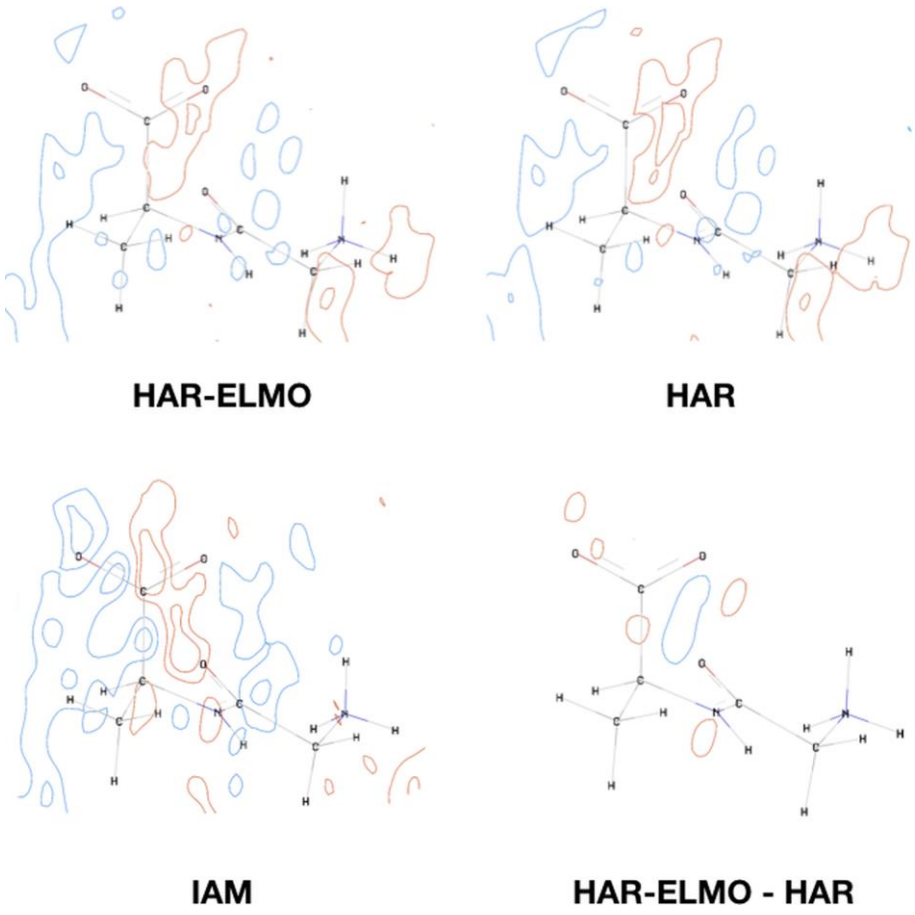

Figure S40: Residual density maps for Gly-*L*-Ala in the plane of the carboxylic group for the HAR-ELMO, HAR and IAM refinements at 100 K. The difference between the HAR-ELMO and HAR residual density maps is also shown. Contour levels: 0.05 and 0.10 eÅ^{-3} for the HAR-ELMO, HAR and IAM maps and 0.02 eÅ^{-3} for the HAR-ELMO – HAR difference map. Colours in the residual density maps: blue (positive) and red (negative).

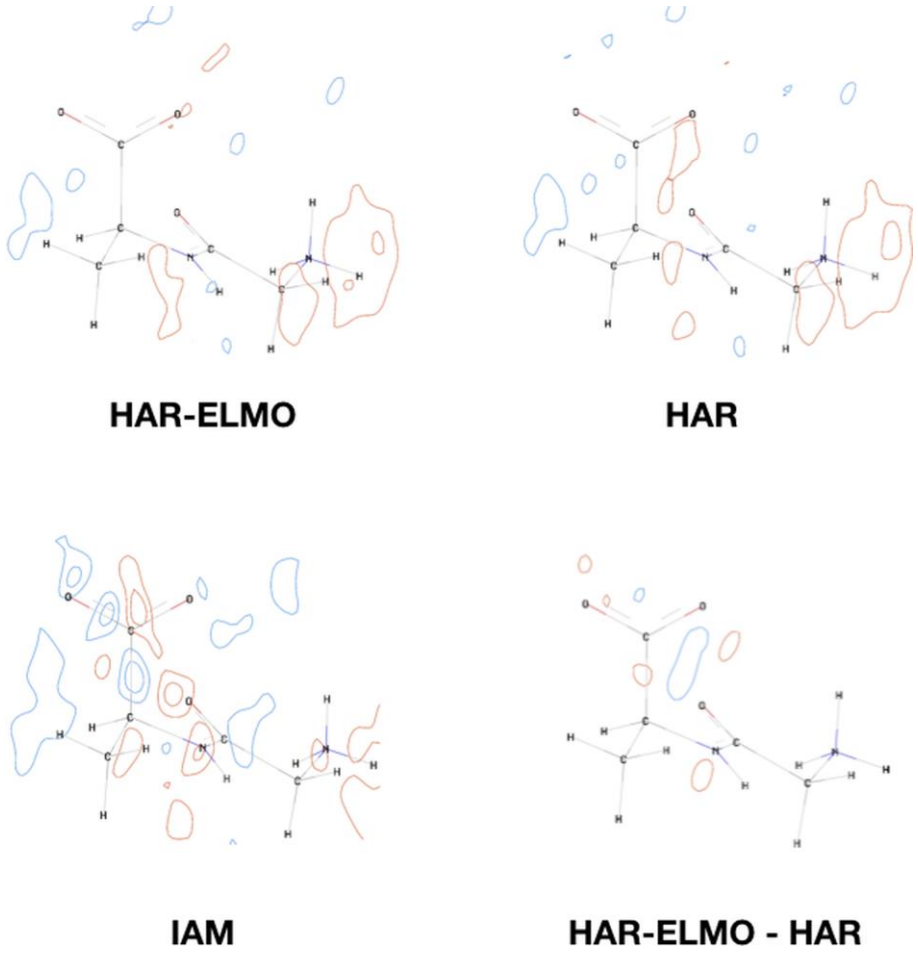

Figure S41: Residual density maps for Gly-*L*-Ala in the plane of the carboxylic group for the HAR-ELMO, HAR and IAM refinements at 150 K. The difference between the HAR-ELMO and HAR residual density maps is also shown. Contour levels: 0.05 and 0.10 eÅ^{-3} for the HAR-ELMO, HAR and IAM maps and 0.02 eÅ^{-3} for the HAR-ELMO – HAR difference map. Colours in the residual density maps: blue (positive) and red (negative).

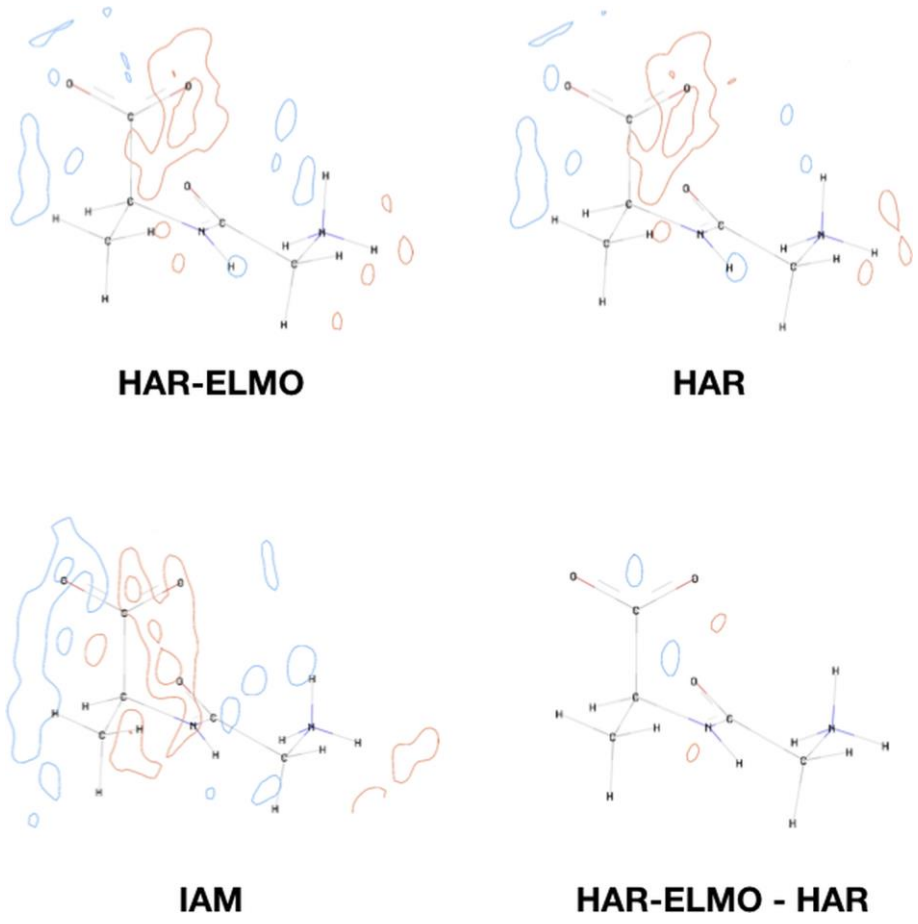

Figure S42: Residual density maps for Gly-*L*-Ala in the plane of the carboxylic group for the HAR-ELMO, HAR and IAM refinements at 295 K. The difference between the HAR-ELMO and HAR residual density maps is also shown. Contour levels: 0.05 and 0.10 eÅ^{-3} for the HAR-ELMO, HAR and IAM maps and 0.02 eÅ^{-3} for the HAR-ELMO – HAR difference map. Colours in the residual density maps: blue (positive) and red (negative).

Gly-*L*-Ala – Residual Densities (peptide bond plane)

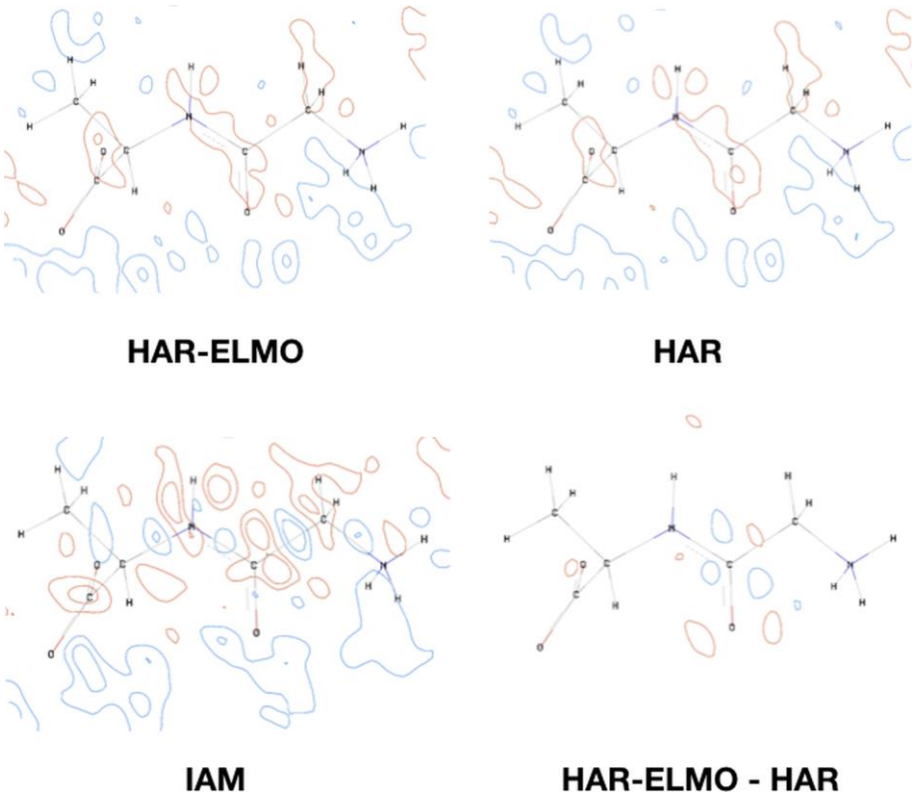

Figure S43: Residual density maps for Gly-*L*-Ala in the plane of the peptide bond for the HAR-ELMO, HAR and IAM refinements at 12 K. The difference between the HAR-ELMO and HAR residual density maps is also shown. Contour levels: 0.05 and 0.10 eÅ^{-3} for the HAR-ELMO, HAR and IAM maps and 0.02 eÅ^{-3} for the HAR-ELMO – HAR difference map. Colours in the residual density maps: blue (positive) and red (negative).

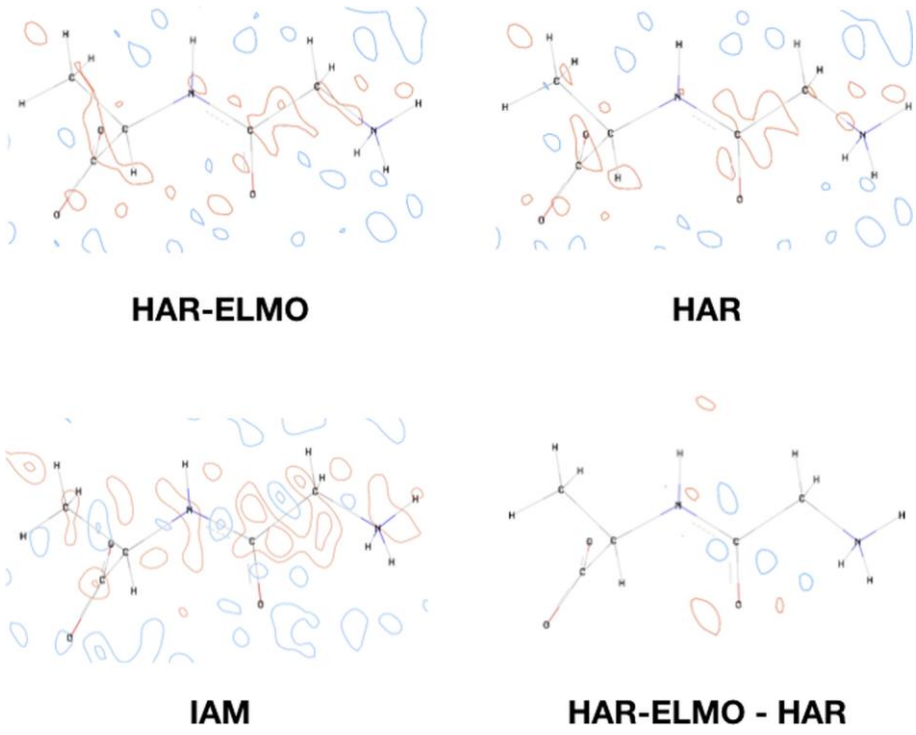

Figure S44: Residual density maps for Gly-*L*-Ala in the plane of the peptide bond for the HAR-ELMO, HAR and IAM refinements at 50 K. The difference between the HAR-ELMO and HAR residual density maps is also shown. Contour levels: 0.05 and 0.10 eÅ^{-3} for the HAR-ELMO, HAR and IAM maps and 0.025 eÅ^{-3} for the HAR-ELMO – HAR difference map. Colours in the residual density maps: blue (positive) and red (negative).

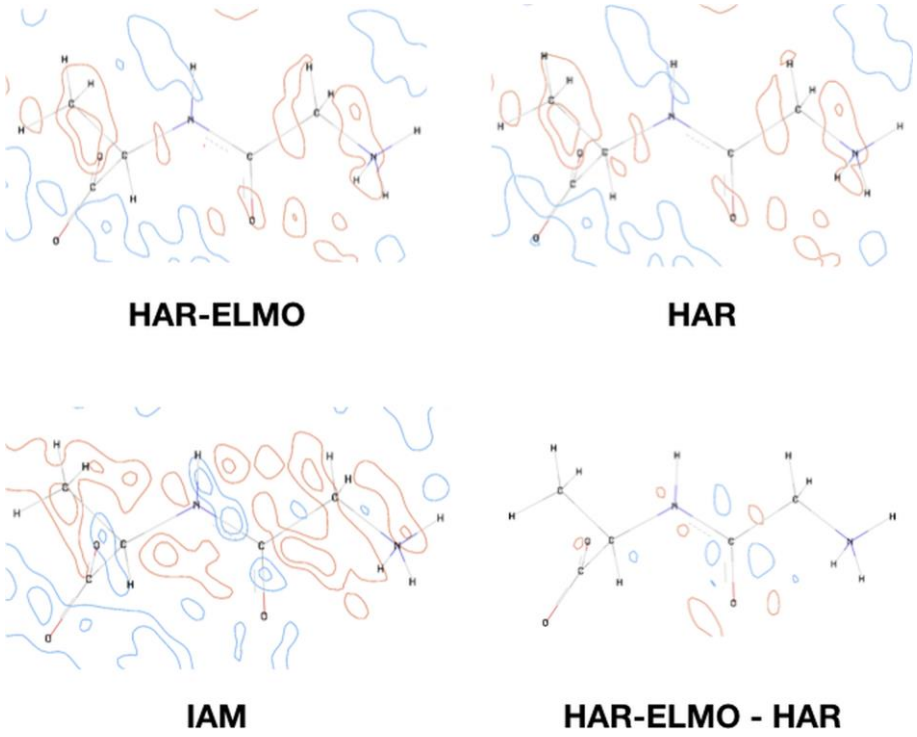

Figure S45: Residual density maps for Gly-*L*-Ala in the plane of the peptide bond for the HAR-ELMO, HAR and IAM refinements at 100 K. The difference between the HAR-ELMO and HAR residual density maps is also shown. Contour levels: 0.05 and 0.10 eÅ^{-3} for the HAR-ELMO, HAR and IAM maps and 0.02 eÅ^{-3} for the HAR-ELMO – HAR difference map. Colours in the residual density maps: blue (positive) and red (negative).

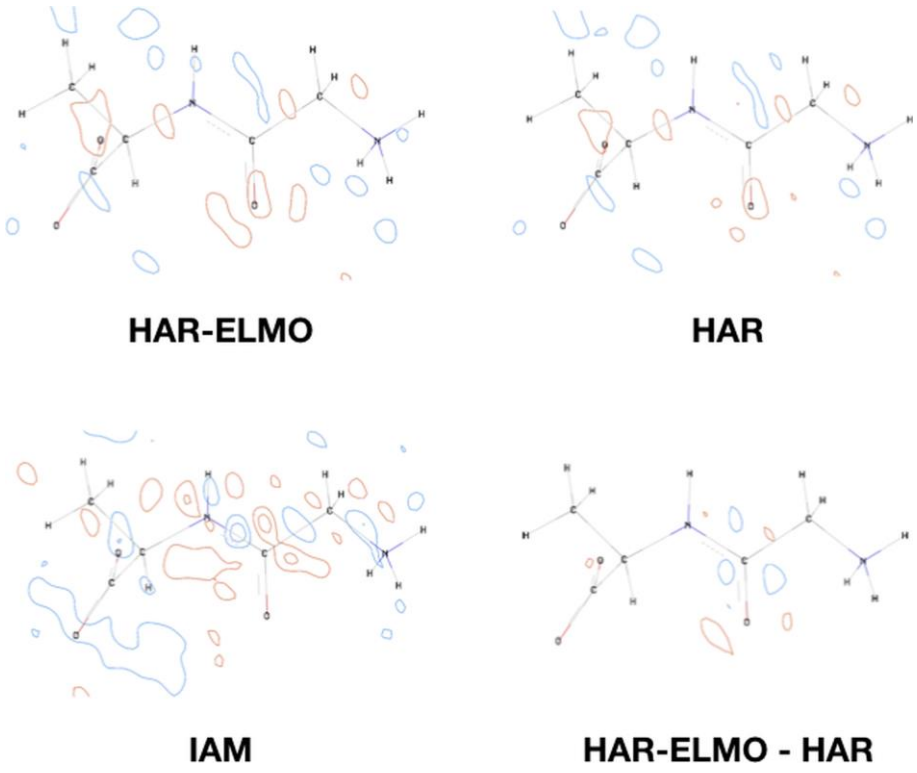

Figure S46: Residual density maps for Gly-*L*-Ala in the plane of the peptide bond for the HAR-ELMO, HAR and IAM refinements at 150 K. The difference between the HAR-ELMO and HAR residual density maps is also shown. Contour levels: 0.05 and 0.10 eÅ^{-3} for the HAR-ELMO, HAR and IAM maps and 0.02 eÅ^{-3} for the HAR-ELMO – HAR difference map. Colours in the residual density maps: blue (positive) and red (negative).

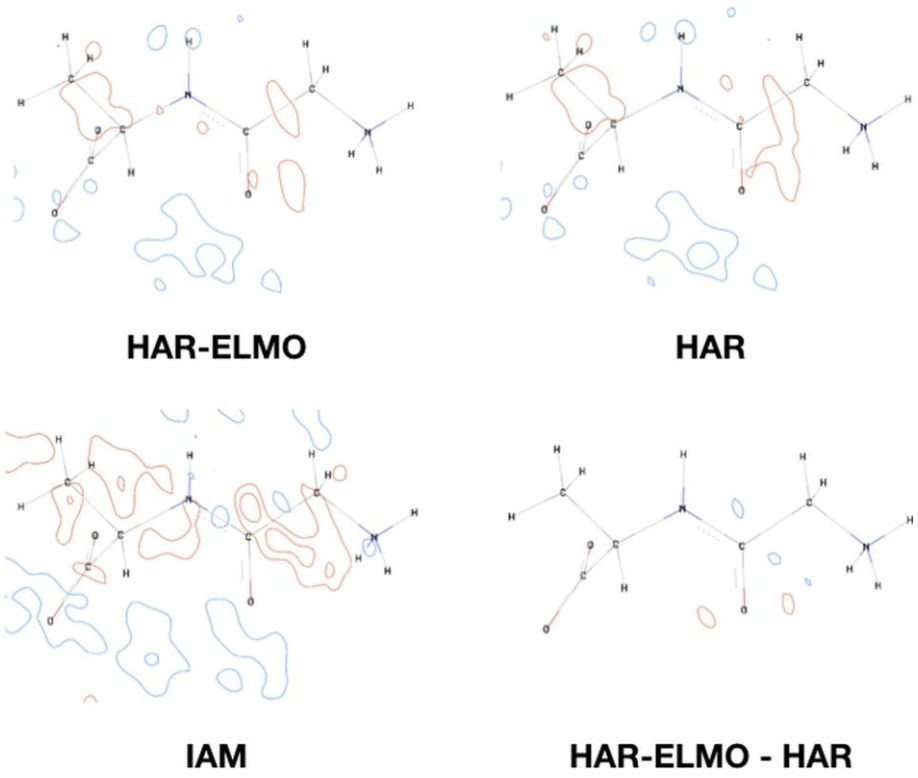

Figure S47: Residual density maps for Gly-*L*-Ala in the plane of the peptide bond for the HAR-ELMO, HAR and IAM refinements at 295 K. The difference between the HAR-ELMO and HAR residual density maps is also shown. Contour levels: 0.05 and 0.10 eÅ^{-3} for the HAR-ELMO, HAR and IAM maps and 0.02 eÅ^{-3} for the HAR-ELMO – HAR difference map. Colours in the residual density maps: blue (positive) and red (negative).

L-alanine – Residual Densities (carboxylate group plane)

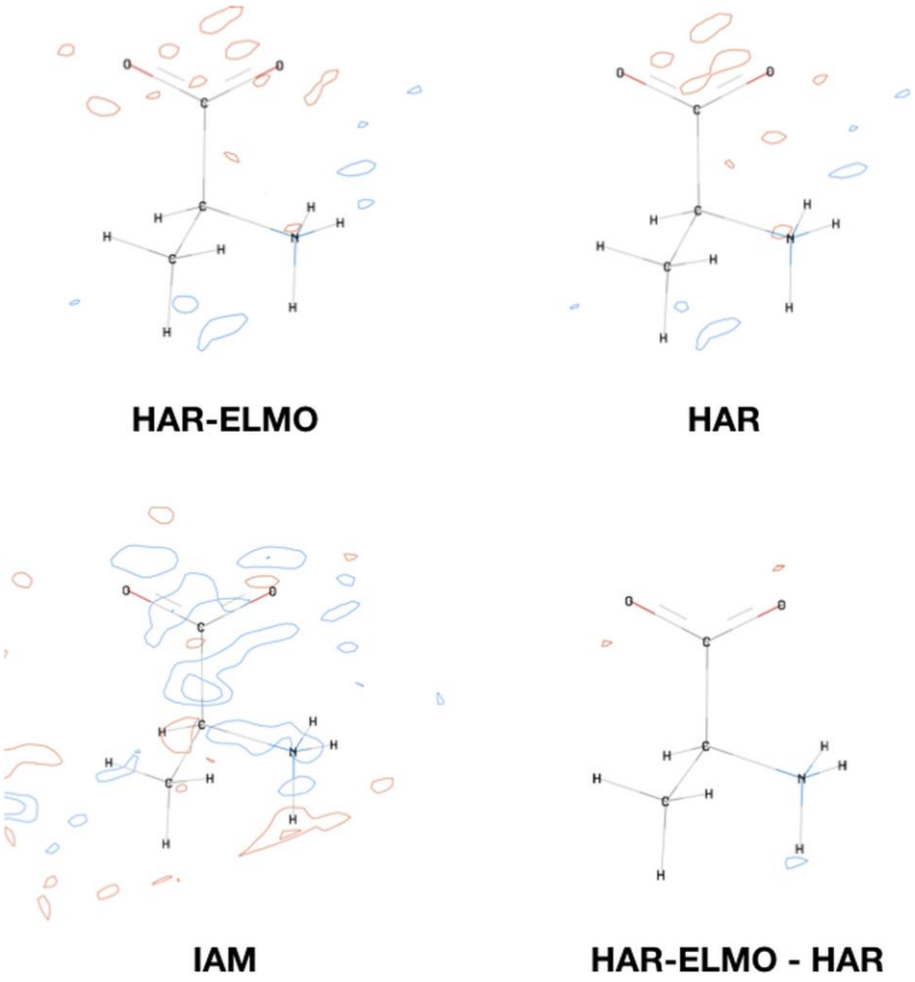

Figure S48: Residual density maps for *L*-Ala in the plane of the carboxylic group for the HAR-ELMO, HAR and IAM refinements at 23 K. The difference between the HAR-ELMO and HAR residual density maps is also shown. Contour levels: 0.05 and 0.10 eÅ^{-3} for the HAR-ELMO, HAR and IAM maps and 0.025 eÅ^{-3} for the HAR-ELMO – HAR difference map. Colours in the residual density maps: blue (positive) and red (negative).

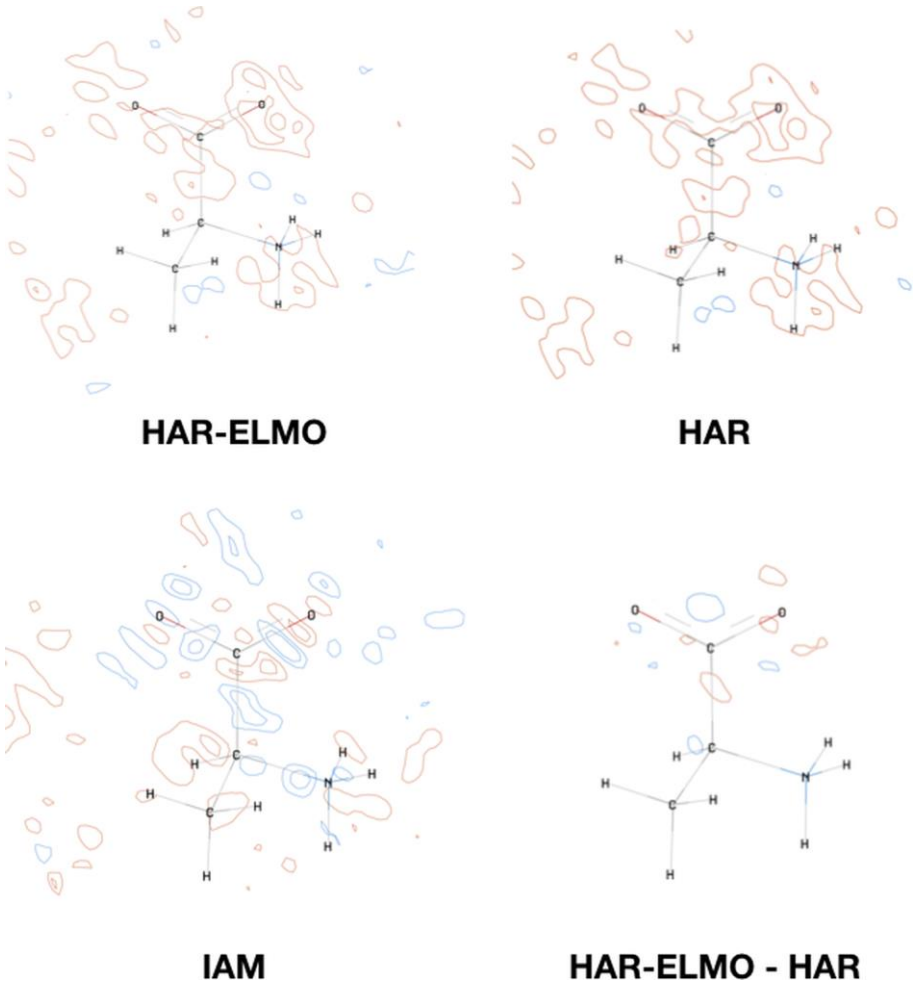

Figure S49: Residual density maps for *L*-Ala in the plane of the carboxylic group for the HAR-ELMO, HAR and IAM refinements at 100 K. The difference between the HAR-ELMO and HAR residual density maps is also shown. Contour levels: 0.05 and 0.10 eÅ^{-3} for the HAR-ELMO, HAR and IAM maps and 0.025 eÅ^{-3} for the HAR-ELMO – HAR difference map. Colours in the residual density maps: blue (positive) and red (negative).

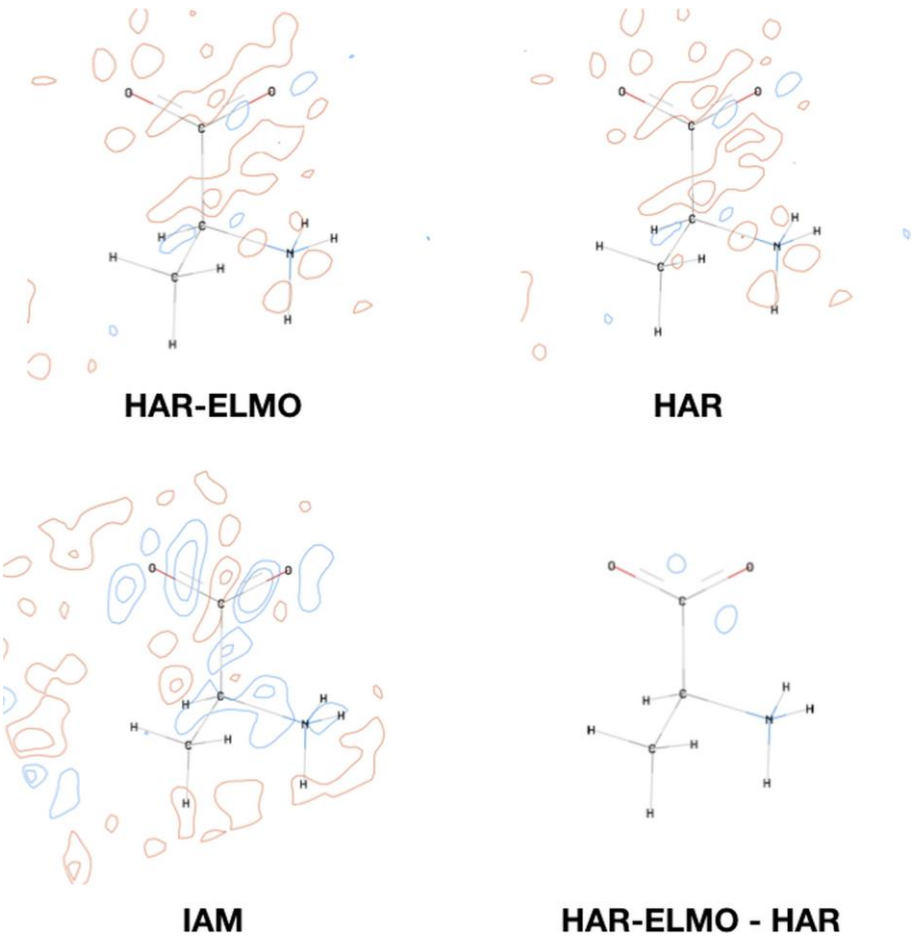

Figure S50: Residual density maps for *L*-Ala in the plane of the carboxylic group for the HAR-ELMO, HAR and IAM refinements at 150 K. The difference between the HAR-ELMO and HAR residual density maps is also shown. Contour levels: 0.05 and 0.10 eÅ^{-3} for the HAR-ELMO, HAR and IAM maps and 0.025 eÅ^{-3} for the HAR-ELMO – HAR difference map. Colours in the residual density maps: blue (positive) and red (negative).

L-alanine – Residual Densities (NCC plane)

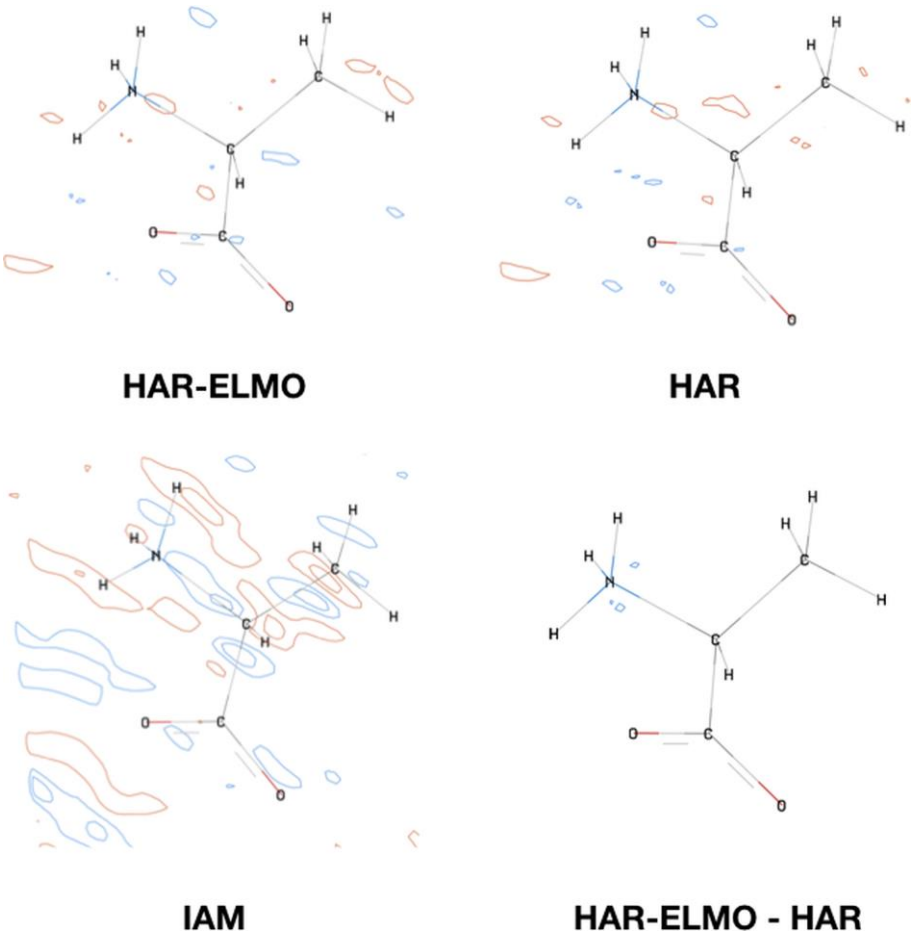

Figure S51: Residual density maps for *L*-Ala in the N-Cα-Cβ plane for the HAR-ELMO, HAR and IAM refinements at 23 K. The difference between the HAR-ELMO and HAR residual density maps is also shown. Contour levels: 0.05 and 0.10 eÅ^{-3} for the HAR-ELMO, HAR and IAM maps and 0.025 eÅ^{-3} for the HAR-ELMO – HAR difference map. Colours in the residual density maps: blue (positive) and red (negative).

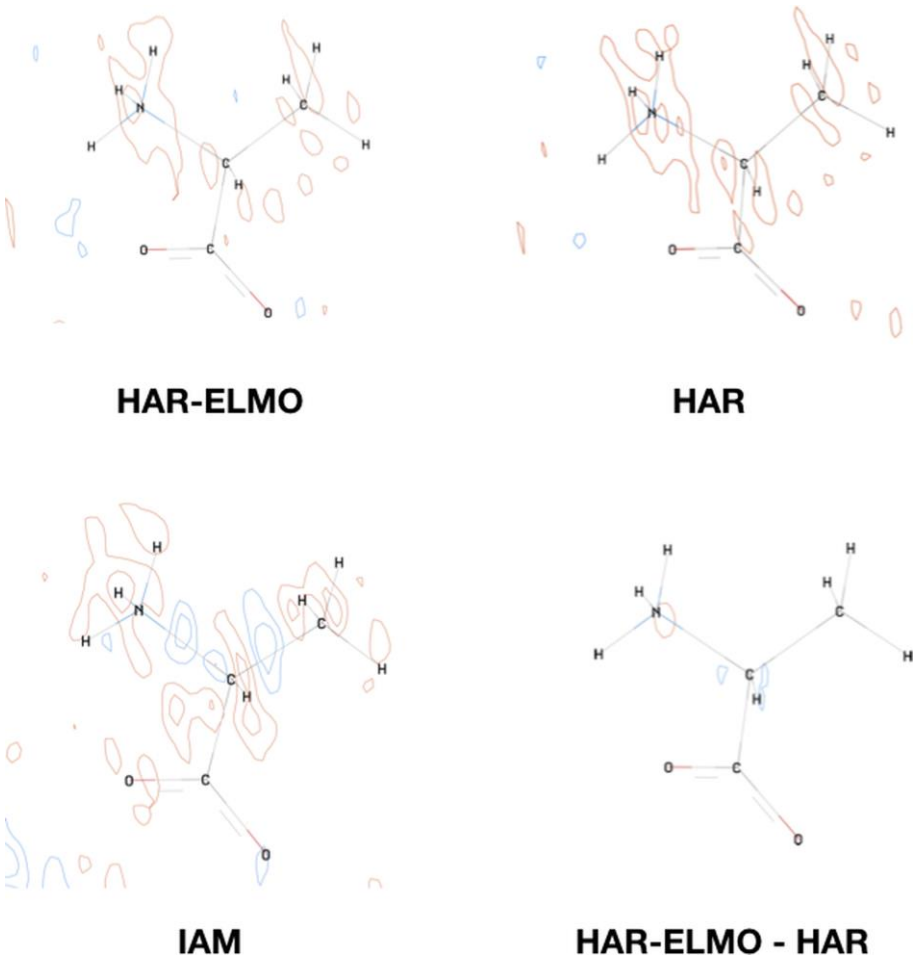

Figure S52: Residual density maps for *L*-Ala in the N-Cα-Cβ plane for the HAR-ELMO, HAR and IAM refinements at 100 K. The difference between the HAR-ELMO and HAR residual density maps is also shown. Contour levels: 0.05 and 0.10 eÅ^{-3} for the HAR-ELMO, HAR and IAM maps and 0.025 eÅ^{-3} for the HAR-ELMO – HAR difference map. Colours in the residual density maps: blue (positive) and red (negative).

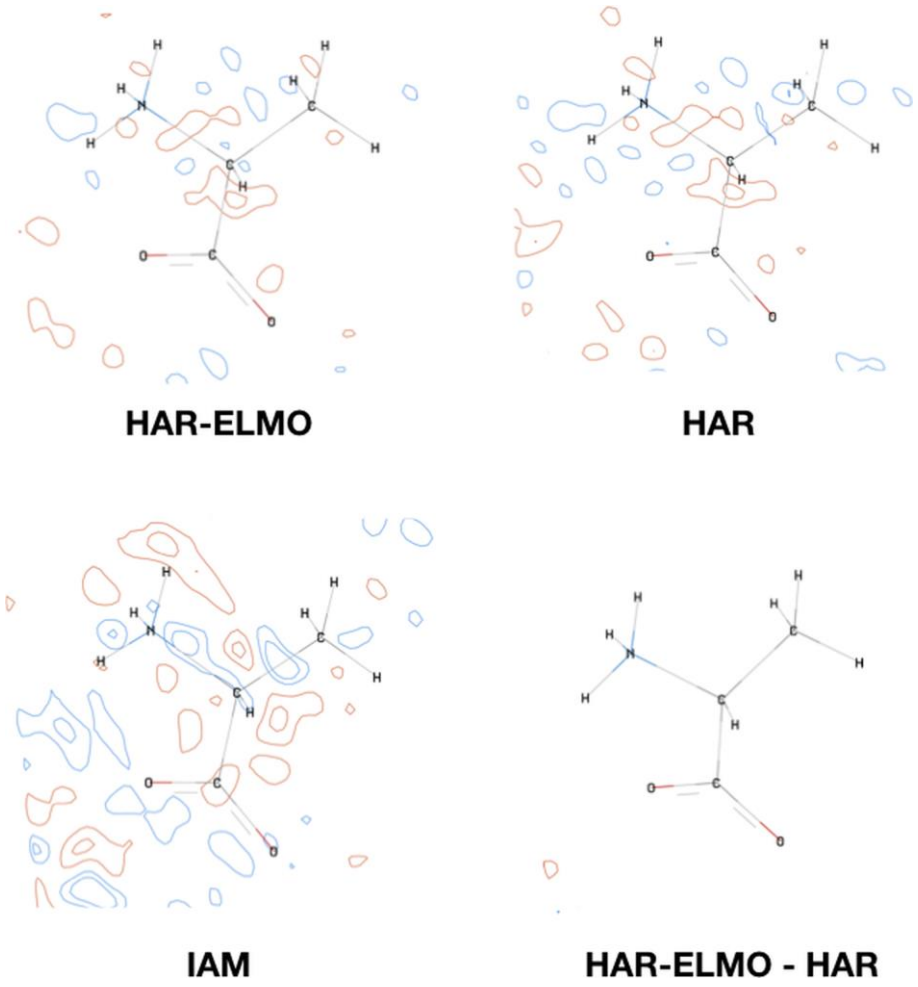

Figure S53: Residual density maps for *L*-Ala in the N-Cα-Cβ plane for the HAR-ELMO, HAR and IAM refinements at 150 K. The difference between the HAR-ELMO and HAR residual density maps is also shown. Contour levels: 0.05 and 0.10 eÅ^{-3} for the HAR-ELMO, HAR and IAM maps and 0.025 eÅ^{-3} for the HAR-ELMO – HAR difference map. Colours in the residual density maps: blue (positive) and red (negative).

Deformation Densities

The difference between HAR-ELMO and HAR deformation densities for all structures (compare Figure S54 to Figure S77) clearly accentuates some systematic features in the regions of oxygen lone pairs and of the most polarizable hydrogen atoms. This is most likely due to the strict localization applied in the construction of the ELMO wavefunction, in contrast to maximal electron delocalization of the wavefunction used in the traditional HAR procedure. This will impact on the description of intermolecular interactions and, hence, it is the reason for the differences in the ADPs of the peptide hydrogen atom in Gly-*L*-Ala (compare Figure S5). We will discuss impacts and mitigations of this phenomenon in a separate study.

Gly-*L*-Ala – Deformation Densities (carboxylate group plane)

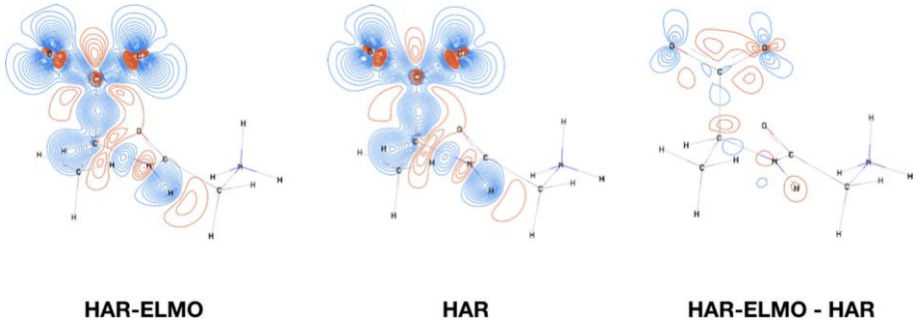

Figure S54: Deformation density maps for Gly-*L*-Ala in the plane of the carboxylic group for the HAR-ELMO and HAR refinements at 12 K. The difference between the HAR-ELMO and HAR deformation density maps is also shown. Contour levels: from 0.05 to 1.00 eÅ^{-3} with a step of 0.05 eÅ^{-3}. Colours in the deformation density maps: blue (positive) and red (negative).

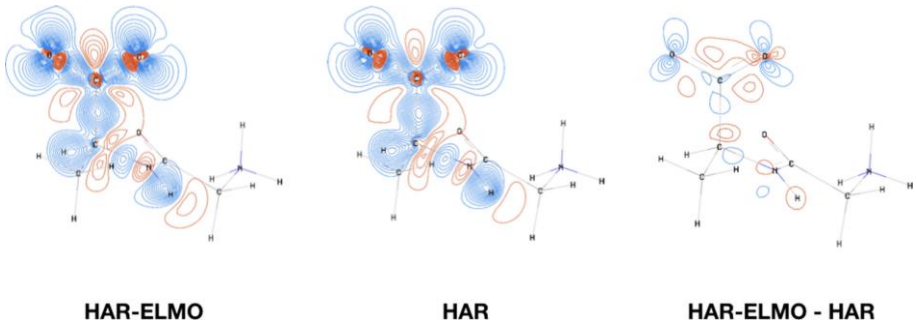

Figure S55: Deformation density maps for Gly-*L*-Ala in the plane of the carboxylic group for the HAR-ELMO and HAR refinements at 50 K. The difference between the HAR-ELMO and HAR deformation density maps is also shown. Contour levels: from 0.05 to 1.00 eÅ^{-3} with a step of 0.05 eÅ^{-3}. Colours in the deformation density maps: blue (positive) and red (negative).

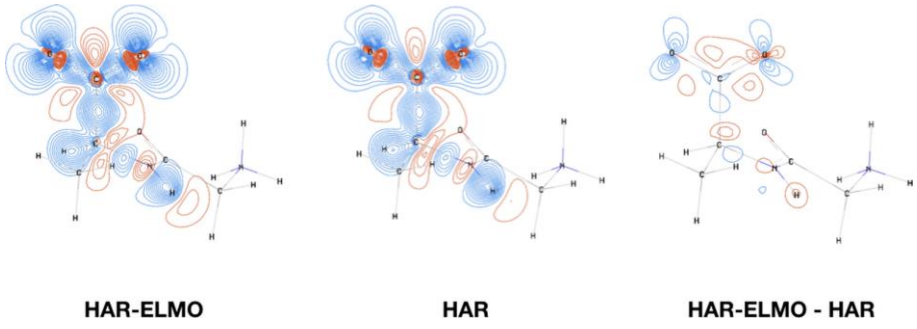

Figure S56: Deformation density maps for Gly-*L*-Ala in the plane of the carboxylic group for the HAR-ELMO and HAR refinements at 100 K. The difference between the HAR-ELMO and HAR deformation density maps is also shown. Contour levels: from 0.05 to 1.00 eÅ^{-3} with a step of 0.05 eÅ^{-3}. Colours in the deformation density maps: blue (positive) and red (negative).

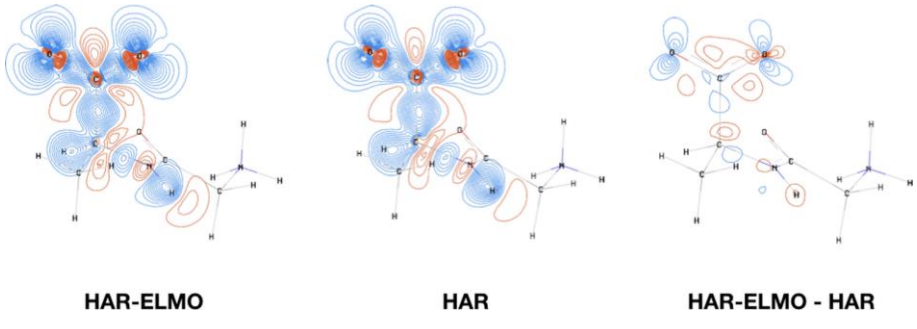

Figure S57: Deformation density maps for Gly-*L*-Ala in the plane of the carboxylic group for the HAR-ELMO and HAR refinements at 150 K. The difference between the HAR-ELMO and HAR deformation density maps is also shown. Contour levels: from 0.05 to 1.00 eÅ^{-3} with a step of 0.05 eÅ^{-3}. Colours in the deformation density maps: blue (positive) and red (negative).

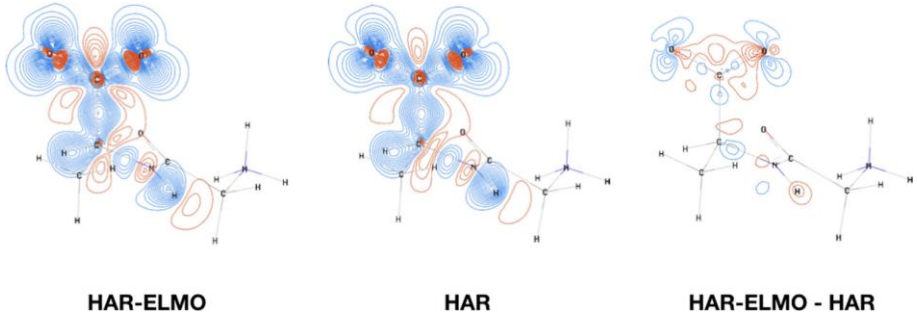

Figure S58: Deformation density maps for Gly-*L*-Ala in the plane of the carboxylic group for the HAR-ELMO and HAR refinements at 295 K. The difference between the HAR-ELMO and HAR deformation density maps is also shown. Contour levels: from 0.05 to 1.00 eÅ^{-3} with a step of 0.05 eÅ^{-3}. Colours in the deformation density maps: blue (positive) and red (negative).

Gly-*L*-Ala – Deformation Densities (peptide bond plane)

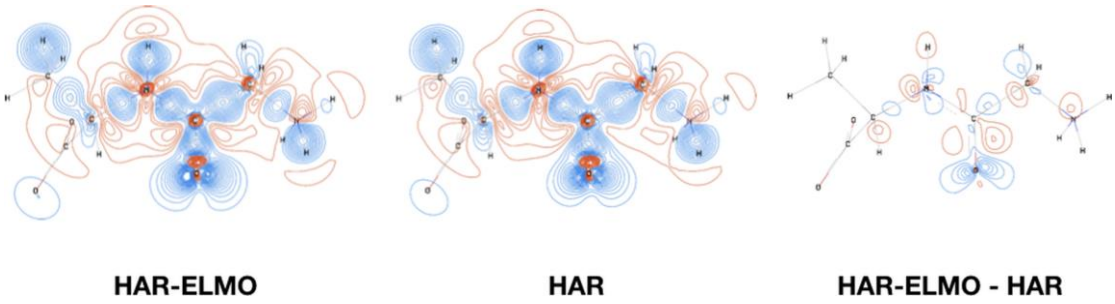

Figure S59: Deformation density maps for Gly-*L*-Ala in the plane of the peptide bond for the HAR-ELMO and HAR refinements at 12 K. The difference between the HAR-ELMO and HAR deformation density maps is also shown. Contour levels: from 0.05 to 1.00 eÅ^{-3} with a step of 0.05 eÅ^{-3}. Colours in the deformation density maps: blue (positive) and red (negative).

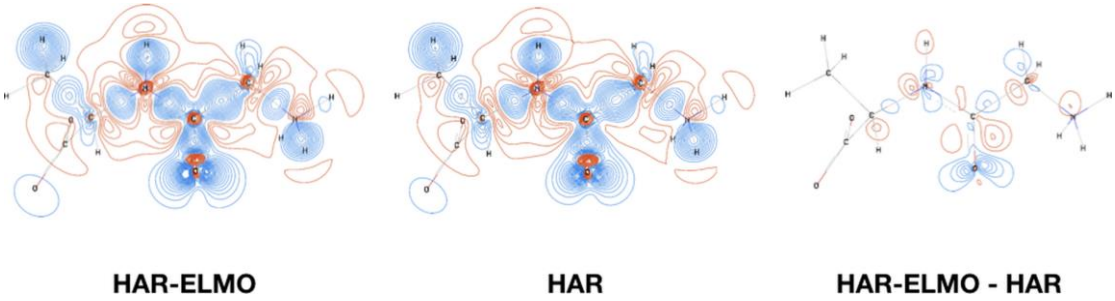

Figure S60: Deformation density maps for Gly-*L*-Ala in the plane of the peptide bond for the HAR-ELMO and HAR refinements at 50 K. The difference between the HAR-ELMO and HAR deformation density maps is also shown. Contour levels: from 0.05 to 1.00 eÅ^{-3} with a step of 0.05 eÅ^{-3}. Colours in the deformation density maps: blue (positive) and red (negative).

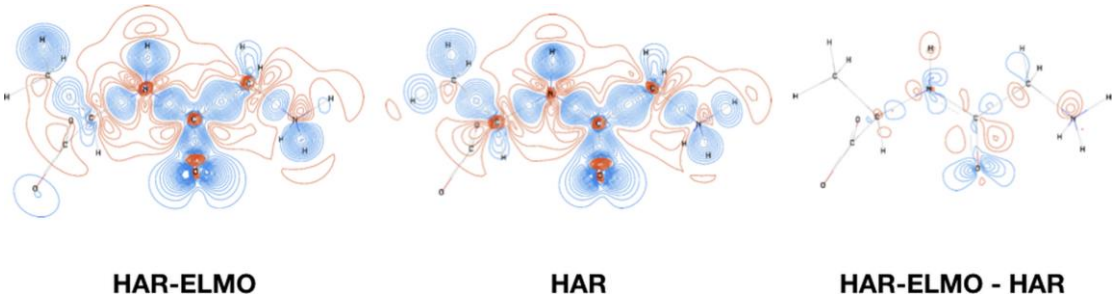

Figure S61: Deformation density maps for Gly-*L*-Ala in the plane of the peptide bond for the HAR-ELMO and HAR refinements at 100 K. The difference between the HAR-ELMO and HAR deformation density maps is also shown. Contour levels: from 0.05 to 1.00 eÅ^{-3} with a step of 0.05 eÅ^{-3}. Colours in the deformation density maps: blue (positive) and red (negative).

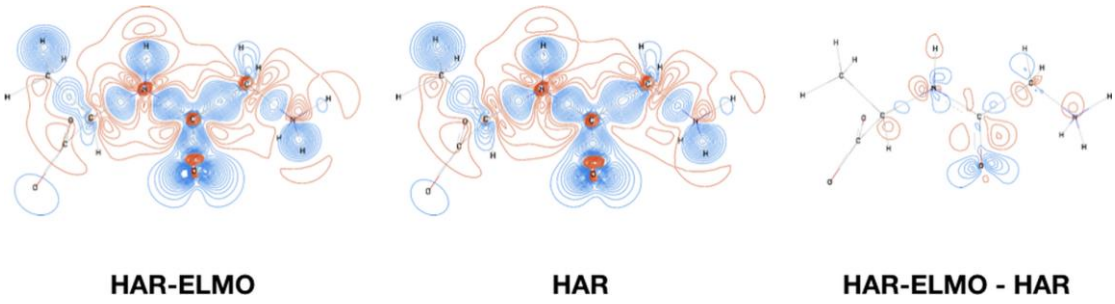

Figure S62: Deformation density maps for Gly-*L*-Ala in the plane of the peptide bond for the HAR-ELMO and HAR refinements at 150 K. The difference between the HAR-ELMO and HAR deformation density maps is also shown. Contour levels: from 0.05 to 1.00 eÅ^{-3} with a step of 0.05 eÅ^{-3}. Colours in the deformation density maps: blue (positive) and red (negative).

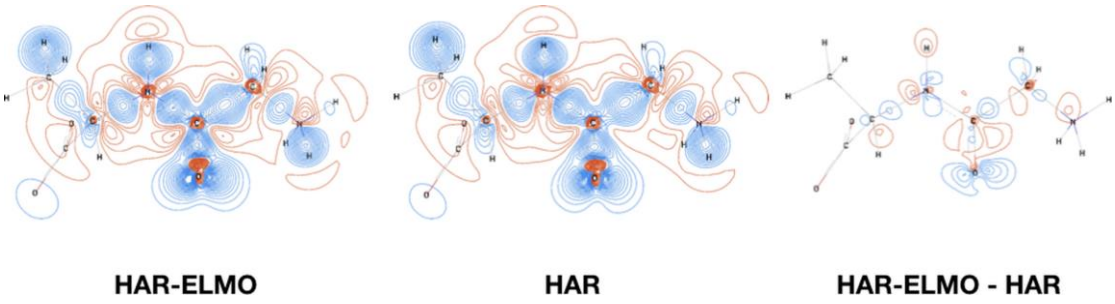

Figure S63: Deformation density maps for Gly-*L*-Ala in the plane of the peptide bond for the HAR-ELMO and HAR refinements at 295 K. The difference between the HAR-ELMO and HAR deformation density maps is also shown. Contour levels: from 0.05 to 1.00 eÅ^{-3} with a step of 0.05 eÅ^{-3}. Colours in the deformation density maps: blue (positive) and red (negative).

L-alanine – Deformation Densities (carboxylate group plane)

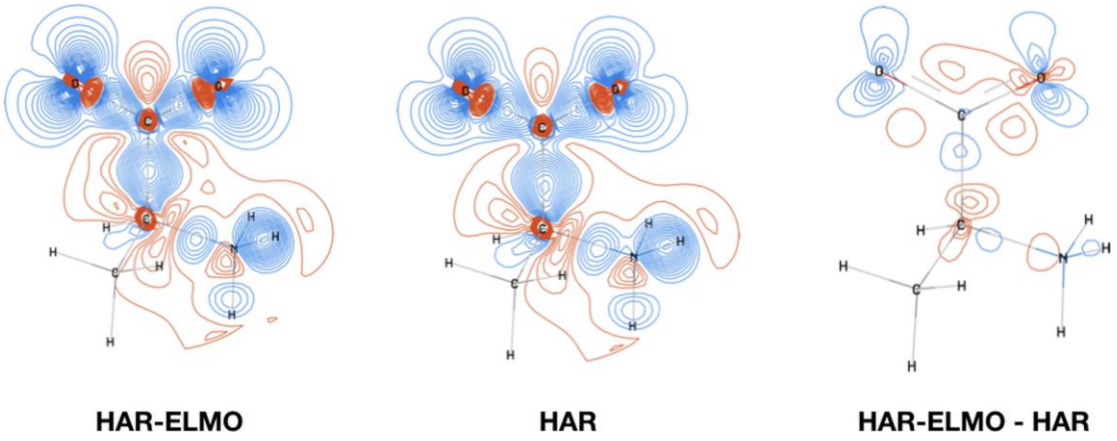

Figure S64: Deformation density maps for *L*-Ala in the plane of the carboxylic group for the HAR-ELMO and HAR refinements at 23 K. The difference between the HAR-ELMO and HAR deformation density maps is also shown. Contour levels: from 0.05 to 1.00 eÅ^{-3} with a step of 0.05 eÅ^{-3}. Colours in the deformation density maps: blue (positive) and red (negative).

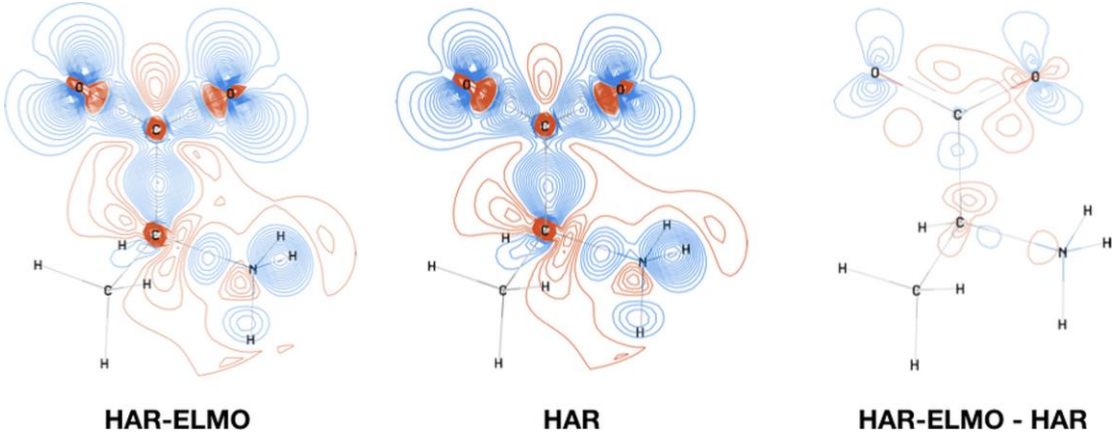

Figure S65: Deformation density maps for *L*-Ala in the plane of the carboxylic group for the HAR-ELMO and HAR refinements at 100 K. The difference between the HAR-ELMO and HAR deformation density maps is also shown. Contour levels: from 0.05 to 1.00 eÅ^{-3} with a step of 0.05 eÅ^{-3}. Colours in the deformation density maps: blue (positive) and red (negative).

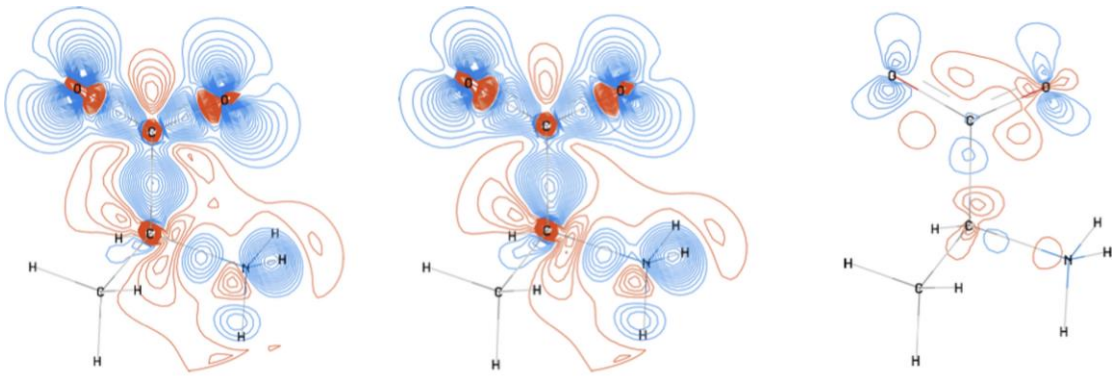

Figure S66: Deformation density maps for *L*-Ala in the plane of the carboxylic group for the HAR-ELMO and HAR refinements at 150 K. The difference between the HAR-ELMO and HAR deformation density maps is also shown. Contour levels: from 0.05 to 1.00 eÅ^{-3} with a step of 0.05 eÅ^{-3}. Colours in the deformation density maps: blue (positive) and red (negative).

L-alanine – Deformation Densities (NCC plane)

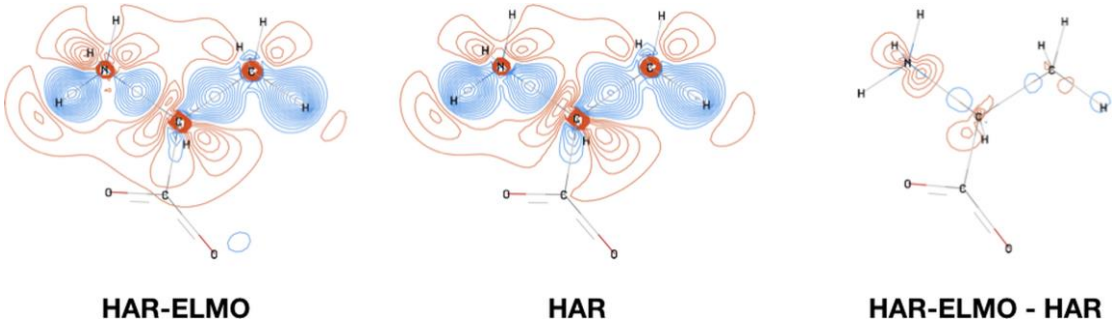

Figure S67: Deformation density maps for *L*-Ala in the N-Cα-Cβ plane for the HAR-ELMO and HAR refinements at 23 K. The difference between the HAR-ELMO and HAR deformation density maps is also shown. Contour levels: from 0.05 to 1.00 eÅ^{-3} with a step of 0.05 eÅ^{-3}. Colours in the deformation density maps: blue (positive) and red (negative).

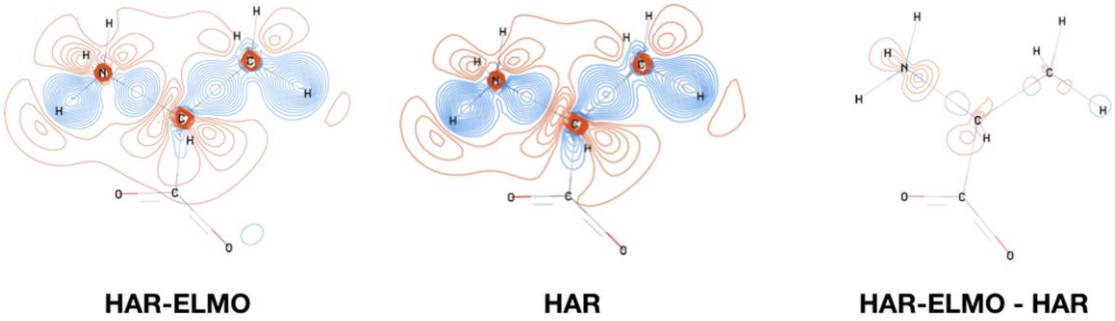

Figure S68: Deformation density maps for *L*-Ala in the N-Cα-Cβ plane for the HAR-ELMO and HAR refinements at 100 K. The difference between the HAR-ELMO and HAR deformation density maps is also shown. Contour levels: from 0.05 to 1.00 eÅ^{-3} with a step of 0.05 eÅ^{-3}. Colours in the deformation density maps: blue (positive) and red (negative).

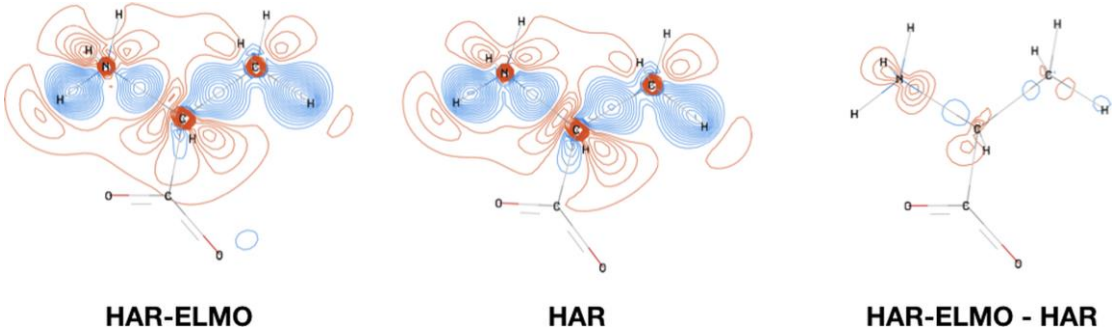

Figure S69: Deformation density maps for *L*-Ala in the N-Cα-Cβ plane for the HAR-ELMO and HAR refinements at 150 K. The difference between the HAR-ELMO and HAR deformation density maps is also shown. Contour levels: from 0.05 to 1.00 eÅ^{-3} with a step of 0.05 eÅ^{-3}. Colours in the deformation density maps: blue (positive) and red (negative).

Gly-*L*-Ala – 3D Deformation Densities

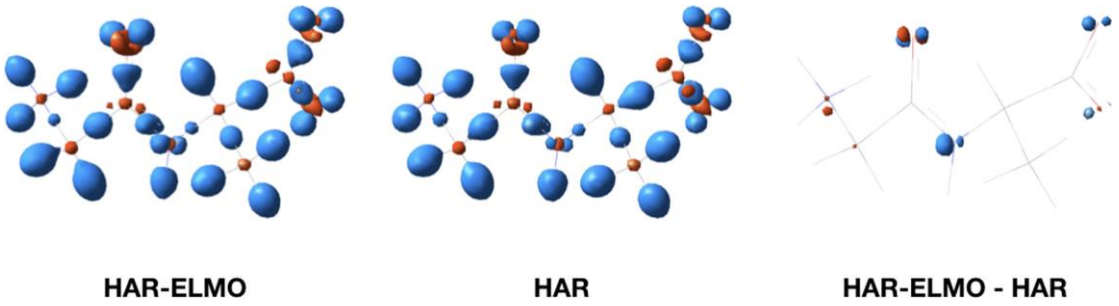

Figure S70: Deformation densities of Gly-*L*-Ala corresponding to the HAR-ELMO and HAR refinements at 12 K (isosurface level: 0.4 eÅ^{-3}). The difference between the HAR-ELMO and HAR deformation densities is also shown (isosurface level: 0.2 eÅ^{-3}). Colours in the deformation density plots: blue (positive) and red (negative).

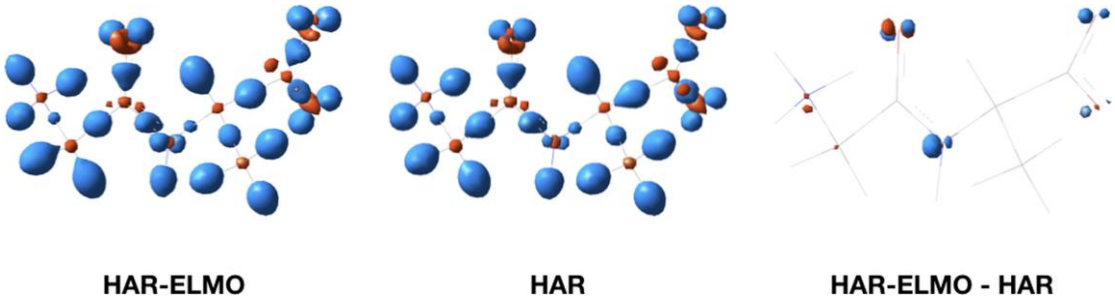

Figure S71: Deformation densities of Gly-*L*-Ala corresponding to the HAR-ELMO and HAR refinements at 50 K (isosurface level: 0.4 eÅ^{-3}). The difference between the HAR-ELMO and HAR deformation densities is also shown (isosurface level: 0.2 eÅ^{-3}). Colours in the deformation density plots: blue (positive) and red (negative).

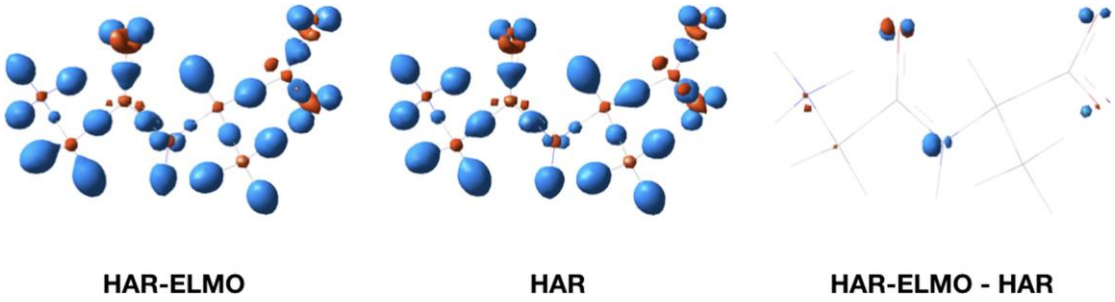

Figure S72: Deformation densities of Gly-*L*-Ala corresponding to the HAR-ELMO and HAR refinements at 100 K (isosurface level: 0.4 eÅ^{-3}). The difference between the HAR-ELMO and HAR deformation densities is also shown (isosurface level: 0.2 eÅ^{-3}). Colours in the deformation density plots: blue (positive) and red (negative).

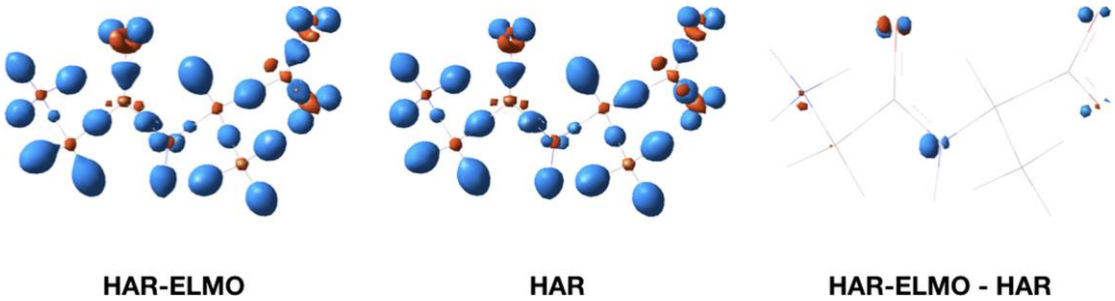

Figure S73: Deformation densities of Gly-*L*-Ala corresponding to the HAR-ELMO and HAR refinements at 150 K (isosurface level: 0.4 eÅ^{-3}). The difference between the HAR-ELMO and HAR deformation densities is also shown (isosurface level: 0.2 eÅ^{-3}). Colours in the deformation density plots: blue (positive) and red (negative).

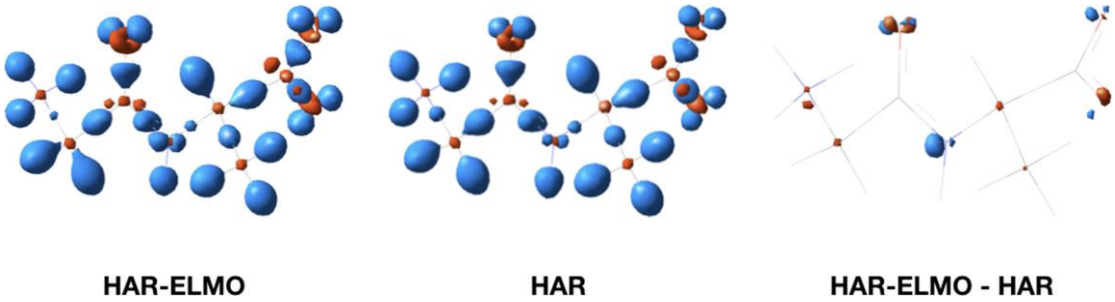

Figure S74: Deformation densities of Gly-*L*-Ala corresponding to the HAR-ELMO and HAR refinements at 295 K (isosurface level: 0.4 eÅ^{-3}). The difference between the HAR-ELMO and HAR deformation densities is also shown (isosurface level: 0.2 eÅ^{-3}). Colours in the deformation density plots: blue (positive) and red (negative).

L-alanine – 3D Deformation Densities

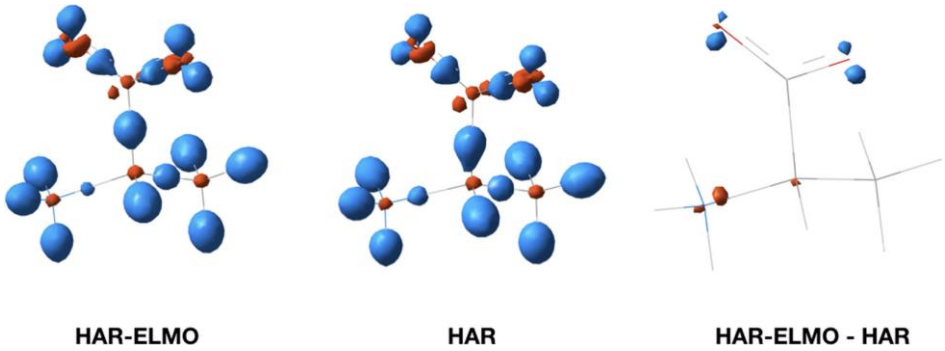

Figure S75: Deformation densities of *L*-Ala corresponding to the HAR-ELMO and HAR refinements at 23 K (isosurface level: 0.4 eÅ^{-3}). The difference between the HAR-ELMO and HAR deformation densities is also shown (isosurface level: 0.2 eÅ^{-3}). Colours in the deformation density plots: blue (positive) and red (negative).

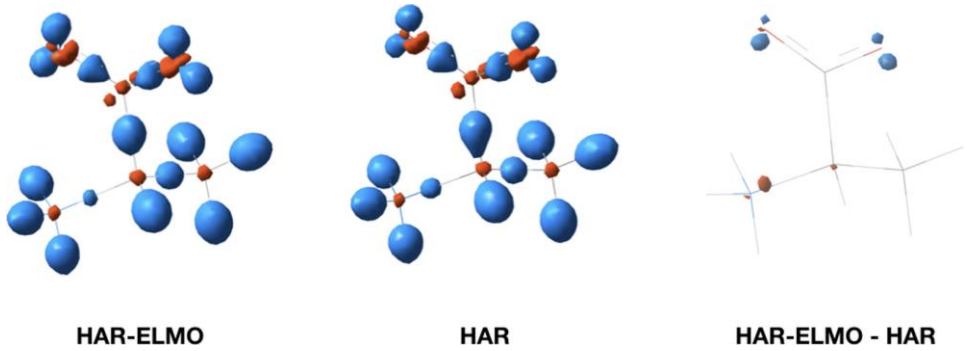

Figure S76: Deformation densities of *L*-Ala corresponding to the HAR-ELMO and HAR refinements at 100 K (isosurface level: 0.4 eÅ^{-3}). The difference between the HAR-ELMO and HAR deformation densities is also shown (isosurface level: 0.2 eÅ^{-3}). Colours in the deformation density plots: blue (positive) and red (negative).

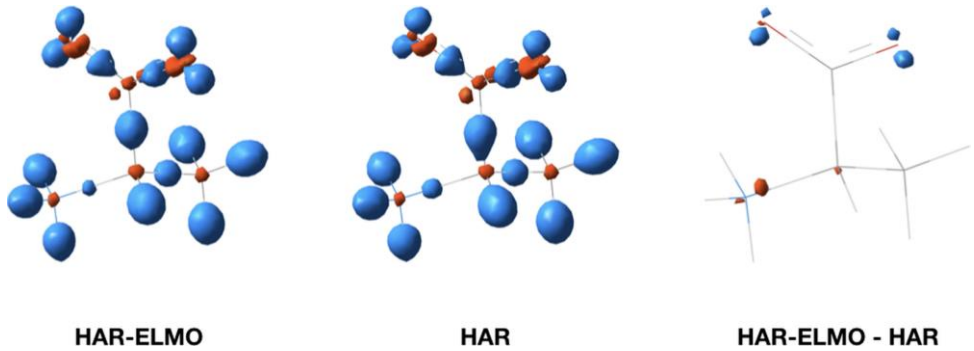

Figure S77: Deformation densities of *L*-Ala corresponding to the HAR-ELMO and HAR refinements at 150 K (isosurface level: 0.4 eÅ^{-3}). The difference between the HAR-ELMO and HAR deformation densities is also shown (isosurface level: 0.2 eÅ^{-3}). Colours in the deformation density plots: blue (positive) and red (negative).

Polypeptides and Protein Refinements

Refinement details

Fibril-forming segment of the human prion protein (original PDB file: 2OL9)[S15]

All the new refinements (IAM, HAR and HAR-ELMO) of the fibril-forming segment of the human prion protein were successfully completed including refinement of hydrogen atoms that were previously missing from the deposited structure. To accomplish this task, we treated all the hydrogen atoms isotropically except those belonging to the water molecules and hydrogen atom H1D, which were geometrically added through the *tleap* software associated with the AMBER Molecular Dynamics package[S16]. All the water molecules were kept fixed during the refinements.

Some of the ADPs in all refinements (IAM, HAR and HAR-ELMO) are NPD, even for non-hydrogen atoms. Anyway, for HAR-ELMO, X-H bond distances are still reasonable (see main text). This shows that HAR-ELMO is feasible for low-quality data, and opens the method for evaluation of many already deposited polypeptide and protein structures in the future.

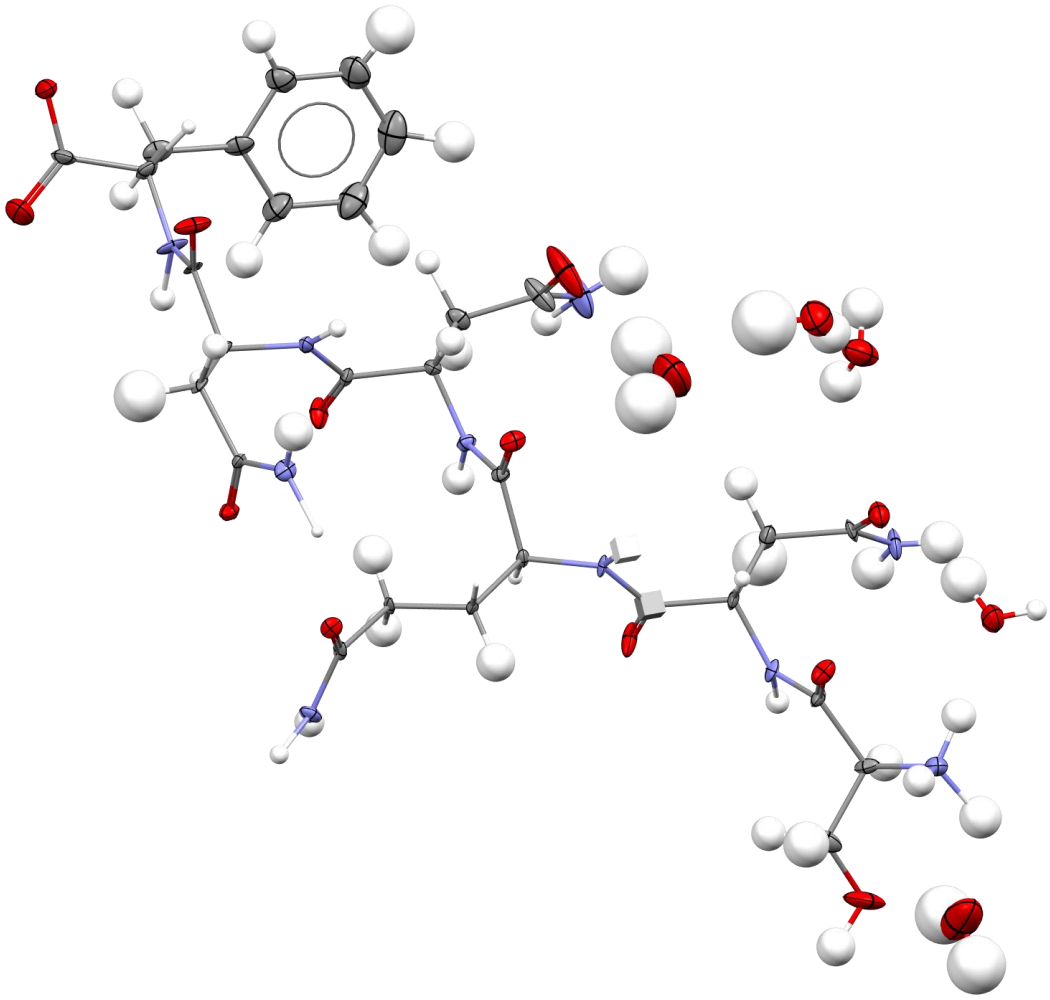

Figure S78: HAR molecular structure of the fibril-forming segment of the human prion protein with ADPs at 50% probability. NPD atoms depicted as boxes.

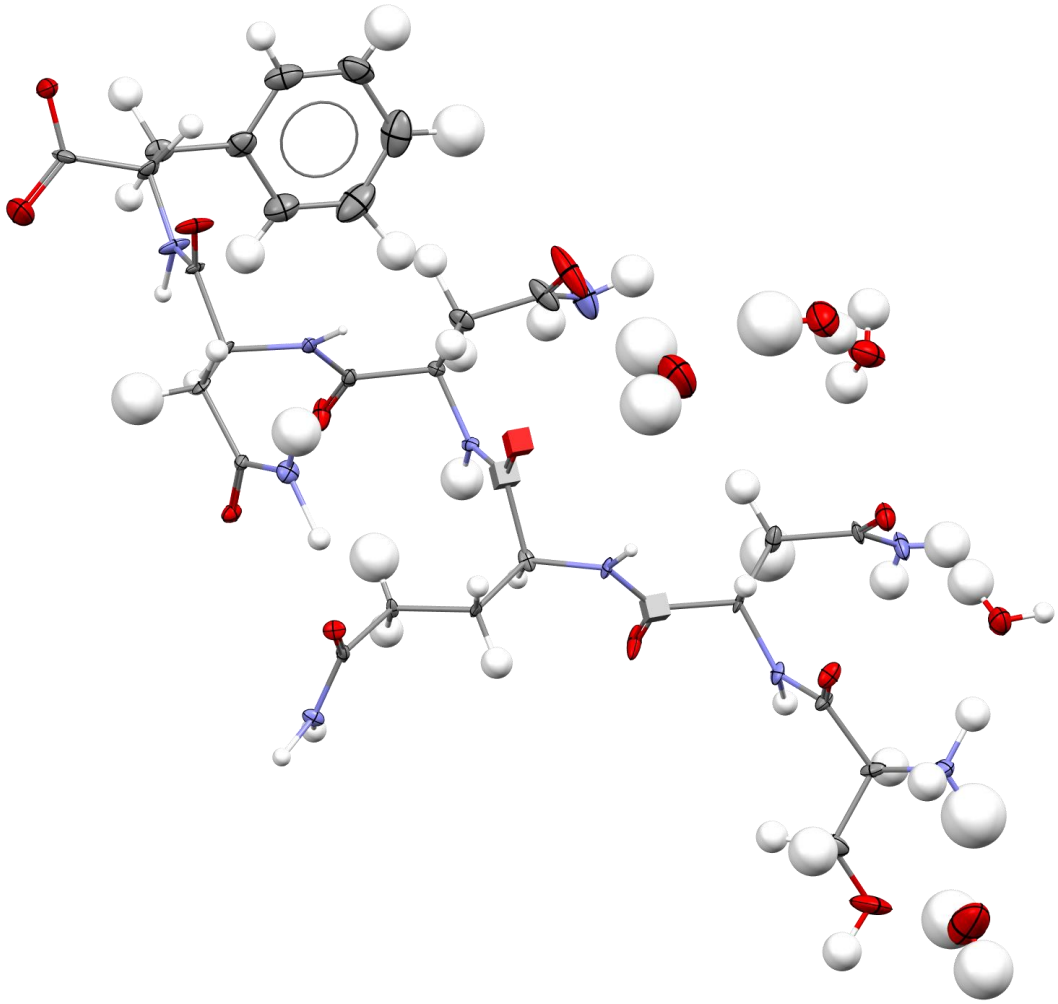

Figure S79: HAR-ELMO molecular structure of the fibril-forming segment of the human prion protein with ADPs at 50% probability. NPD atoms depicted as boxes.

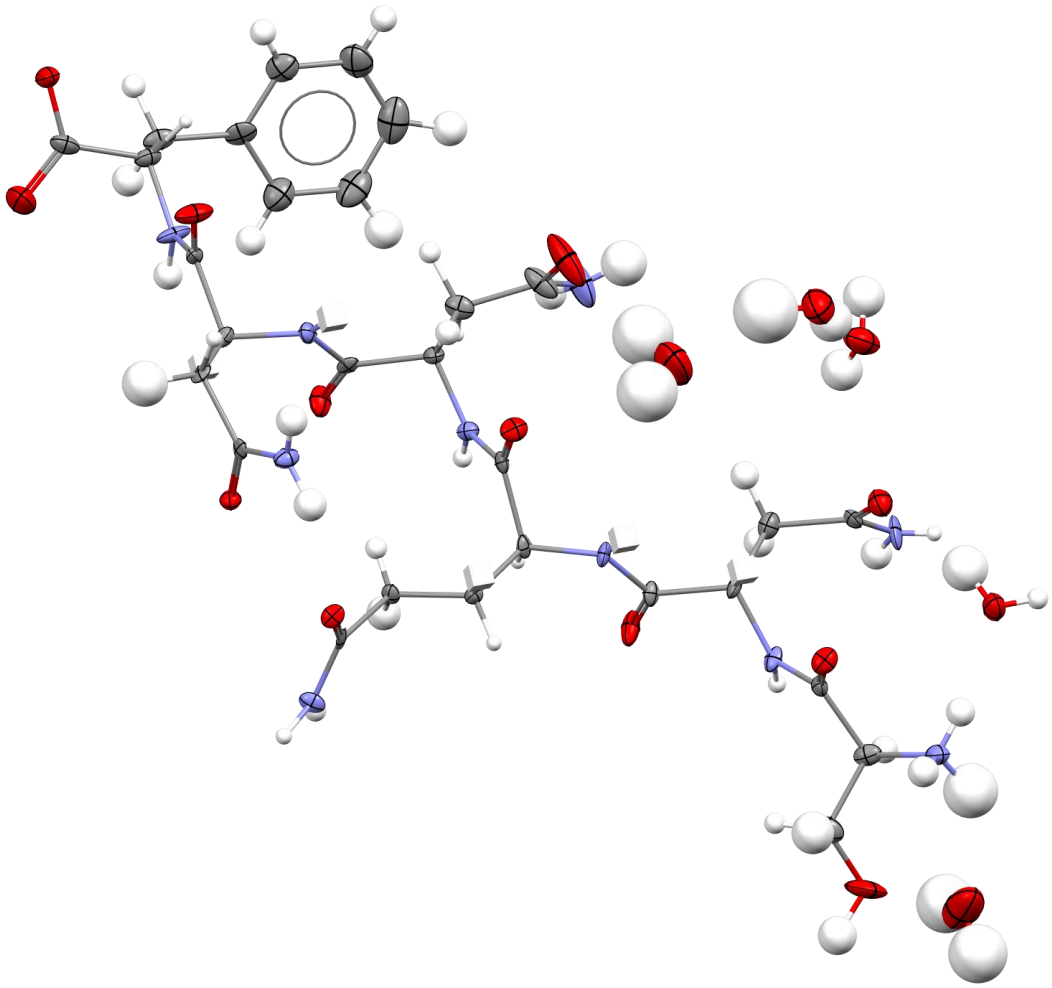

Figure S80: IAM molecular structure of the fibril-forming segment of the human prion protein with ADPs at 50% probability. NPD atoms depicted as boxes.

Table S20: Measurement details for the fibril-forming segment of the human prion protein (previously deposited in the protein data bank by Sawaya *et al.*[S15]). Information missing in this table was not given in the original paper and deposited structure.

PDB code	2OL9
Chemical formula	$C_{29}H_{42}N_{10}O_{12}\cdot 5(H_2O)$
M*$_r$ *(u)	812.80
Crystal system	Triclinic
Space group	*P*1
***a, b, c* (Å)**	14.0020, 4.8790, 15.1000
α, β, γ (°)	75.2340, 75.880, 78.8940
***V* (*Å*^{3})**	957.96
Z	1
Diffractometer	ALS BEAMLINE 8.2.2 diffractometer
Radiation type	Synchrotron
Wavelength (Å)	0.88560
Temperature (K)	100
Crystal size (mm)	
Absorption cor.	-
***μ* (mm^{-1})**	0.20
Tmin	-
Tmax	-
Extintion correction.	none
Resolution (Å)	0.85
hkl ranges	$h = -14, 15$ $k = -4, 4$ $l = 0, 17$
Theta min	1.887
Theta max	31.359
Theta full	31.359
Complet. (max)	0.8211
Complet. (full)	0.8211
Refl. Measured	3264
Unique refl.	2680
Unique obs. refl.	2642
Obs. criteria	$F > 0$ & F/u(F) > 3.0 & $\|F\_calc\| > 10^{-3}$
***R*int**	0.036
***R*sym**	-

Table S21: Refinement of X-ray data for the fibril-forming segment of the human prion protein. CCDC deposition nos.: 1917596-1917598.

	HAR	**HAR-ELMO**	**IAM**
R*[*F*>3σ(*F*)], *wR*(*F*), *S	0.044, 0.052, 3.15	0.047, 0.057, 3.45	0.045, 0.053, 3.20
No. of reflections	2642	2642	2642
No. of parameters	624	624	624
No. of restraints	0	0	0
No. of constraints	349	349	349
H-atom treatment	H atoms treated isotropically.	H atoms treated isotropically.	H atoms treated isotropically.
$(\Delta/\sigma)_{max}$	0.004	< 0.001	< 0.001
$\Delta\rho_{max}$, $\Delta\rho_{min}$ (eÅ^{-3})	0.51, −0.39	0.51, −0.41	0.50, −0.38

Leu-Enkephalin (original CSD entry GEWWAG01)[S17]

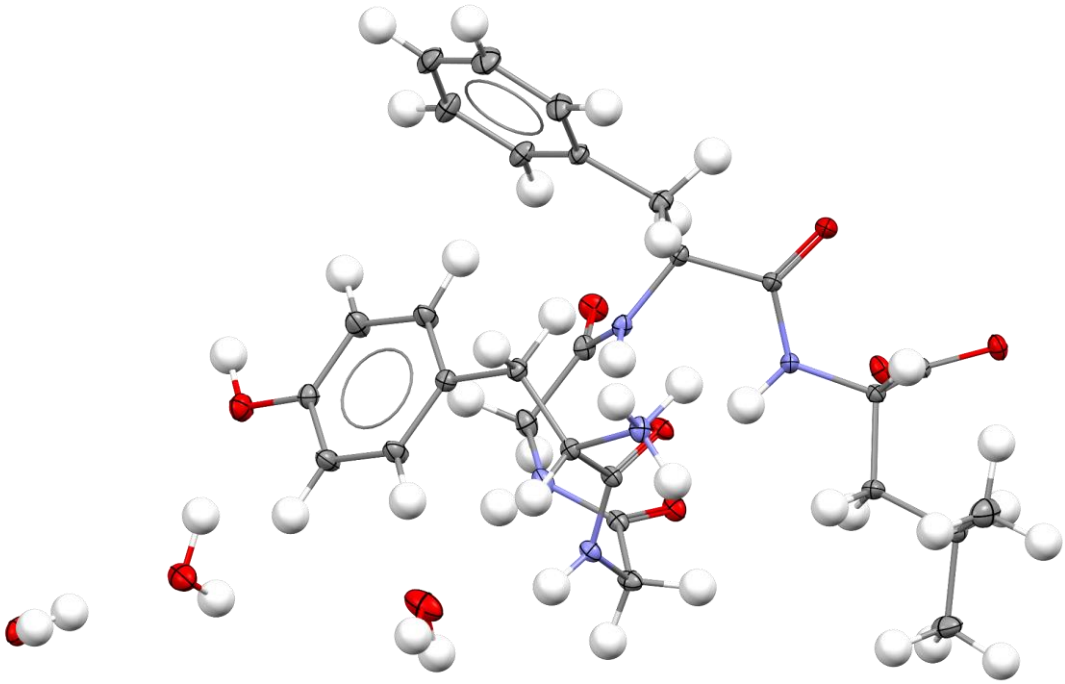

Figure S81: HAR molecular structure of Leu-enkephalin with ADPs depicted at a 50% probability level.

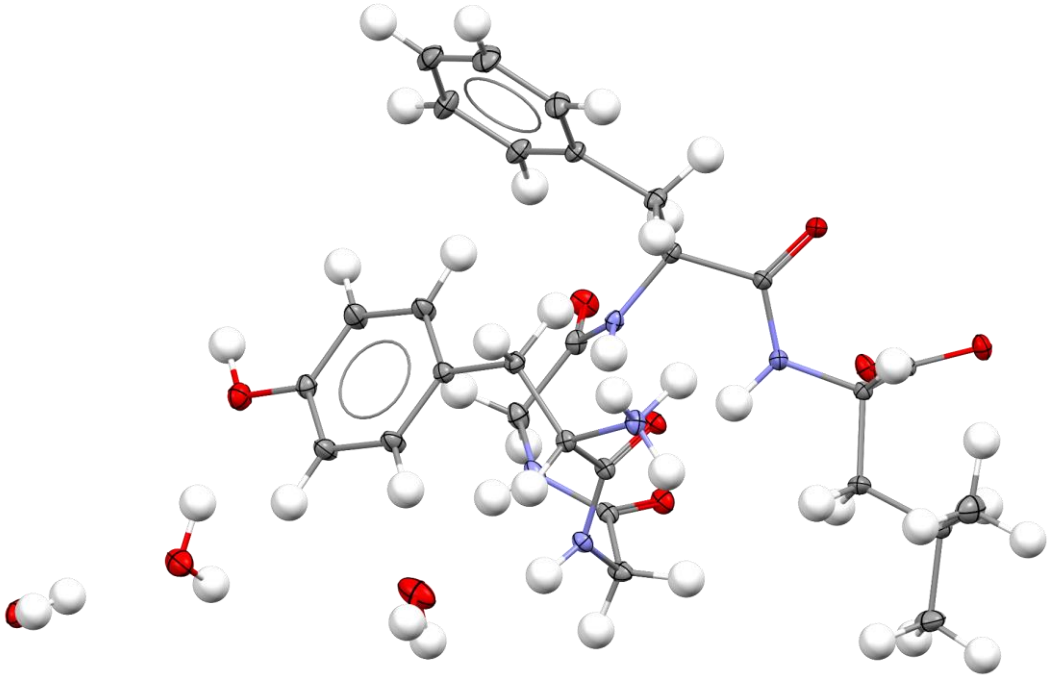

Figure S82: HAR-ELMO molecular structure of Leu-enkephalin with ADPs depicted at a 50% probability level.

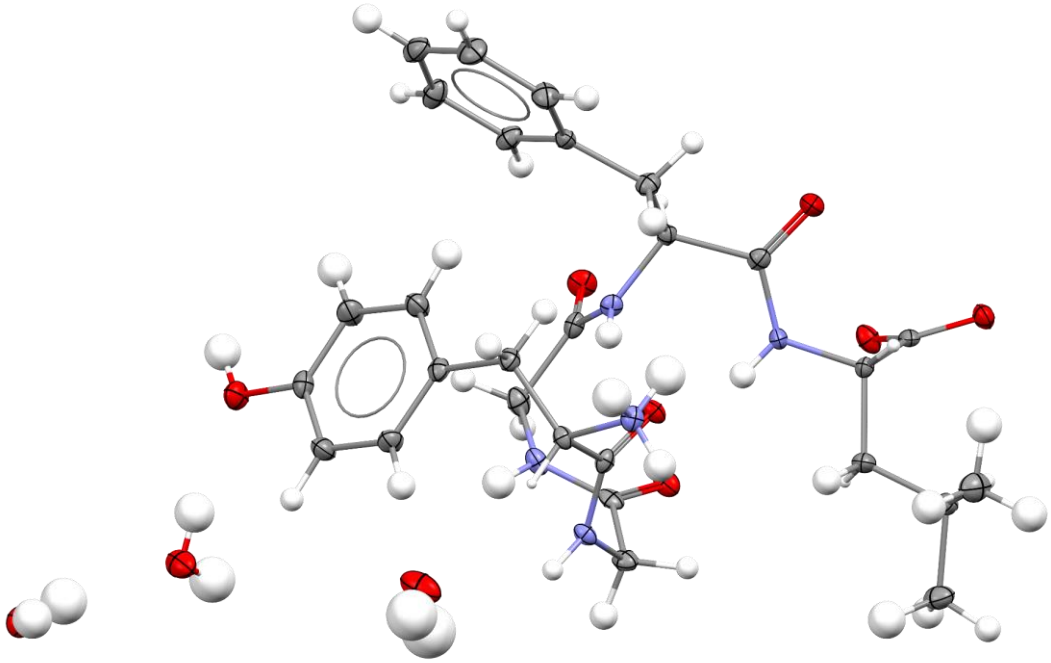

Figure S83: IAM molecular structure of Leu-enkephalin with ADPs depicted at a 50% probability level.

Table S22: Measurement details for Leu-enkephalin (previously deposited. in the Cambridge structural database by Pichon-Pesme *et al.*[S17]). Information missing in this table was not given in the original paper and deposited structure.

CSD entry	GEWWAG01
Chemical formula	$C_{28}H_{37}N_5O_7 \cdot 3(H_2O)$
***M*r (u)**	609.68
Crystal system	Orthorhombic
Space group	$P2_12_12_1$
***a, b, c* (Å)**	10.851 (4), 13.095 (3), 21.192 (4)
***V* (Å^3)**	3011.3 (14)
Z	4
Diffractometer	CAD4F diffractometer
Radiation type	MoKα
Wavelength (Å)	0.71073
Temperature (K)	100
Crystal size (mm)	-
Absorption cor.	-
***μ* (mm^{-1})**	0.10
***T*min**	-
***T*max**	-
Extintion correction.	none
Resolution (Å)	0.43
hkl ranges	*h= 0, 24* *k= 0, 29* *l= 0, 45*
Theta min	1.828
Theta max	54.797
Theta full	25.242
Complet. (max)	0.526
Complet. (full)	0.959
Refl. Measured	40844
Unique refl.	10777
Unique obs. refl.	5851
Obs. criteria	$F > 0$ & $F/u(F) > 3.0$ & $\|F\_calc\| > 10^{-3}$
***R*int**	-
***R*merge**	-

Table S23: Refinement of X-ray data for Leu-enkephalin. CCDC deposition nos.: 1917730-1917732.

	HAR	**HAR-ELMO**	**IAM**
R*[*F*>3σ(*F*)], *wR*(*F*), *S	0.042, 0.023, 0.71	0.043, 0.024, 0.74	0.056, 0.034, 1.03
No. of reflections	5851	5851	5851
No. of parameters	560	560	560
No. of restraints	0	0	0
No. of constraints	215	215	215
H-atom treatment	H atoms treated isotropically.	H atoms treated isotropically.	H atoms treated isotropically.
$(\Delta/\sigma)_{max}$	0.006	< 0.001	< 0.001
$\Delta\rho_{max}$, $\Delta\rho_{min}$ (eÅ^{-3})	0.20, −0.22	0.21, −0.22	0.29, −0.32

Crambin (original PDB file: 1EJG [S18]***)***

The X-ray data set used in this study is the one associated with the PDB structure 1EJG previously deposited for the protein crambin. Notwithstanding the authors reported a refinement including solvent molecules, these were not present in the deposited PDB file. Fourier difference maps clearly showed regions of solvent residual densities that were not modelled. Consequently, the PLATON/SQUEEZE tool was applied to calculate the void space and extract its scattering contribution from the reflection list. Missing hydrogen atoms were placed according to calculated positions using the *tleap* utility of the AMBER Molecular Dynamics package.[S16] Furthermore, since at the moment HAR and HAR-ELMO techniques cannot properly treat disorder, only the atoms belonging to the major components in the disordered parts of the protein were modelled by assigning them full occupancies.

After this preliminary step, an unconstrained structure refinement of crambin was performed against the modified set of structure factors, using the IAM procedure inside the software TONTO, at maximum resolution (d=0.54 Å) and one considering a subset of the data set (d=0.73 Å). Subsequently, HAR-ELMO and another IAM were performed with parameters for all atoms belonging to the disordered regions kept fixed, based on the values obtained from the first IAM. Other than these, a few other atoms belonging to the outermost flexible loop of crambin were also kept fixed to guarantee convergence and a high precision of the final structure. In all cases, all the refined hydrogen atoms were treated isotropically, while all the refined non-hydrogen atoms were treated anisotropically.

For the sake of completeness, we report the list of atoms that we fixed during the refinements in Table S24.

Table S24: Crambin atoms (with corresponding residues and labels in the original PDB file) that were fixed during the HAR-ELMO refinements.

Label in cif file	Residue		Label in pdb file
N3	THR	1	N
H1	THR	1	H1
H2	THR	1	H2
H3	THR	1	H3
C7	THR	1	CB
H8	THR	1	HB
H4	THR	1	HG1
C8	THR	1	CG2
H5	THR	1	HG21
H6	THR	1	HG22
H7	THR	1	HG23
C4	THR	2	CA
C9	THR	2	CB
H15	THR	2	HB
O4	THR	2	OG1
H11	THR	2	HG1
C10	THR	2	CG2
H12	THR	2	HG21
H13	THR	2	HG22
H14	THR	2	HG23
H309	CYS	4	HB3
H18	PRO	5	HB2
H19	PRO	5	HB3
H26	SER	6	HG
C64	ILE	7	C
O30	ILE	7	O
C65	ILE	7	CA
H40	ILE	7	HA
C75	ILE	7	CB
H39	ILE	7	HB
C76	ILE	7	CG1
H34	ILE	7	HG12
H35	ILE	7	HG13
C78	ILE	7	CG2
H36	ILE	7	HG21
H37	ILE	7	HG22
H38	ILE	7	HG23
C77	ILE	7	CD1
H31	ILE	7	HD11
H32	ILE	7	HD12
H33	ILE	7	HD13

Label in cif file	Residue		Label in pdb file
C121	GLU	23	CG
H158	GLU	23	HG2
H159	GLU	23	HG3
C122	GLU	23	CD
O39	GLU	23	OE1
O40	GLU	23	OE2
H164	ALA	24	HB1
H165	ALA	24	HB2
H166	ALA	24	HB3
C124	LEU	25	CB
H176	LEU	25	HB2
H177	LEU	25	HB3
C125	LEU	25	CG
H175	LEU	25	HG
C126	LEU	25	CD1
H169	LEU	25	HD11
H170	LEU	25	HD12
H171	LEU	25	HD13
C127	LEU	25	CD2
H173	LEU	25	HD21
H174	LEU	25	HD22
H172	LEU	25	HD23
H188	THR	28	HG21
H189	THR	28	HG22
H190	THR	28	HG23
C21	TYR	29	CA
H201	TYR	29	HA
C132	TYR	29	CG
C133	TYR	29	CD1
H198	TYR	29	HD1
C137	TYR	29	CD2
H195	TYR	29	HD2
C134	TYR	29	CE1
H197	TYR	29	HE1
C136	TYR	29	CE2
H196	TYR	29	HE2
C135	TYR	29	CZ
O42	TYR	29	OH
H194	TYR	29	HH
H203	THR	30	HG1
H204	THR	30	HG21
H205	THR	30	HG22
H206	THR	30	HG23

Table S24: continued.

Label in cif file	Residue		Label in pdb file
N29	VAL	8	N
H41	VAL	8	H
C63	VAL	8	CA
H49	VAL	8	HA
C79	VAL	8	CB
H48	VAL	8	HB
C80	VAL	8	CG1
H42	VAL	8	HG11
H43	VAL	8	HG12
H44	VAL	8	HG13
C81	VAL	8	CG2
H45	VAL	8	HG21
H46	VAL	8	HG22
H47	VAL	8	HG23
C85	ARG	10	CD
H61	ARG	10	HD2
H62	ARG	10	HD3
H60	ARG	10	HE1
N33	ARG	10	NE
C86	ARG	10	CZ
N34	ARG	10	NH1
H56	ARG	10	HH11
H57	ARG	10	HH12
N35	ARG	10	NH2
H58	ARG	10	HH21
H59	ARG	10	HH22
C88	ASN	12	CB
H76	ASN	12	HB2
H77	ASN	12	HB3
C89	ASN	12	CG
N36	ASN	12	ND2
H74	ASN	12	HD21
H75	ASN	12	HD22
O36	ASN	12	OD1
C92	PHE	13	CD1
H84	PHE	13	HD1
C93	PHE	13	CE1
H83	PHE	13	HE1
C94	PHE	13	CZ
H82	PHE	13	HZ
C96	PHE	13	CD2
H80	PHE	13	HD2
C95	PHE	13	CE2
H81	PHE	13	HE2

Label in cif	Residue		Label in pdb file
H296	ILE	33	HD12
C195	ILE	34	CB
H292	ILE	34	HB
C196	ILE	34	CG1
H288	ILE	34	HG12
H287	ILE	34	HG13
C198	ILE	34	CG2
H289	ILE	34	HG21
H290	ILE	34	HG22
H291	ILE	34	HG23
C197	ILE	34	CD1
H284	ILE	34	HD11
H285	ILE	34	HD12
H286	ILE	34	HD13
H276	ILE	35	HG12
H277	ILE	35	HG13
H278	ILE	35	HG21
H279	ILE	35	HG22
H280	ILE	35	HG23
H273	ILE	35	HD11
H274	ILE	35	HD12
H275	ILE	35	HD13
C188	PRO	36	CB
H270	PRO	36	HB2
H271	PRO	36	HB3
C189	PRO	36	CG
H269	PRO	36	HG2
H268	PRO	36	HG3
H257	GLY	37	H
H261	ALA	38	HA
H258	ALA	38	HB1
H259	ALA	38	HB2
H260	ALA	38	HB3
H265	THR	39	H
C185	THR	39	CB
H255	THR	39	HB
O64	THR	39	OG1
C186	THR	39	CG2
H251	THR	39	HG1
H252	THR	39	HG21
H253	THR	39	HG22
H254	THR	39	HG23

Table S24: continued.

Label in cif file	Residue		Label in pdb file
H126	LEU	18	HD11
H127	LEU	18	HD12
H128	LEU	18	HD13
H123	LEU	18	HD21
H124	LEU	18	HD22
H125	LEU	18	HD23
C114	PRO	19	CB
H133	PRO	19	HB2
H134	PRO	19	HB3
C113	PRO	19	CG
H135	PRO	19	HG2
H136	PRO	19	HG3
C112	PRO	19	CD
H137	PRO	19	HD2
H138	PRO	19	HD3
C34	PRO	22	C
O15	PRO	22	O
C35	PRO	22	CA
H156	PRO	22	HA
C119	PRO	22	CB
H151	PRO	22	HB2
H150	PRO	22	HB3
C118	PRO	22	CG
H152	PRO	22	HG2
H153	PRO	22	HG3
C117	PRO	22	CD
H155	PRO	22	HD2
H154	PRO	22	HD3

Label in cif file	Residue		Label in pdb file
H246	PRO	41	HB2
H247	PRO	41	HB3
H245	PRO	41	HG2
H244	PRO	41	HG3
C180	ASP	43	CB
H235	ASP	43	HB2
H236	ASP	43	HB3
C181	ASP	43	CG
O62	ASP	43	OD1
O63	ASP	43	OD2
C170	ASN	46	CB
H217	ASN	46	HB2
H218	ASN	46	HB3
C171	ASN	46	CG
N55	ASN	46	ND2
H215	ASN	46	HD21
H216	ASN	46	HD22
O60	ASN	46	OD1

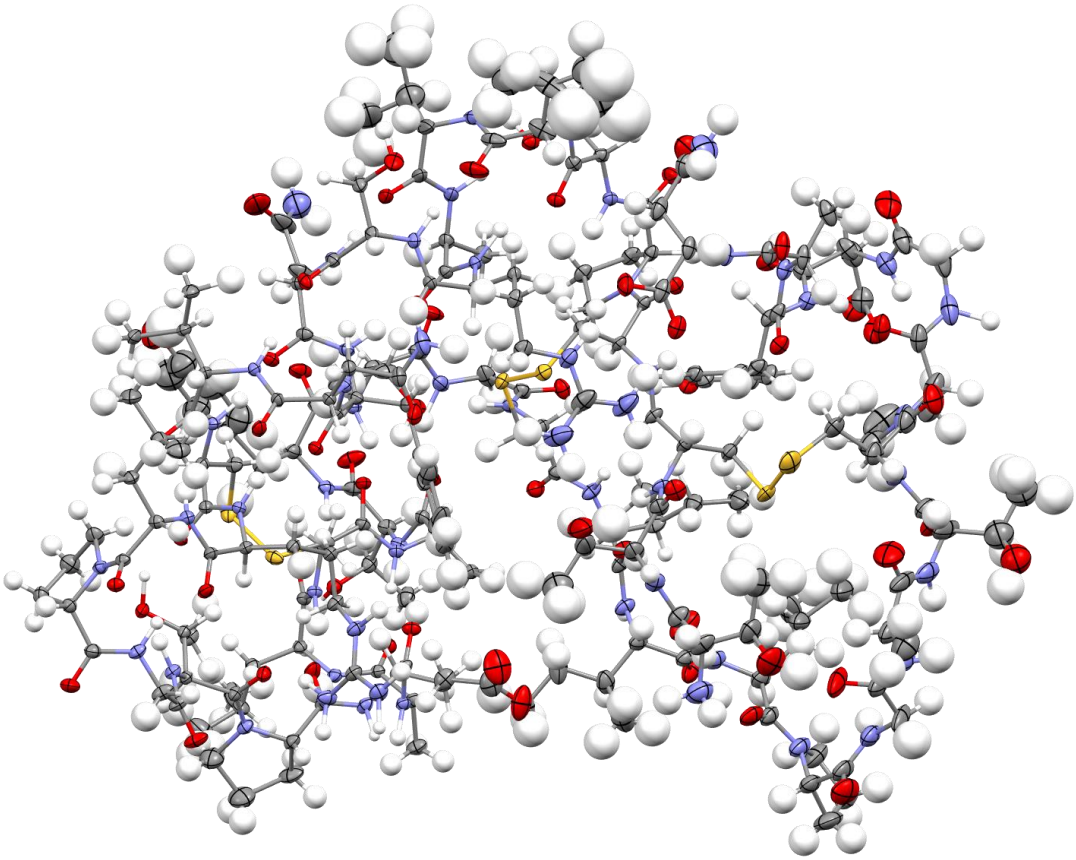

Figure S84: HAR-ELMO molecular structure of crambin (0.54 Å resolution data-set) with ADPs at a 50% probability level.

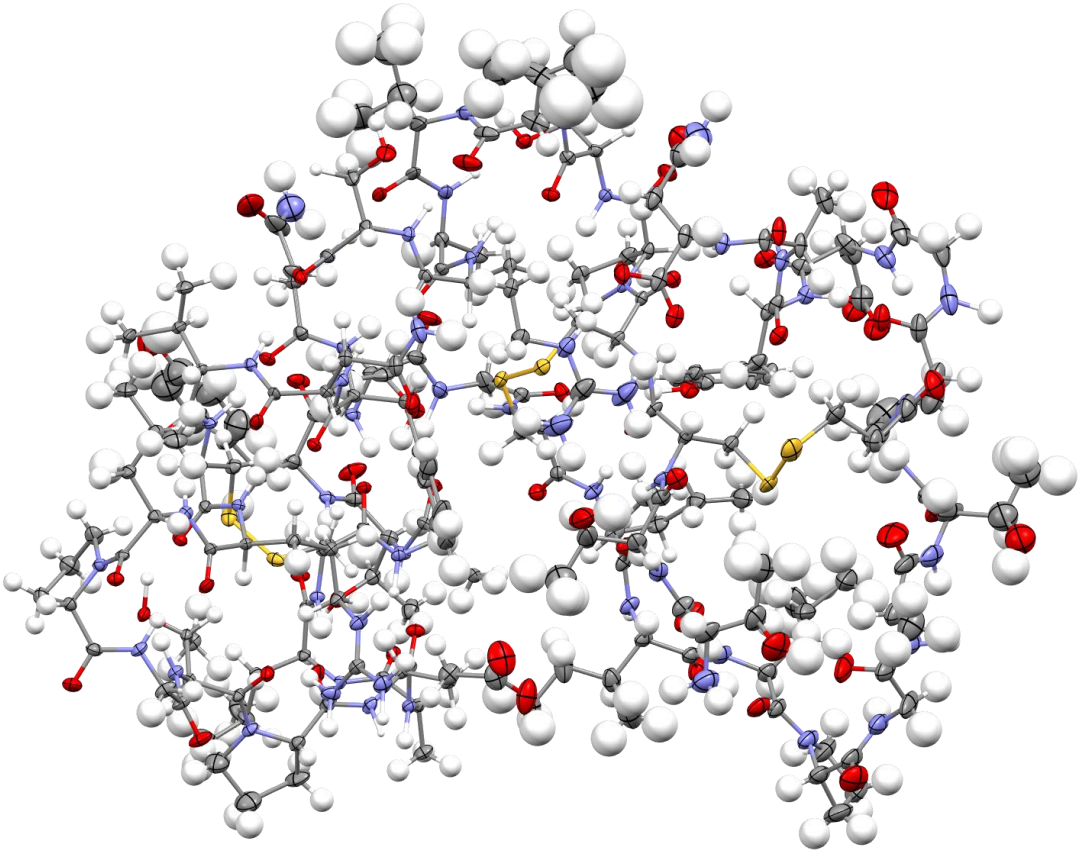

Figure S85: HAR-ELMO molecular structure of crambin (0.73 Å resolution data-set) with ADPs at a 50% probability level.

Table S25: Measurement details for crambin (previously deposited in the protein data bank by Jelsch *et al.*[S18]). Information missing in this table was not given in the original paper and deposited structure.

PDB code	1EJG	
Chemical formula	$C_{202}H_{315}N_{55}O_{64}S_6$	
***M*r (u)**	4730.48	
Crystal system	Monoclinic	
Space group	$P2_1$	
***a, b, c* (Å)**	40.824, 18.498, 22.371	
β (°)	90.47	
***V* (Å^3)**	16893.17	
Z	2	
Diffractometer	300-mm MarResearch imaging plate diffractometer	
Radiation type	Synchrotron	
Wavelength (Å)	0.54000	
Temperature (K)	100	
Crystal size (mm)	-	
Absorption cor.	none	
***μ* (mm^{-1})**	0.06	
***T*min**	-	
***T*max**	-	
Extintion correction.	none	
Resolution (Å)	0.54	0.73
hkl ranges	*h= -75, 75* *k= 0, 34* *l= 0, 41*	*h= -55, 55* *k= 0, 25* *l= 0, 30*
Theta min	0.692	0.692
Theta max	30.021	21.707
Theta full	18.905	18.905
Complet. (max)	0.976	0.992
Complet. (full)	0.994	0.994
Refl. Measured	489969	489969
Unique refl.	112233	46479
Unique obs. refl.	96139	45265
Obs. criteria	$F > 0$ & $F/u(F) > 3.0$ & $\|F\_calc\| > 10^{-3}$	$F > 0$ & $F/u(F) > 3.0$ & $\|F\_calc\| > 10^{-3}$
***R*int**	0.070	0.055

Table S26: Refinement of X-ray data for crambin.

	HAR-ELMO (0.54 Å)	**IAM (0.54 Å)**	**HAR-ELMO (0.73 Å)**	**IAM (0.73 Å)**
R[F>3σ(F)], wR(F), S	0.072, 0.084, 2.24	0.070, 0.083, 2.21	0.062, 0.079, 2.77	0.062, 0.078, 2.74
No. of reflections	96139	96139	45265	45265
No. of parameters	2965	2965	2965	2965
No. of restraints	0	0	0	0
No. of constraints	2814	2814	2814	2814
H-atom treatment	H atoms treated by a mixture of independent and constrained refinement	H atoms treated by a mixture of independent and constrained refinement	H atoms treated by a mixture of independent and constrained refinement	H atoms treated by a mixture of independent and constrained refinement
$(\Delta/\sigma)_{max}$	< 0.001	< 0.001	< 0.001	0.0516
$\Delta\rho_{max}$, $\Delta\rho_{min}$ (eÅ^{-3})	1.47, −0.77	1.51, −0.75	0.94, −0.68	0.96, −0.68

Comparison of hydrogen bond distances

Table S27: Averaged X-H bond distances (in Å) according to the Allen-Bruno classes[S19] for the fibril-forming segment of the human prion protein. The last column refers to the number of bond lengths in the class.

Allen-Bruno class	Neutron Reference [S19]	HAR	HAR-ELMO	IAM	#
X–H (all)		1.09(11)[a] 1.09(11)[b]	1.07(14)[a] 1.07(13)[b]	0.95(11)[a] 0.95(11)[b]	42[a] 41[b]
Z_3–Csp^3–H	1.098(11)	1.17(8)	1.13(10)	1.01(10)	6
Z_2–Csp^3–H_2	1.091(17)	1.12(9)	1.11(11)	1.01(10)	14
C_2–Csp^3–H_2	1.092(17)	1.11(9)	1.11(11)	1.01(11)	12
C(ar)–H	1.083(17)	1.08(7)	1.07(14)	0.96(8)	5
Z–O–H	0.983(25)	0.966(4)	0.967(4)	0.966(4)	1[c]
C(any)–O–H	0.980(21)	0.966(4)	0.967(4)	0.966(4)	1[c]
Csp^3–O–H	0.970(12)	0.966(4)	0.967(4)	0.966(4)	1[c]
N^+–H	1.036(16)	1.12(15)	1.04(5)	0.94(9)	3
Csp^2– N–H_2 (all)	1.013(9)	1.04(14)[a] 1.02(13)[b]	1.02(23)[a] 0.97(19)[b]	0.86(10)[a] 0.84(10)[b]	8[a] 7[b]
Csp^2– N–H_2 (N amido)	1.010(8)	1.04(14)[a] 1.02(13)[b]	1.02(23)[a] 0.97(19)[b]	0.86(10)[a] 0.84(10)[b]	8[a] 7[b]
Csp^2– N–H_2 (N pl)	1.012(8)	1.04(14)[a] 1.02(13)[b]	1.02(23)[a] 0.97(19)[b]	0.86(10)[a] 0.84(10)[b]	8[a] 7[b]
Z_2–N–H	1.027(16)	1.04(10)	1.04(11)	0.85(8)	5

[a] Including outliers.

[b] Excluding outliers. Outliers are defined as being outside the geometric criterion

$$d(i-j) < R(i) + R(j) + 0.4\ \text{Å}$$

[c] The values are the averages with the standard uncertainty of the bond lengths. If there is only one value in the Allen Bruno class, the bond length is taken from the CIF file and the error is the experimental error.

Table S28: Averaged X-H bond distances (in Å) according to the Allen-Bruno classes[S19] for Leu-enkephalin. The last column refers to the number of bond lengths in the class.

Allen-Bruno class	Neutron Reference[S19]	HAR	HAR-ELMO	IAM	#
X–H (all)		1.04(6)	1.04(7)	0.80(33)	43
Z_3–Csp^3–H	1.098(11)	1.08(3)	1.09(4)	0.59(49)	10
C_3–Csp^3–H	1.091(17)	1.09(3)	1.10(4)	0.44(51)	7
Z_2–Csp^3–H_2	1.092(17)	1.08(3)	1.09(3)	0.88(31)	10
C_2–Csp^3–H_2	1.083(17)	1.09(3)	1.10(3)	0.97(3)	6
C(ar)–H	0.983(25)	1.05(3)	1.05(3)	0.84(32)	9
Z–O–H	0.980(21)	0.97(5)	0.97(6)	0.85(6)	7
C(any)–O–H	1.098(11)	0.98(2)	0.99(2)	0.82(2)	1
C(ar) –O–H	0.992(17)	0.98(2)	0.99(2)	0.82(2)	1
N^+–H	1.036(16)	1.03(3)	1.00(5)	0.92(4)	3
Z_2–N–H	1.027(16)	0.96(2)	0.97(3)	0.84(5)	4

Table S29: Averaged X-H bond distances (in Å) according to the Allen-Bruno classes[S19] for crambin for both resolutions. The last column refers to the number of bond lengths in the class.

		Resolution = 0.54 Å			Resolution = 0.73 Å		
Allen-Bruno class	Neutron Reference[S19]	HAR-ELMO	IAM	#	HAR-ELMO	IAM	#
X–H (all)		1.11(12)[a]	0.97(9)[a]	173[a]	1.10(10)[a]	0.96(9)[a]	173[a]
		1.10(10)[b]	0.96(9)[b]	167[b]	1.10(10)[b]	0.95(9)[b]	172[b]
Z_3–Csp^3–H	1.098(11)	1.12(10)[a]	0.98(9)[a]	43[a]	1.10(9)[a]	0.96(9)[a]	43[a]
		1.11(8)[b]	0.97(7)[b]	41[b]	1.10(8)[b]	0.95(7)[b]	42[b]
C_3–Csp^3–H	1.091(17)	1.09(10)	0.96(7)	4	1.08(6)	0.95(4)	4
Z_2–Csp^3–H_2	1.092(17)	1.11(11)[a]	0.98(9)[a]	55[a]	1.10(10)	0.97(9)	55
		1.10(10)[b]	0.97(9)[b]	53[b]			
C_2–Csp^3–H_2	1.083(17)	1.10(10)[a]	0.97(8)[a]	24[a]	1.09(9)	0.96(8)	24
		1.09(9)[b]	0.97(8)[b]	23[b]			
Z–Csp^3–H_3	1.077(26)	1.13(18)[a]	0.98(11)[a]	23[a]	1.09(13)	0.97(11)	23
		1.10(13)[b]	0.97(11)[b]	21[b]			
C–Csp^3–H_3	1.077(29)	1.13(18)[a]	0.98(11)[a]	23[a]	1.09(13)	0.97(11)	23
		1.10(13)[b]	0.97(11)[b]	21[b]			
C(ar)–H	0.983(25)	1.10(11)	0.96(9)	4	1.07(9)	0.95(6)	4
Z–O–H	0.983(25)	1.04(7)	0.91(6)	4	1.03(8)	0.91(8)	4
C(any)–O–H	0.980(21)	1.04(7)	0.91(6)	4	1.03(8)	0.91(8)	4
Csp^3–O–H	0.970(12)	1.02(7)	0.90(8)	3	1.01(8)	0.89(9)	3
C(ar) –O–H	0.992(17)	1.09(4)	0.93(4)	1[c]	1.10(5)	0.94(4)	1[c]

Table S29: continued.

		Resolution = 0.54 Å			Resolution = 0.73 Å		
Allen-Bruno class	Neutron Reference[S19]	HAR-ELMO	IAM	#	HAR-ELMO	IAM	#
Csp^2– N–H_2 (all)	1.013(9)	1.05(6)	0.90(11)	6	1.04(7)	0.90(7)	6
Csp^2– N–H_2 (N amido)	1.010(8)	1.00(1)	0.82(12)	2	0.98(8)	0.83(6)	2
Csp^2– N–H_2 (N pl)	1.012(8)	1.08(4)	0.95(5)	4	1.07(3)	0.94(5)	4
Z_2–N–H	1.027(16)	1.10(1)	0.95(8)	38	1.10(10)	0.94(9)	38

[a] Including outliers.
[b] Excluding outliers. Outliers are defined as being outside the geometric criterion

$$d(i-j) < R(i) + R(j) + 0.4\ \text{Å}$$

[c] The values are the averages with the standard uncertainty of the bond lengths. If there is only one value in the Allen Bruno class, the bond length is taken from the CIF file and the error is the experimental error.

Comparison of residual and deformation densities

Fibril segment – Residual Densities

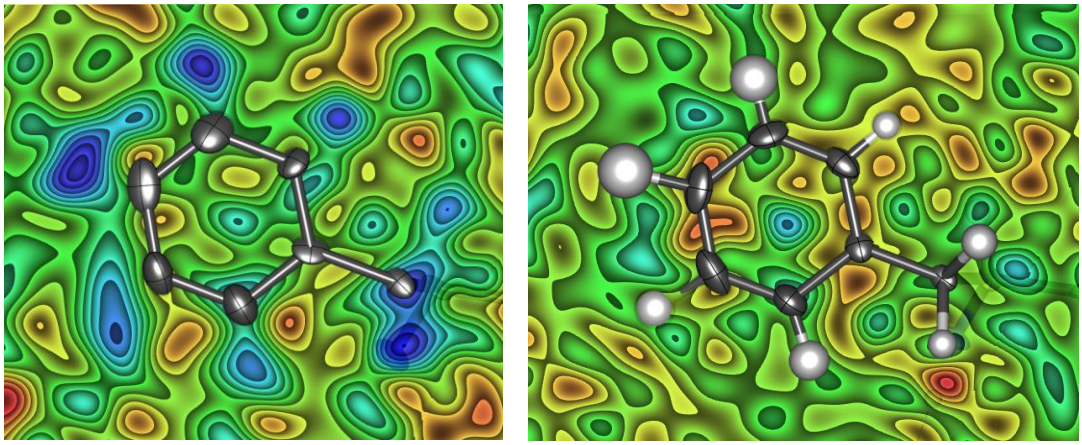

(a) **(b)**

Figure S86: Phenyl group in the fibril-forming segment of the human prion protein: a) without hydrogen atoms as deposited, b) with hydrogen atoms refined in the HAR-ELMO procedure. For (a) and (b) min and max values are -0.2 and 0.3 eÅ^{-3} and contour lines at 0.05 eÅ^{-3} interval. Colour code: from blue (positive), through green (zero) to red (negative). ADPs at 50% probability.

Leu-enkephalin – Residual Densities

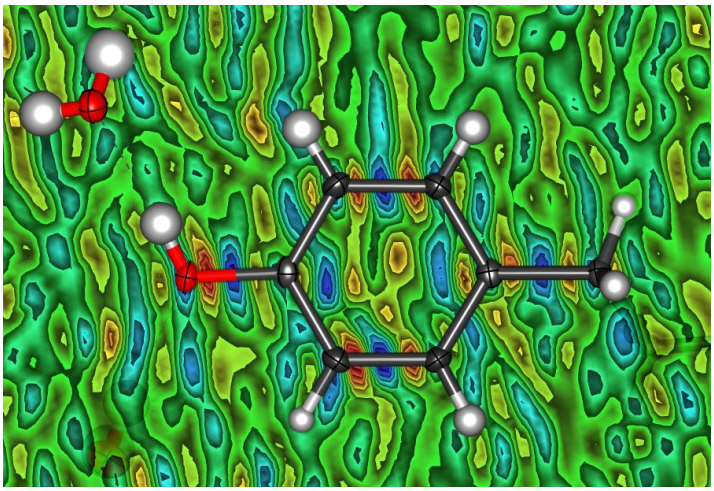

Figure S87: Residual density map for Leu-enkephalin in the plane of the TYR group for the IAM refinement. Min and max values are -0.2 and 0.3 eÅ^{-3}, contour lines at 0.05 eÅ^{-3} interval. Colour code: from blue (positive), through green (zero) to red (negative). ADPs at 50% probability.

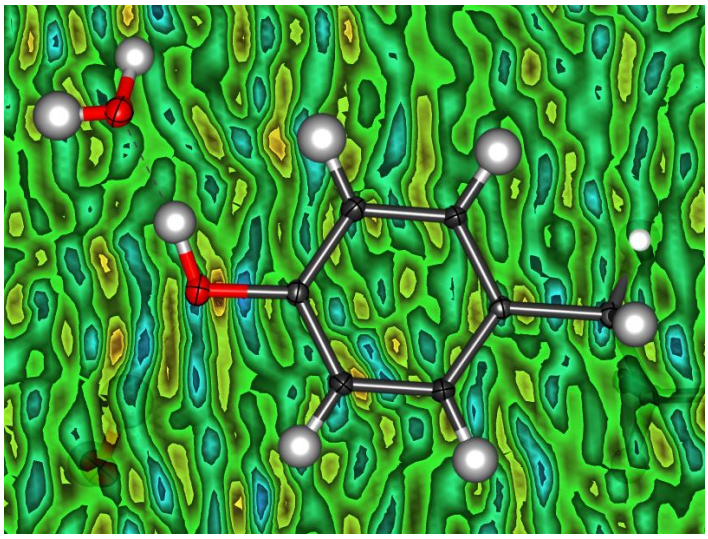

Figure S88: Residual density map for Leu-enkephalin in the plane of the TYR group for the HAR-ELMO refinement. Min and max values are -0.2 and 0.3 eÅ^{-3}, contour lines at 0.05 eÅ^{-3} interval. Colour code: from blue (positive), through green (zero) to red (negative). ADPs at 50% probability.

Crambin – Deformation Densities

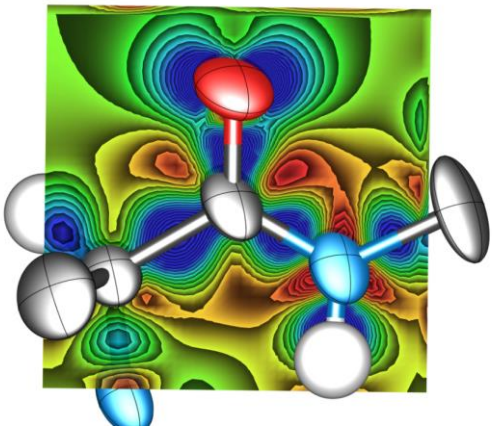

Figure S89: Deformation density map for crambin in the plane of a PRO group (residue 36) for the HAR-ELMO refinement with reflections up to 0.54 Å resolution. Colour code: from blue (positive), through green (zero) to red (negative). ADPs at 50% probability.

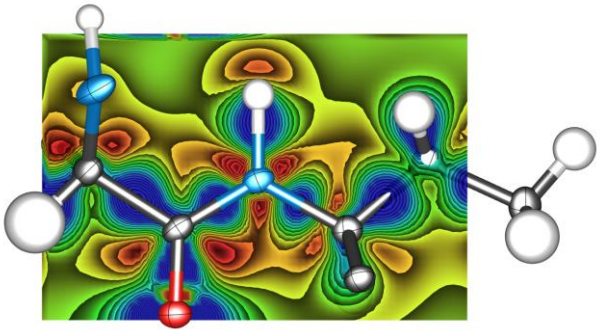

Figure S90: Deformation density map for crambin in the plane of an ALA group (residue 9) for the HAR-ELMO refinement with reflections up to 0.54 Å resolution. Colour code: from blue (positive), through green (zero) to red (negative). ADPs at 50% probability.

Crambin – 3D Deformation Densities

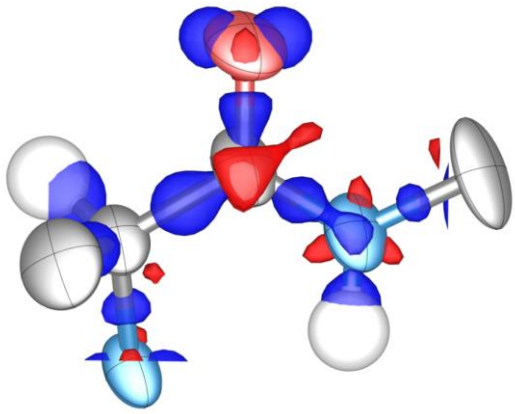

Figure S91: Deformation density of crambin residue 36 (PRO) corresponding to the HAR-ELMO refinement with reflections up to a resolution of 0.54 Å (isosurface level: 0.05 eÅ^{-3}). Colour scheme: blue (positive) and red (negative). ADPs at 50% probability.

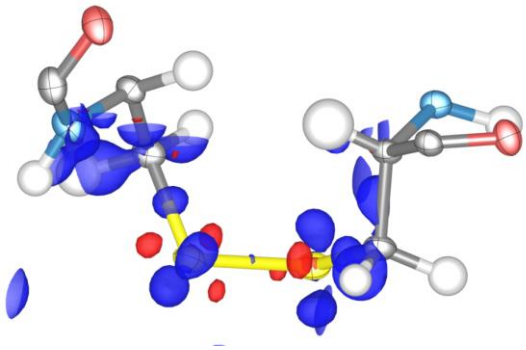

Figure S92: Deformation density of crambin around the disulphide bond between residues 32 (CYX) and 4 (CYX) corresponding to the HAR-ELMO refinement with reflections up to a resolution of 0.54 Å (isosurface level: 0.05 eÅ^{-3}). Colour scheme: blue (positive) and red (negative). ADPs at 50% probability. The sulphur lone pairs are clearly visible.

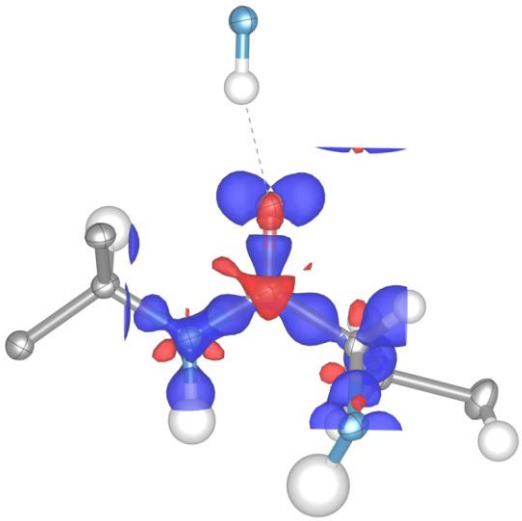

Figure S93: Deformation density of crambin (hydrogen bond between residues 25 (LEU) and 29 (THR)) corresponding to the HAR-ELMO refinement with reflections up to a resolution of 0.54 Å (isosurface level: 0.05 eÅ^{-3}). Colour scheme: blue (positive) and red (negative).

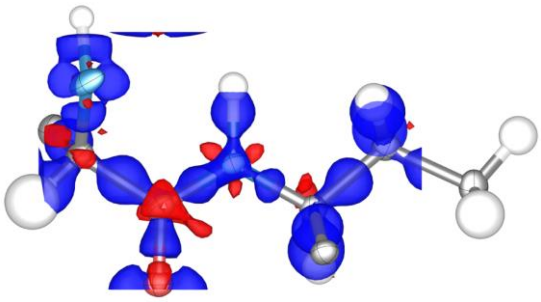

Figure S94: Deformation density of crambin residue 9 (ALA) corresponding to the HAR-ELMO refinement with reflections up to a resolution of 0.54 Å (isosurface level: 0.05 eÅ^{-3}). Colour scheme: blue (positive) and red (negative).

Interaction Energies and Hirshfeld Surface Analysis for the fibril-forming segment of the human prion protein.

Dimer model interaction energies were calculated using the procedure outlined in references S20 and S21 and implemented in the software CrystalExplorer. The colour code in Table S30 shows which molecule is the partner forming the dimer with respect to the central molecule shown in Figure S95. Red and green refer to parallel strands, which are symmetry-related, yellow and purple to head-to-tail contacts, also symmetry-related, and blue to co-crystallized water.

Table S30: Interaction Energies (kJ/mol) calculated at B3LYP/6-31G(d,p) level between dimers found in the crystal structure of the fibril-forming segment of the human prion protein. As discussed in the text, the parallel strands are not the main interactions in terms of energy. R is the distance between molecular centroids (mean atomic positions). The total energies are the sum of the four energy components, properly scaled according to the scale factors k shown below.

	R (Å)	E_ele	E_pol	E_dis	E_rep	E_tot
	4.88	-221.5	-129.6	-169.7	499.5	-169.3
	4.88	-221.5	-129.6	-169.7	499.5	-169.3
	22.07	-182.7	-42.5	-11.2	52.1	-202.2
	22.07	-182.7	-42.5	-11.2	52.1	-202.2
	10.01	-113.2	-36.8	-14.0	101.3	-96.5

Energy Model	k_ele	k_pol	k_disp	k_rep
CE-B3LYP ... B3LYP/6-31G(d,p) electron densities	1.057	0.740	0.871	0.618

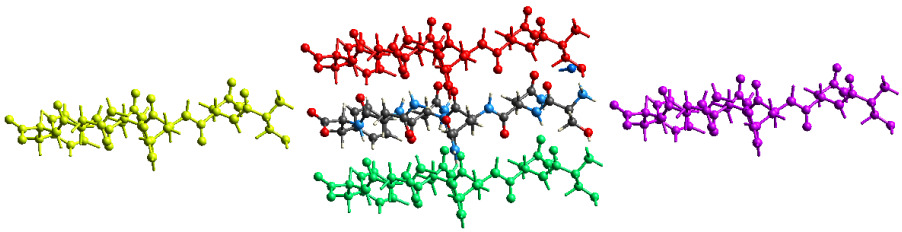

(a)

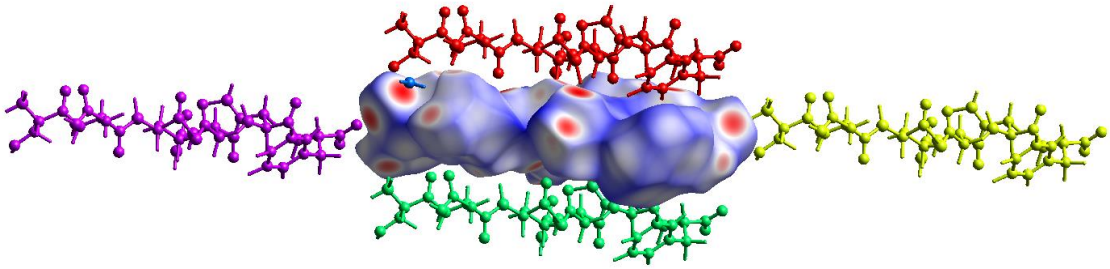

(b)

Figure S95: Symmetry-generated cluster around a central molecule of the fibril-forming segment of the human prion protein, colour coded according to Table S30. In b) a Hirshfeld surface is plotted around the central molecule with the property d_{norm} mapped onto it. Red areas show close contacts such as hydrogen bonds. Details about Hirshfeld Surface Analysis can be found in ref. S22.

Refinement of coordination compounds

Specific model molecule for ELMOs of coordination compounds. For the sake of completeness, in Figure S96 we report the Lewis structure of the coordination compounds investigated in this paper: $(Ph_3P)_2Hg(CN)_2$ (see Figure S96-A) and $(Ph_3P)_2Hg(NO_3)_2$ (see Figure S96-B).

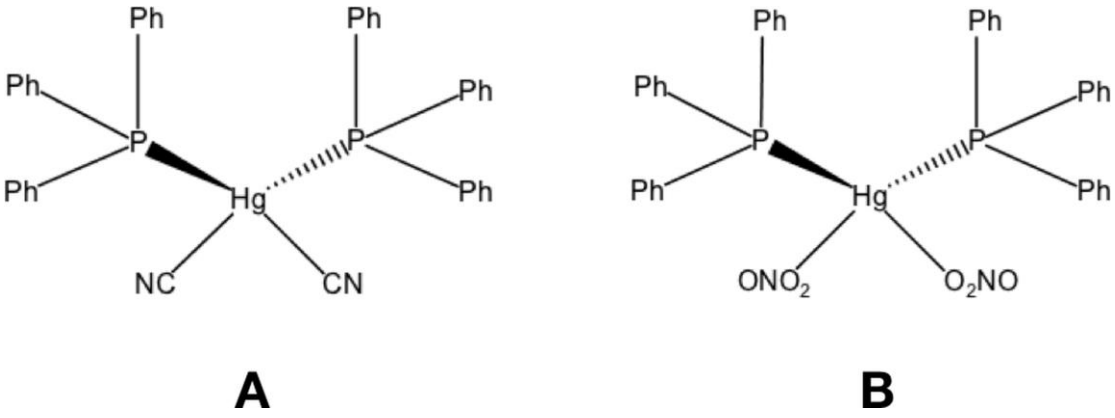

Figure S96: Coordination compounds investigated in the paper: (A) $(Ph_3P)_2Hg(CN)_2$ and (B) $(Ph_3P)_2Hg(NO_3)_2$

As mentioned earlier, the ELMOs used in the HAR-ELMO refinements of these two coordination compounds were obtained by performing ELMO calculations on tailor-made model molecules. In fact, the current ELMO libraries cover only the subunits for the twenty natural amino acids and water. The model systems adopted for the ELMO computations are depicted in Figure S97.

For model molecule $(H_3P)_2Hg(CN)_2$ (see Figure S97-A), we computed the following ELMOs to describe:

- all the Hg core electrons;
- all the electrons of the CN^- ligands, including the electron pairs delocalized between the carbon atoms and Hg. This means that, for each ligand, we considered an ELMO delocalized between C and Hg to describe the bonds between the two atoms;
- the lone-pair electrons of the phosphorous atoms delocalized between P and Hg. In other words, we computed ELMOs delocalized between each of the P atoms and Hg to describe the different P-Hg bonds.

For model molecule $(H_3P)_2Hg(NO_3)_2$ (see Figure S97-B), we computed the following ELMOs to describe:

- all the Hg core electrons;
- all the electrons of the NO_3^- ligands, including the electron pairs delocalized between the oxygen atoms and Hg. This means that, for each ligand, we also considered ELMOs delocalized between the O atoms and Hg to describe the four Hg-O bonds of the system (see Figure S97-D for details);
- the lone-pair electrons of the phosphorous atoms delocalized between P and Hg. In other words, we computed ELMOs delocalized between each of the P atoms and Hg to describe the different P-Hg bonds.

To fully take into account the non-equivalence of the two Hg-O dative bonds provided by each nitrate ligand, we considered a geometry for model molecule $(H_3P)_2Hg(NO_3)_2$ characterized by different Hg-O bond lengths within the same nitrate ligand (2.845 Å and 2.467 Å).

For triphenylphosphine (see Figure S97-C) we computed all the ELMOs needed to describe all the electrons of the PPh_3 ligands, except for those associated with the lone pair of the phosphorus atom.

All the ELMO calculations on the model molecules were performed using the DZP-DKH basis set and adopting localization schemes corresponding to the Lewis structures of the molecules under exam.

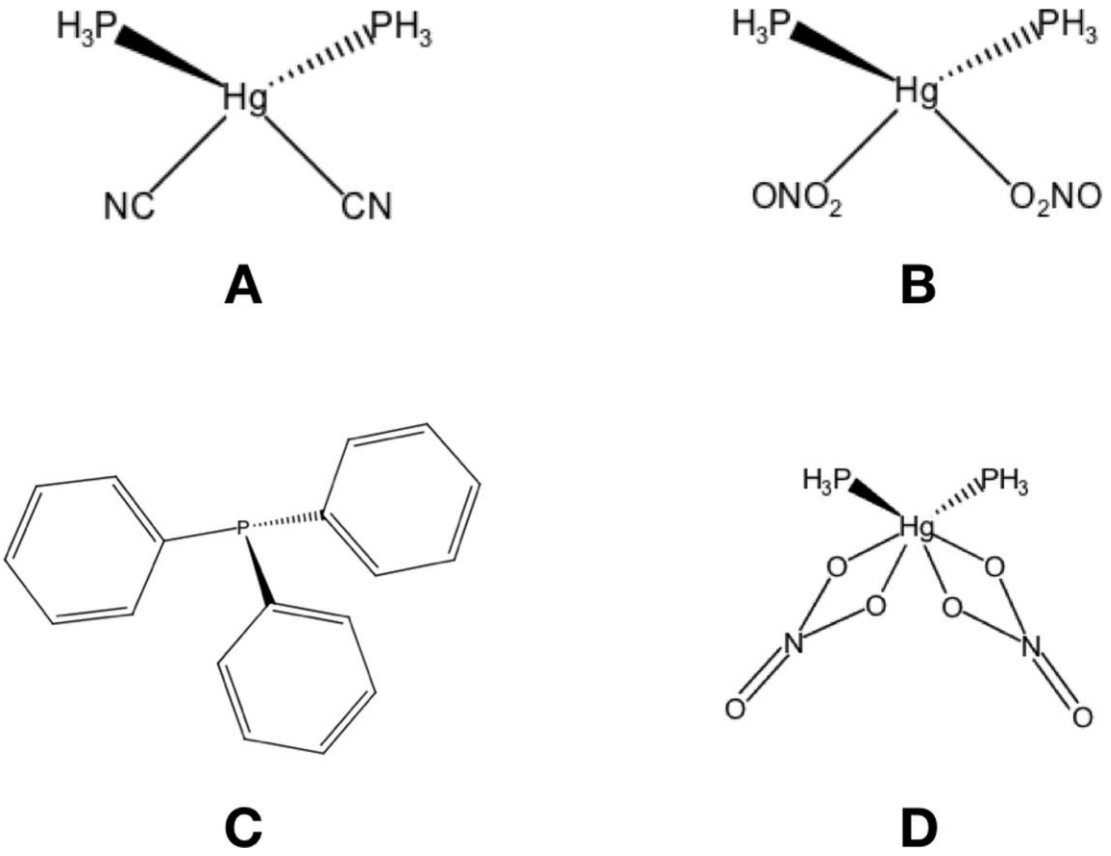

Figure S97: Model molecules used for the computations of the ELMOs used in the HAR-ELMO refinements of the two coordination compounds investigated in this study: A) $(H_3P)_2Hg(CN)_2$, B) $(H_3P)_2Hg(NO_3)_2$ and, C) triphenylphosphine (PPh_3). Figure D is another representation of model molecule $(H_3P)_2Hg(NO_3)_2$ with the details of the two non-equivalent bonds between the oxygen atoms and Hg.

Table S31: Measurement details for the X-ray diffraction experiments of $(Ph_3P)_2Hg(NO_3)_2$ and $(Ph_3P)_2Hg(CN)_2$.

Chemical formula	$(Ph_3P)_2Hg(NO_3)_2$	$(Ph_3P)_2Hg(CN)_2$
Mr (u)	849.15	777.17
Crystal system	monoclinic	orthorhombic
Space group	C 2/c	P na2_1
***a, b, c, β* (Å)**	13.2836(4) 13.8899(4) 17.7854(5) 91.070 (1)	17.9310(5) 9.8963(3) 18.1031(5)
***V* (Å^3)**	3280.97(16)	3212.41(16)
Z	4	4
Radiation type	X-ray (MoKα)	X-ray (MoKα)
Wavelength (Å)	0.71073	0.71073
Temperature (K)	100(1)	100(1)
Crystal size (mm)	0.26x0.22x 0.19	0.17x0.11x 0.09
Absorption cor.	multi-scan	multi-scan
***μ* (mm^{-1})**	4.813	4.895
***T*min**	0.30	0.53
***T*max**	0.40	0.64
Extinction cor:[S10]	none	none
Resolution (Å)	0.50	0.55
hkl ranges	*h*=-26, 26 *k*=-27, 27 *l*=-35, 35	*h*=-32, 32 *k*=-17, 17 *l*=-32, 32
Theta min	2.12	2.35
Theta max	45.29	40.25
Theta full	39.39	40.25
Complet. (max)	0.995	1.000
Complet. (full)	1.000	1.000
Refl. Measured	124199	269147
Unique refl.	13738	10335
Unique obs. refl.	13031	9846
Obs. criteria	F>0 F/u(F)>3.0 |F_calc|>10^{-3}	F>0 F/u(F)>3.0 |F_calc|>10^{-3}
***R*int**	0.0263	0.0359
***R*sigma**	0.0134	0.0262
CCDC number	1917593	1917594

Table S32: Refinement of X-ray data for $(Ph_3P)_2Hg(NO_3)_2$ and $(Ph_3P)_2Hg(CN)_2$.

$(Ph_3P)_2Hg(NO_3)_2$	IAM	HAR-ELMO, isotropic	HAR-ELMO, anisotropic
R*[*F*>3*σ*(*F*)], *wR*(*F*), *S	0.0204, 0.0221, 3.070	0.0163, 0.0153, 2.114	0.0162, 0.0151, 2.098
No. of reflections	13031	13031	13031
No. of parameters	277	277	352
H-atom treatment	H atoms refined isotropically	H atoms refined isotropically	All H-atom parameters refined (anisotropically)
$\Delta\rho_{max}$, $\Delta\rho_{min}$ (eÅ^{-3})	2.072, −0.843	1.632, −0. 669	1.632, −0.680
$(Ph_3P)_2Hg(NO_3)_2$	HAR, relativistic	HAR, isotropic	HAR, anisotropic
R*[*F*>3*σ*(*F*)], *wR*(*F*), *S	0.0150, 0.0135, 1.875	0.0163, 0.0149, 2.072	0.0162, 0.0148, 2.057
No. of reflections	13031	13031	13031
No. of parameters	352	277	352
H-atom treatment	All H-atom parameters refined (anisotropically)	H atoms refined isotropically	All H-atom parameters refined (anisotropically)
$\Delta\rho_{max}$, $\Delta\rho_{min}$ (eÅ^{-3})	1.149, −0.805	1.664, −0.675	1.672, −0.675
$(Ph_3P)_2Hg(CN)_2$	IAM	HAR-ELMO, isotropic	HAR-ELMO, anisotropic
R*[*F*>3*σ*(*F*)], *wR*(*F*), *S	0.0215, 0.0211, 2.080	0.0188, 0.0165, 1.632	0.0187, 0.0163, 1.619
No. of reflections	9846	9846	9846
No. of parameters	504	504	657
H-atom treatment	H atoms refined isotropically	H atoms refined isotropically	All H-atom parameters refined (anisotropically)
$\Delta\rho_{max}$, $\Delta\rho_{min}$ (eÅ^{-3})	1.299, −1.021	1.130, −1.015	1.118, −0.994

Table S32: continued.

$(Ph_3P)_2Hg(CN)_2$	-	HAR, isotropic	HAR, anisotropic
$R[F>3\sigma(F)]$, $wR(F)$, S		0.0188, 0.0165, 1.626	0.0187, 0.0162, 1.613
No. of reflections		9846	9846
No. of parameters		504	657
H-atom treatment		H atoms refined isotropically	All H-atom parameters refined (anisotropically)
$\Delta\rho_{max}$, $\Delta\rho_{min}$ (eÅ^{-3})		1.143, −1.016	1.132, −0.995

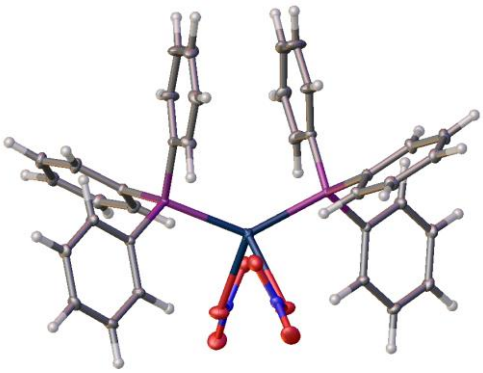

(a) HAR-ELMO, isotropic

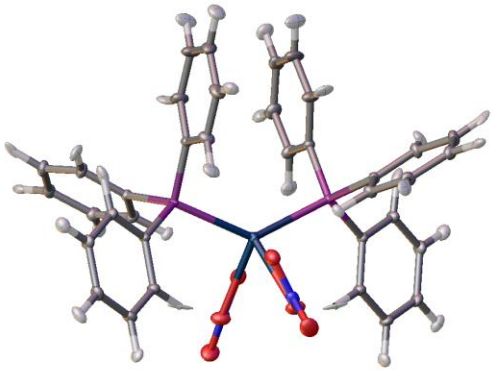

(b) HAR-ELMO, anisotropic

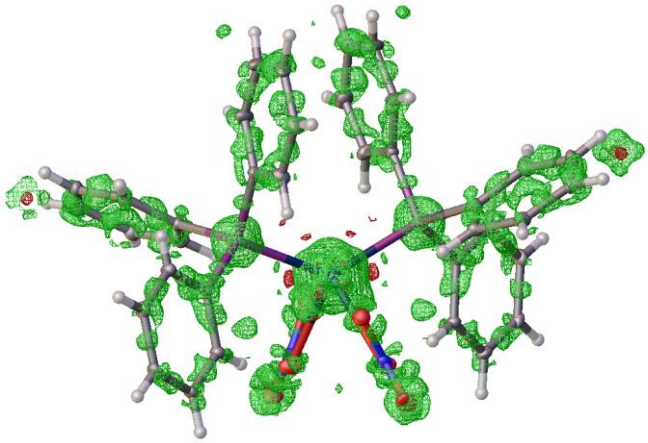

(c) IAM, -0.843/+2.072 eÅ^{-3}

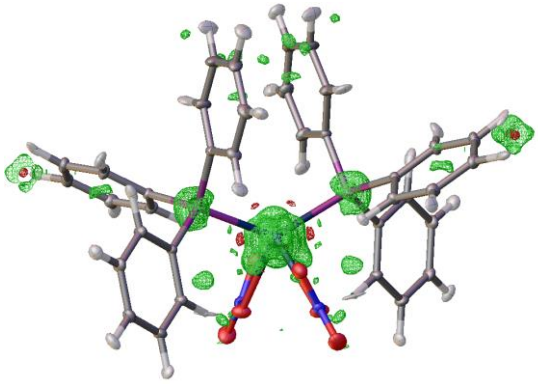

(d) HAR-ELMO, -0.680/+1.632 eÅ^{-3}

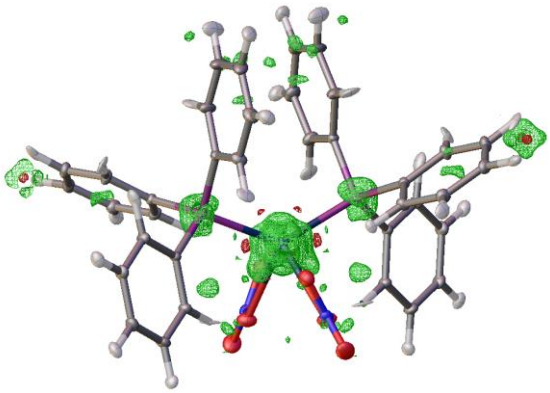

(e) HAR, -0.675/+1.672 eÅ^{-3}

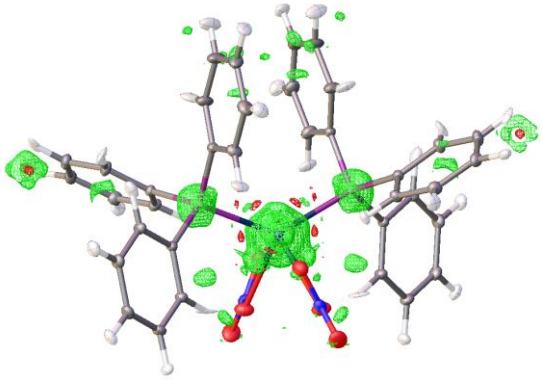

(f) HAR at B3LYP-IOTC, -0.805/+1.149 eÅ^{-3}

Figure S98: $(Ph_3P)_2Hg(NO_3)_2$. HAR-ELMO molecular structures using (a) isotropic displacement parameters and (b) anisotropic displacement parameters for the hydrogen atoms. (c) Residual density distribution after IAM refinement with minimum and maximum values, (d) after anisotropic HAR-ELMO, (e) after anisotropic HAR at the same level of theory (HF/ DZP-DKH), (f) after HAR at B3LYP-IOTC level. Isovalue = $\pm$ 0.2 eÅ^{-3}, green=positive, red=negative. ADPs at 50% probability level.

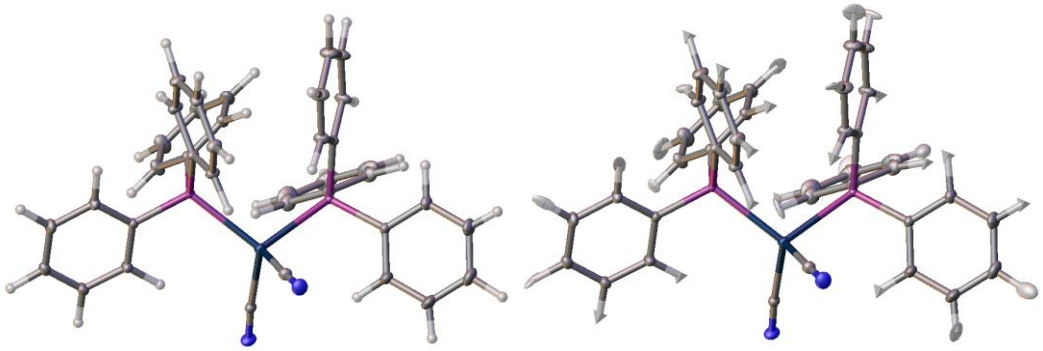

(a) HAR-ELMO, isotropic (b) HAR-ELMO, anisotropic

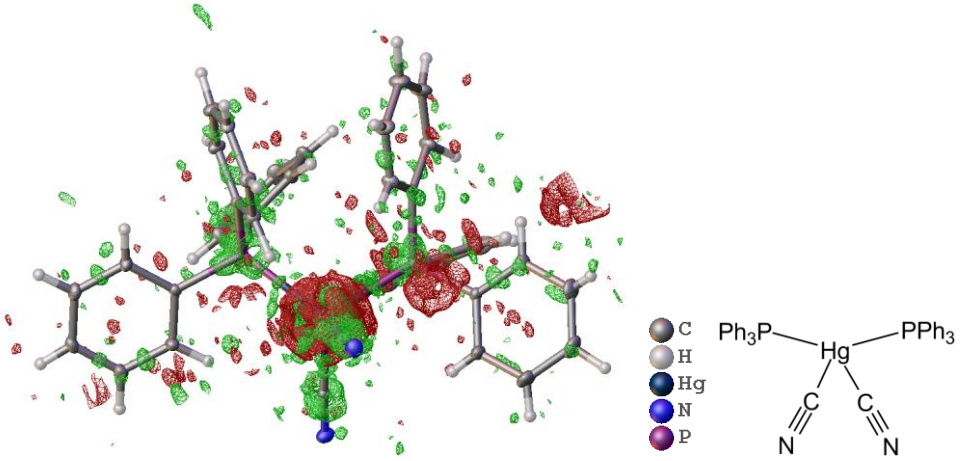

(c) IAM, -1.021/+1.299 eÅ^{-3}

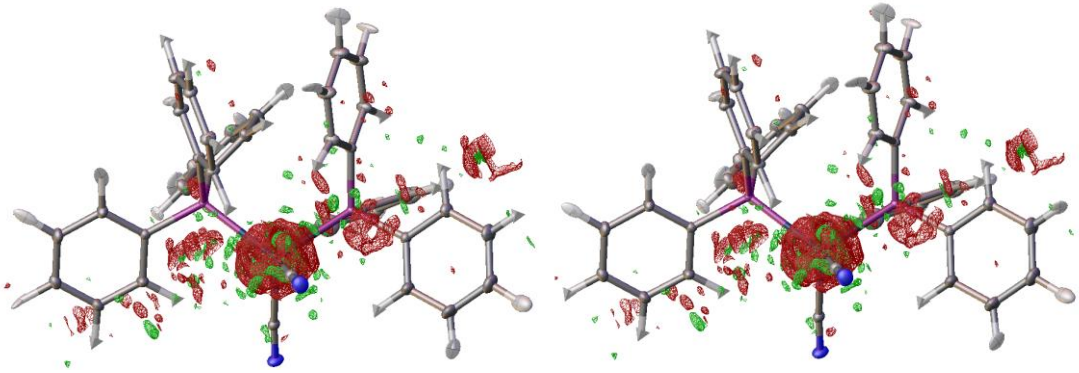

(d) HAR-ELMO, -0.944/+1.118 eÅ^{-3} (e) HAR, -0.995/+1.132 eÅ^{-3}

Figure S99: $(Ph_3P)_2Hg(CN)_2$. HAR-ELMO molecular structures using (a) isotropic displacement parameters and (b) anisotropic displacement parameters for the hydrogen atoms. (c) Residual density distribution after IAM refinement with minimum and maximum values, (d) after anisotropic HAR-ELMO, (e) after anisotropic HAR at the same level of theory (HF/DZP-DKH). Isovalue = $\pm$ 0.2 eÅ^{-3}, green=positive, red=negative. ADPs at 50% probability level.

Graphical visualization software used

Globally, throughout manuscript and supporting information, deformation densities, residual densities, ELI-D and ESPs were visualized using GaussView,[S23] VESTA,[S24] VMD[S25] and Olex2[S26]. For the crambin model (Fig 2a) UCSF Chimera was used.[S27]

References

S1. Stoll, H.; Wagenblast, G; Preuss, H. On the Use of Local Basis Sets for Localized Molecular Orbitals. *Theor. Chim. Acta* **1980**, *57*,169−178.

S2. Philipp, D. M.; Friesner, R. A. Mixed Ab Initio QM/MM Modeling Using Frozen Orbitals and Tests with Alanine Dipeptide and Tetrapeptide. *J. Comput. Chem.* **1999**, *20*, 1468-1494.

S3. Meyer, B.; Guillot, B.; Ruiz-Lopez, M. F.; Genoni, A. Libraries of Extremely Localized Molecular Orbitals. 1. Model Molecules Approximation and Molecular Orbitals Transferability. *J. Chem. Theory. Comput.* **2016**, *12*, 1052-1067.

S4. Meyer, B.; Guillot, B.; Ruiz-Lopez, M. F.; Jelsch, C.; Genoni, A. Libraries of Extremely Localized Molecular Orbitals. 2. Comparison with the Pseudoatoms Transferability. *J. Chem. Theory. Comput.* **2016**, *12*, 1068-1081.

S5. Meyer, B.; Genoni, A. Libraries of Extremely Localized Molecular Orbitals. 3. Construction and Preliminary Assessment of the New Databanks. *J. Phys. Chem. A* **2018**, *122*, 8965-8981.

S6. Ferré, N.; Assfeld, X.; Rivail, J.-L. Specific Force Field Parameters Determination for the Hybrid Ab Initio QM/MM LSCF Method. *J. Comput. Chem.* **2002**, *23*, 610-624.

S7. Capelli, S.; Bürgi, H.-B.; Dittrich, B.; Grabowsky, S.; Jayatilaka, D. Hirshfeld atom refinement. *IUCrJ* **2014**, *1*, 361-379.

S8. Destro, R.; Marsh, R. E.; Bianchi, R. A low-temperature (23 K) study of *L*-alanine. *J. Phys. Chem.* **1998**, *92*, 966–973.

S9. Capelli, S. C.; Bürgi, H.-B.; Mason, S. A.; Jayatilaka, D. Glycyl-*L*-alanine: a multi-temperature neutron study. *Acta Cryst. C* **2014**, *70*, 949–952.

S10. Larson, A. C. In *Crystallographic Computing*; Ahmed, F. R., Ed.; Munskgaard: Copenhagen, Denmark, 1970; pp 291-294.

S11. Fugel, M.; Jayatilaka, D.; Hupf, E.; Overgaard, J.; Hathwar, V. R.; Macchi, P.; Turner, M. J.; Howard, J. A. K.; Dolomanov, O. V.; Puschmann, H.; Iversen, B. B.; Bürgi, H.-B.; Grabowsky, S. Probing the accuracy and precision of Hirshfeld atom refinement with HARt interfaced with Olex2. *IUCrJ* **2018**, *5*, 32-44.

S12. Morgenroth, W.; Overgaard, J.; Clausen, H. F.; Svendsen, H.; Jørgensen, M. R. V.; Larsen, F. K; Iversen, B. B. Helium cryostat synchrotron charge densities determined using a large CCD detector – the upgraded beamline D3 at DESY. *J. Appl. Cryst.* **2008**, *41*, 846–853.

S13. Jørgensen, M. R. V.; Hathwar, V. R.; Sist, M.; Wang, X.; Hoffmann, C. M.; Briseno, A. L.; Overgaard, J.; Iversen, B. B. Accurate atomic displacement parameters from time-of-flight neutron-diffraction data at TOPAZ. *Acta Cryst. A* **2014**, *70*, 679–681.

S14. Meindl, K.; Henn, J. Foundations of residual-density analysis. *Acta Cryst. A* **2008**, *64*, 404–418.

S15. Sawaya, M. R.; Sambashivan, S.; Nelson, R.; Ivanova, M. I.; Sievers, S. A.; Apostol, M. I.; Thompson, M. J.; Balbirnie, M.; Wiltzius, J. J. W.; McFarlane, H. T.; Madsen, A. Ø.; Riekel, C.; Eisenberg, D. Atomic structures of amyloid cross-β spines reveal varied steric zippers. *Nature* **2007**, *447*, 453–457.

S16. Case, D. A.; Ben-Shalom, I. Y.; Brozell, S. R.; Cerutti, D. S.; Cheatham, T. E., III; D. Cruzeiro, V. W.; Darden, T. A.; Duke, R. E.; Ghoreishi, D.; Gilson, M. K.; Gohlke, H.; Goetz, A. W.; Greene, D.; Harris, R.; Homeyer, N.; Izadi, S.; Kovalenko, A.; Kurtzman, T.; Lee, T. S.; LeGrand, S.; Li, P.; Lin, C.; Liu, J.; Luchko, T.; Luo, R.; Mermelstein, D. J.; Merz, K. M.; Miao, Y.; Monard, G.; Nguyen, C.; Nguyen, H.; Omelyan, I.; Onufriev, A.; Pan, F.; Qi, R.; Roe, D. R.; Roitberg, A.; Sagui, C.; Schott-Verdugo, S.; Shen, J.; Simmerling, C. L.; Smith, J.; Salomon-Ferrer, R.; Swails, J.; Walker, R. C.; Wang, J.; Wei, H.; Wolf, R. M.; Wu, X.; Xiao, L.; York, D. M.; Kollman, P. A. *AMBER 2018*, University of California, San Francisco: San Francisco, CA, USA, 2018.

S17. Pichon-Pesme, V.; Lecomte, C.; Wiest, R.; Bernard, M. Modeling fragments for the *ab initio* determination of electron density in polypeptides. An experimental and theoretical approach to the electron distribution in Leu-enkephalin trihydrate. *J. Am. Chem. Soc*. **1992**, *114*, 2713-2715.

S18. Jelsch, C.; Teeter, M. M.; Lamzin, V.; Pichon-Pesme, V.; Blessing, R. H.; Lecomte, C. Accurate protein crystallography at ultra-high resolution: valence electron distribution in crambin. *Proc. Natl. Acad. USA* **2000**, *97*, 3171-3176.

S19. Allen, F. H.; Bruno, I. J. Bond lengths in organic and metal-organic compounds revisited: X-H bond lengths from neutron diffraction data. *Acta Cryst. B* **2010**, *66*, 380–386.

S20. Turner, M. J.; Grabowsky, S.; Jayatilaka, D.; Spackman, M. Accurate and Efficient Model Energies for Exploring intermolecular Interactions in Molecular Crystals. *J. Phys. Chem. Lett.* **2014**, *5*, 4249-4255.

S21. Mackenzie, C. F.; Spackman, P. R.; Jayatilaka, D.; Spackman, M. CrystalExplorer model energies and energy frameworks: extension to metal coordination compounds, organic salts, solvates and open-shell systems. *IUCrJ* **2017**, *4*, 575-587.

S22. Spackman, M. A.; Jayatilaka, D. Hirshfeld surface analysis. *CrystEngComm* **2009**, *11*, 19-32.

S23. Dennington, R.; Keith, T. A.; Millam, J. M. *GaussView, Version 6*; Semichem Inc.: Shawnee Mission, KS, USA, 2016.

S24. Momma, K.; Izumi, F. VESTA 3 for three-dimensional visualization of crystal, volumetric and morphology data. *J. Appl. Cryst.* **2011**, *44*, 1272-1276.

S25. Humphrey, W.; Dalke, A.; Schulten, K. VMD - Visual Molecular Dynamics. *J. Molec. Graphics* **1996**, *14*, 33-38.

S26. Dolomanov, O. V.; Bourhis, L. J.; Gildea, R. J.; Howard, J. A. K.; Puschmann, H. OLEX2: a complete structure solution, refinement and analysis program *J. Appl. Cryst.* **2009**, *42*, 339-341.

S27. Pettersen, E. F.; Goddard, T. D.; Huang, C. C.; Couch, G. S.; Greenblatt, D. M.; Meng, E. C.; Ferrin, T. E. UCSF Chimera - a visualization system for exploratory research and analysis. *J Comput Chem.* **2004**, *25***,** 1605-1612.